Exploring processes to improve electroactivity in *Shewanella oneidensis* MR-1

Understanding biofilm formation and cytochrome *c* maturation

Ana V. Silva

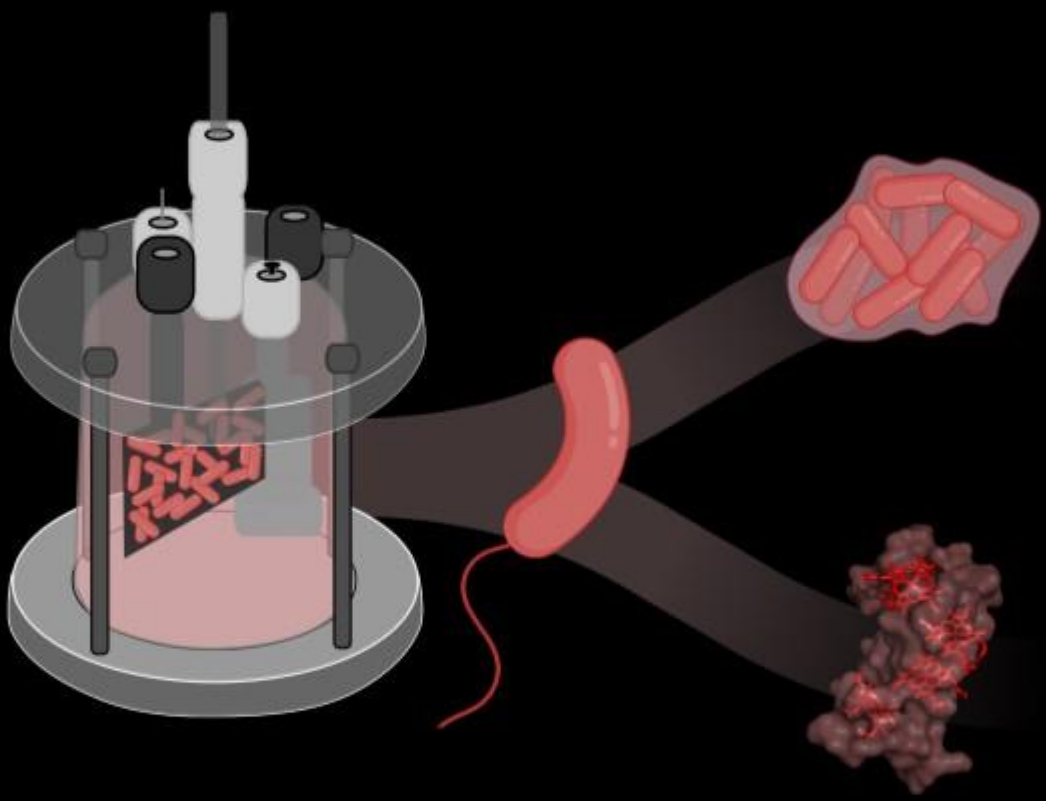

Dissertation presented to obtain the Ph.D degree in Molecular Biosciences

Instituto de Tecnologia Química e Biológica António Xavier | Universidade Nova de Lisboa

Oeiras,
February, 2023

UNIVERSIDADE NOVA DE LISBOA

Exploring processes to improve electroactivity in *Shewanella oneidensis* MR-1

Understanding biofilm formation and cytochrome *c* maturation

Ana V. Silva

Dissertation presented to obtain the Ph.D. degree in Molecular Biosciences

Instituto de Tecnologia Química e Biológica António Xavier | Universidade Nova de Lisboa

Oeiras, February, 2023

The research described in this thesis was performed under the supervision of:

Professor Ricardo O. Louro
Instituto de Tecnologia Química e Biológica António Xavier, Universidade Nova de Lisboa, Avenida da República, 2780-157 Oeiras, Portugal

Doctor Catarina M. Paquete
Instituto de Tecnologia Química e Biológica António Xavier, Universidade Nova de Lisboa, Avenida da República, 2780-157 Oeiras, Portugal

All work was performed at:

- Instituto de Tecnologia Química e Biológica António Xavier, Universidade Nova de Lisboa, Oeiras, Portugal
- Institute for Applied Biology, Karlsruhe Institute of Technology, Karlsruhe, Germany

"She is Not Fragile Like a Flower, She is Fragile Like a Bomb" Frida Khalo

A todos os que fizeram de mim quem sou, dedico esta tese. Principalmente a ti, que me fizeste filha, e a ti, que me fizeste mãe.

Agradecimentos

Em primeiro lugar, agradeço aos meus orientadores, sem os quais nunca se faria uma tese:

- Ricardo O. Louro – Quando procurava um laboratório para fazer a minha tese de mestrado, todos me fizeram sentir "a mais", como se ter um estudante fosse um fardo. O Ricardo fez-me sentir o oposto, que seria uma mais-valia e uma necessidade do laboratório! Agradeço por todas as vezes que, tal como na primeira, me fez sentir especial e valorizada.

- Catarina M. Paquete – A ti, que tão bem me mostraste como podem estar erradas as primeiras impressões, tenho muito a agradecer. Agradeço a amizade, as conversas fora de horas, a calma nos momentos de pânico e todas as vezes que fizeste este trabalho andar para a frente. Tens um dom muito especial de, a cada conversa, me dar força, motivação e inspiração.

Agradeço a todos os meus colegas IBN, os presentes e os que já voaram para outras andanças. Em particular, não posso deixar de agradecer a:

- Nazua Costa – A minha mamã loba, cocó orientadora, *Pseudomona* nas horas vagas, agradeço a introdução à vida científica, todo o *tough love*, que na verdade é tudo o que uma pessoa precisa, todo o apoio, dentro e fora "de campo", a amizade, as horas extra e tantas outras coisas! E obviamente (como tanto gostas desta palavra) e acima de tudo, teres-me dado o meu primeiro coraçãozinho fora do peito! A minha afilhada, a quem também agradeço a motivação extra para a tese e para a vida no geral e todo o amor que só ela me sabe dar! Se não têm alguém que olha para vocês como a Camila olha para a sua madrinha… arranjem!

- Maria Firmino – A minha aluna prodígio! A única que passou em todos os testes para integrar a família loba! É e será sempre difícil separar o que te agradecer para esta tese com o que te agradecer na vida! És uma força

da natureza que, tendo visto o pior que ela tem para oferecer, te esforças por tornar melhor a de todos com quem te cruzas! És das pessoas mais especiais que conheço e um obrigada nunca será suficiente!

- Bruno Fonseca – A melhor pessoa do mundo disfarçada de pequena bestinha. Agradeço desde o início, por me dares o benefício da dúvida quando mais ninguém o fez. Por toda a boa disposição e humor negro que tanto gosto! Por teres sempre a capacidade de aliviar o *mood* e olhar para tudo com um sorriso no rosto e uma piada prontinha a sair. O tempo no laboratório contigo passa-se muito melhor!

- Inês Trindade – A minha companheira desta aventura! Estivemos sempre juntas, lado a lado durante esta jornada a ser confundidas por toda a gente, até o Sr. Google, esse grande sábio! Agradeço-te todas as piadas, os bons momentos, a companhia e a ajuda, que ofereces sempre sem hesitar! Devolvo-te aquilo que me escreveste e que muito me marcou: se evoluímos por estar rodeadas de pessoas espetaculares, tu certamente contribuíste muito para a minha evolução! Obrigada por apoiares e incentivares sempre as minhas tentativas de pôr alguma ordem neste sítio!

- Alexandra Alves, Anaisa Coelho e Ricardo Soares – a vocês, que me acompanharam em boa parte do tempo deste doutoramento, agradeço o bom ambiente no laboratório, a entreajuda e a diversão que nos caracteriza. Sem vocês não teria sido a mesma coisa!

Agradeço à minha família ter-me feito o que sou, ter aceitado sempre quem sou e o caminho que quis percorrer, em suma, o apoio incondicional

- Mamã – Nunca terei palavras para te agradecer, não as há em nenhum idioma! Como se poderia agradecer à melhor pessoa do mundo a sorte de ser sua filha? Não tenho sequer por onde começar, o apoio e amor incondicionais? O esforço por fazer sempre o melhor para mim? A ajuda

em todas as horas? Não dá… continuarei até ao fim dos nossos dias a fazer por te agradecer, com a certeza de que nunca serei capaz.

- Pai – Agradeço por acreditares sempre que posso ser melhor, que posso ser A melhor. Com esse teu jeito particular de mostrar amor que só nós sabemos interpretar e com a tua ironia sempre presente, és o senhor guelras rabugento mais fofinho do mundo!

- Miguel Salreta – Obrigada por me fazeres sempre ver o lado mais leve da vida, por seres o yin do meu yang. Tens uma forma descomplicada de ver a vida e de me fazer perceber quando estou a stressar demasiado! Agradeço por aturares as minhas piores e melhores versões e te manteres sempre a meu lado, sempre pronto para me abraçar e apoiar. O que atura mais vezes o meu mau feitio (e não é nada fácil)

- Maria – A ti, meu sonho tornado realidade, que me dificultaste tanto a conclusão desta tese, mas melhoraste mil vezes mais a minha vida.

Agradeço a todos os meus amigos, a família que escolhi e que sempre me apoiou. Aos fidjos di tchon por serem sempre um escape e uma forma de esquecer todos os problemas! Aos que ficam orgulhosos das minhas conquistas como se fossem suas, que estão presentes em todos os momentos, que aturam todos os meus humores, que celebram todas as minhas vitórias e tanto mais que vos poderia agradecer (vou tentar que a ordem seja cronológica para não ferir suscetibilidades), Mó, Dudu e Catarina, os companheiros de sempre e para sempre. Maga, Sara e Patrícia, o melhor que a universidade me deu e que guardo para sempre. Tiago, Diana e Gonçalo os meus aldeões favoritos que me acompanham todos os dias!

Aos meus colegas MolBioS, por terem acompanhado o início desta aventura e tê-la tornado muito mais divertida (nunca esquecerei aquele retiro)! Em especial, agradeço à Cátia Bárria, que se tornou uma grande amiga, sempre

pronta para ajudar no trabalho ou em qualquer outro contexto e que certamente levarei para a vida!

Agradeço ao ITQB e à sua estrutura o ambiente que nos proporciona para desenvolvermos o nosso trabalho e as nossas competências num clima de colaboração e não de competição, pois é isso que nos torna fortes e nos permite estar no topo!

- A todos os grupos de investigação do ITQB, que contribuem para que juntos sejamos mais fortes. Em especial aos laboratórios do 3º piso, aos que nos emprestam sempre coisas em particular os grupos do Tiago Cordeiro, Inês Pereira, Lígia Saraiva e Miguel Teixeira.

- Agradeço a existência das salas de lavagens e aos seus profissionais. Sei como é não os ter e, como tal, reconheço a diferença que fazem! Em especial, agradeço à Cristininha e à Rose todo o carinho com que sempre me trataram, fazendo-me sentir parte da família! Agradeço também a disponibilidade e facilitarem sempre o meu trabalho!

- A todos os técnicos, pelo trabalho exemplar que fazem, tratando o ITQB como uma casa e não como um trabalho, não tenho dúvida que sem vocês este instituto não seria nem de perto nem de longe o que é! Em particular, agradeço à Paula Chicau, ao João Carita e à Cristina Timóteo todo o carinho, amizade e preocupação, comigo e com a minha pequena! Agradeço também a preocupação com o meu trabalho, fazendo sessões de *troubleshooting* como se do vosso se tratasse. Para além de facilitarem muito o meu trabalho também me fazem sentir em casa. E, claro a nossa Isabelinha (Isabel Pacheco) cuja partida deixou um grande vazio! Muito mais que uma técnica, uma companheira, uma amiga, uma conselheira! Muito obrigada!

- A todos os funcionários do gabinete de comunicação, que me ajudaram a despertar para a minha paixão pela comunicação de ciência, em

especial à Joana Lobo Antunes e Renata Ramalho, responsáveis pelo gabinete durante o meu tempo no ITQB, e ao Luís Morgado e Rita Neves que tantas vezes me acompanharam e ajudaram.

To our collaborators, in Portugal and abroad that allowed this work to be carried out in the best way possible:

- Irene Diaz-Moreno – The booster of the System III work, back in my Masters, by providing us with the pBBR plasmid, that started it all!

- Daldal Lab – The ones that introduced me to maturation System I and that allowed me to stay in the field after the Master and took me in across seas both in the lab and outside. For this, I thank all the group, especially Fevzi, Andreia, and Bahia, and all the friends I made in the states.

- Gescher Lab – You always took me in as one of your own, making me feel at home (and even giving me your home, thanks Edi!!) every single day I spent in Germany, and for that, I thank all the group. More than collaborators I made friends, I always had fun and I could always be myself and for that, I thank you, Miri and Laura, which names I will never be able to pronounce correctly (but I'll keep trying). To you, Johannes I thank the encouraging words and the way you always make people feel special and needed! I'll keep waiting for you to take the train to Lisbon!

- Dynamic Structural Biology Lab – For all the mutual help we share, and for being our treasured neighbors ever since the beginning when it was just Marta. I thank Tiago N. Cordeiro and Hugo Monteiro for their help with the System I project. especially thank Guillem Hernadez for the help in all moments and for always being available.

- Control of Gene Expression Lab – Agradeço aos membros do laboratório por sempre me fazerem sentir bem-vinda (mesmo quando vou só cravar coisas) e receberem sempre com carinho e um sorriso na cara. À professora Cecília Arraiano tenho tanto que agradecer, a forma como

consegue sempre enaltecer os alunos, como se sente orgulhosa de nós, da Maria por ter ganho um prémio ainda na barriga, pelo carinho com que sempre me tratou, a mim e à Maria, pela sua preocupação e tantas outras coisas… Agradeço por ter aceite de braços abertos a nossa ideia de trabalhar com *bolA*s e se ter desde sempre disponibilizado para ajudar e transmitir o seu valioso conhecimento na área. À Cátia Bárria agradeço ter-me ensinado tudo o que sabia sobre quantificação de Biofilmes. Agradeço também à Inês J. Silva, Susana Barahona e Ana Alves da Silva terem-me ensinado extração de RNA, RT-PCR e swimmings e pelo seu envolvimento e dedicação neste trabalho.

À minha comissão de tese, Dr. Carlos Salgueiro e Dr. Teresa Catarino pelas divertidas e interessantes reuniões de comissão de tese. Por me "espremerem" e desafiarem, como eu tanto gosto e dessa vossa maneira tão característica.

To my Juri, I thank the time spent on my thesis and all the feedback.

To the person reading this thesis, I thank your time and interest in my work, I hope you enjoy it!

Publications

Silva, A.V., Firmino, M.O., Costa, N.L., Louro, R.O., Paquete, C.M. (2022) "Investigation of the Molecular Mechanisms of the Eukaryotic Cytochrome-*c* Maturation System". Biomolecules 2022, 12, 549. DOI:10.3390/biom12040549

Silva A.V., Edel M., Gescher J., Paquete C.M. (2020) "Exploring the Effects of *bolA* in Biofilm Formation and Current Generation by *Shewanella oneidensis* MR-1", Frontiers in Microbiology DOI: 10.3389/fmicb.2020.00815

Paquete C.M., Rusconi G., **Silva A.V.**, Soares R., Louro R.O.(2019) "A brief survey of the "cytochromome"", chapter 3 in "Advances in Microbial Physiology" edited by Robert K. Poole. DOI: 10.1016/bs.ampbs.2019.07.005

Louro R.O., Costa, N.L., Fernandes A. P., **Silva A.V.**, Trindade I.B., Fonseca B. M., Paquete C.M.(2019) "Exploring the Molecular Mechanisms of Extracellular Electron Transfer for Harnessing Reducing Power in METs: Methodologies and Approaches", Chapter 2.2 in "Microbial Electrochemical Technology Sustainable Platform for Fuels, Chemicals and Remediation A volume in Biomass, Biofuels and Biochemical" edited by S. Venkata Mohan, Sunita Varjani and Ashok Pandey. DOI: 10.1016/B978-0-444-64052-9.00010-8

Silva A.V., Louro R.O.(2017) "Biomolecular NMR Assignment: Illustration Using the Heme Signals in Horse Cytochrome *c*", Journal of Chemical Education. DOI: 10.1021/acs.jchemed.7b00123

In preparation

Silva A.V., Edel M., Soares R., Louro R. O., Gescher J., Paquete C.M. "Exploring the Effects of IbaG in Biofilm Formation and Current Generation by *Shewanella oneidensis* MR-1"

Silva A.V., Costa N.C., Veríssimo A.F., Hernandez G., Monteiro H., Cordeiro T.N., Paquete C.M., Daldal F., Louro R.O. "Maturation of Class II cytochromes *c* does not follow the paradigm proposed for Class I"

Resumo

Os sistemas bioeletroquímicos (BES) são uma plataforma altamente sustentável e versátil para a produção de energia, tratamento de águas residuais, bioremediação ambiental, bioeletrosíntese e biosensores, tendo emergido como uma energia alternativa de baixa pegada ambiental. Como tal, o seu interesse económico, político e científico tem vindo a aumentar, em particular nas últimas duas décadas, quando o problema de sobrepopulação e a crise energética ganharam espaço nas agendas sociais e políticas no mundo e, em particular, na Europa.

Existem diferentes implementações para estas tecnologias, no entanto o seu mecanismo central é comum e assenta na capacidade inata de alguns microrganismos, chamados organismos eletroativos, de acoplar ao seu metabolismo o transporte de eletrões para o interior e/ou exterior da célula. Em particular, a capacidade destes organismos de formar biofilme eletroativos (EAB) na superfície do elétrodo, e de produzir citocromos *c* multihémicos (MHC), são processos chave para o estudo e otimização dos BESs.

A bactéria *Shewanella oneidensis* tem sido estudada ao longo dos anos como um organismo modelo para o desenvolvimento de BES. Esta bactéria halotolerante, anaeróbia facultativa, caracterizada pela sua coloração rosada, é geneticamente manipulável, fácil de cultivar e manter em condições laboratoriais e bem caraterizada em termos dos processos de transferência eletrónica extracelular (EET). A capacidade de este organismo formar EAB é também conhecida e considerada importante para a produção de corrente, com a maior capacidade de produção de biofilme associada à maior produção de corrente.

Os citocromos *c* são definidos pela ligação covalente entre o hemo e a cadeia polipeptídica. Atendendo à sua diversidade, foram divididos em quatro classes, numa divisão baseada na análise das suas sequências. Devido à

ligação covalente que os caracteriza, os citocromos *c* não são formados espontaneamente na natureza, e sistemas de maturação específicos são necessários. Foram descritos três sistemas de maturação principais, sendo o Sistema I (Ccm) e o Sistema III (CcHL) os mais prevalentes na natureza. O Sistema I é o mais complexo, envolvendo 8 a 9 proteínas, dependendo do organismo. Este é o sistema presente em α- e γ-proteobactérias, bem como em algumas β- e δ-proteobactérias, Archaea, deinococci e nas mitocôndrias de plantas e algas vermelhas. Em contraste, o Sistema III é o mais simples, com apenas uma proteína essencial para o seu funcionamento. Este Sistema está presente nas mitocôndrias da maioria dos organismos eucariontes, exceto as plantas.

A primeira parte desta tese é dedicada aos sistemas de maturação de citocromos *c*. Com o objetivo de perceber a maturação dos citocromos *c* da Classe II pelo Sistema I, foram estudadas as interações entre o apocitocromo *c*' e os seus parceiros fisiológicos. Foram examinadas, por NMR e Uv-visível, a interação do apocitocromo *c*' com hemina, porfirina de zinco e proteína CcmI (pertencente ao Sistema I). As características estruturais do apocitocromo *c*' foram também exploradas usando NMR, CD e SAXS. Os resultados mostram que as ligações covalentes entre as cisteínas e o hemo não são formadas espontaneamente *in vivo,* nas condições reportadas para os citocromos *c* da Classe I, ou em qualquer das várias condições testadas. Esta observação, em conjunto com a presença de elementos de estrutura secundária na forma apo da proteína, evidenciam as diferenças no processo de maturação dos citocromos *c* de Classe I e Classe II

A fim de explorar os mecanismos de reconhecimento do Sistema III, o citocromo *c* tetrahémico bacteriano STC, de *S. oneidensis* foi mutado de forma a ser convertido num substrato para o Sistema III, que não o reconhece naturalmente. O objetivo inicial deste trabalho, para além de perceber os mecanismos de reconhecimento do Sistema III, seria melhorar a produção de MHCs pelos organismos eletroativos, ao expressar um Sistema de

maturação mais eficiente. No entanto, os resultados obtidos demonstram que, sendo possível converter o MHCc bacteriano em substrato para o Sistema III, este Sistema, ao contrário do Sistema bacteriano, não é capaz de inserir mais de um hemo por cadeia polipeptídica. Assim, foi possível concluir que a presença da sequência de reconhecimento não é o único fator para a maturação por Sistema III, sendo que a localização desta sequência desempenha também um papel importante.

A segunda parte desta tese é dedicada ao estudo da formação de biofilme por *S. oneidensis* MR-1. Neste contexto, o fator de transcrição *bolA*, anteriormente identificado como central na formação de biofilme por outros organismos, com a sua sobrexpressão levando a aumentos significativos na produção de biofilme, foi objeto de estudo. O efeito deste gene na formação de biofilme e produção de corrente foi explorado em *S. oneidensis* MR-1. Os resultados demonstram que a sobrexpressão deste gene leva ao aumento da produção de biofilme e, consequentemente, a mais produção de corrente. Esta informação é importante para a otimização de organismos eletroativos, no sentido da sua aplicação prática em BESs.

Como seguimento deste trabalho, o segundo gene pertencente à família *bolA*, *ibaG,* foi estudado, bem como os seus efeitos na formação de biofilme e produção de corrente. Os resultados indicam que, apesar da sua homologia e semelhança estrutural prevista, estas proteínas apresentam diferentes modos de ação, produzindo efeitos diferentes na formação de biofilme e produção de corrente. Mais estudos são necessários para a exploração dos mecanismos de regulação de biofilme em *S. oneidensis* MR-1, no sentido da otimização dos processos que ocorrem em BESs.

No geral, este trabalho contribui substancialmente para o conhecimento existente sobre bactérias eletroativas, fornecendo informação relevante em dois processos chave na transferência eletrónica para elétrodos: a maturação de citocromos *c* e a produção de biofilme.

Abstract

Bioelectrochemical systems (BES) are a highly sustainable and versatile platform for electricity production, wastewater treatment, environmental bioremediation, bioelectrosynthesis, and biosensing, emerging as an alternative energy source of low CO_2 footprint. The economic, political, and scientific interest in these technologies has been increasing, particularly in the last two decades, when the global population and energy crisis increased, and the need for a circular economy became a concern in the political and social agendas throughout the world and particularly in Europe.

Different implementations of this technology exist but the central mechanism is common and relies on the innate capability of some microorganisms, known as electroactive organisms, to link their metabolism with the transport of electrons in and out of the cell. In particular, the electroactive biofilm (EAB) formed at the electrode surface and their ability to produce multiheme cytochromes *c* (MHC), are key for the understanding and optimization of BES.

S. oneidensis is a halotolerant, facultative anaerobe characterized by its pinkish color that has been studied over the years as a model organism for the development of BES. It is genetically tractable and easy to manipulate, and its extracellular electron transfer (EET) chain is well studied and characterized, containing a multitude of MHC. The ability of this organism to form EAB is described and was shown to be important for current generation, with thicker biofilms being associated with more current production.

Cytochromes *c* are defined by the covalent bond between the heme cofactor and the polypeptide chain. Due to their diversity, at the beginning of the 1980s, cytochromes *c* were divided into four classes based on sequence analysis. Due to the covalent bond that characterizes them, cytochromes *c* are not spontaneously formed in nature and a dedicated maturation system is required. Three main maturation systems have been described in the literature, being System I (Ccm) and System III (CcHL) the most prevalent.

System I is the most complex maturation system, involving 8 or 9 membrane-associated proteins, depending on the organism. This system is present in α- and γ-proteobacteria, in Archaea, in deinococci, and in the mitochondria of plants and red algae, as well as in some β- and δ-proteobacteria. System III is the simplest maturation system, with only one protein essential for the process. System III is present in the mitochondria of most eukaryotic organisms, except in plants.

In the first part of the thesis, to address the Class II cytochrome *c* maturation by System I, the interactions between apocytochrome *c*' and its physiological binding partners were addressed. Interactions with CcmI and hemin were investigated by NMR and UV-visible spectroscopy and the structural features of apocytochrome *c*' were explored by NMR, SAXS, and CD spectroscopies. Results show that covalent bonds between cysteines and the heme are not spontaneously formed *in vitro*, in the conditions that were reported for Class I cytochromes *c*. This finding, together with the presence of secondary structural elements in the apo form of the protein, highlight the differences in the maturation process of Class I vs Class II cytochromes *c*.

To explore the recognition mechanisms of maturation System III, the bacterial tetraheme cytochrome STC from *S. oneidensis* MR-1, which is not a native substrate for System III, was mutated to be identified as a substrate. The original aim of this work was to improve the electroactive organisms' ability to produce MHCs by expressing a more efficient maturation system while addressing its recognition mechanisms. The results obtained show that it is possible to convert a bacterial cytochrome in a substrate for CcHL, but the presence of the recognition sequence is not the only factor that induces the maturation of a holocytochrome by System III. The location of this sequence in the polypeptide also plays a role in the maturation of the cytochrome *c*. Furthermore, CcHL appears to be able to catalyze the binding of only one heme per polypeptide chain, being unable to assemble multiheme cytochromes *c*, in contrast with bacterial maturation systems.

The second part of this thesis is dedicated to the study of biofilm formation by *S. oneidensis* MR-1. In this scope, the transcription factor *bolA,* previously identified as a central player in biofilm formation in other organisms, with its overexpression leading to increased biofilm, was studied. The effect of this gene on biofilm formation and current production by *S. oneidensis* MR-1 was explored. Results demonstrate that an increased biofilm formation and consequent current generation was achieved by the overexpression of this gene. This information is important to optimize electroactive organisms toward their practical application in METs.

As a follow-up of this work, the second *bolA* family gene present in the *S. oneidensis* MR-1 genome, *ibaG*, was addressed and its effects on biofilm formation and current generation were studied. Results indicate that despite their homology and predicted structural similarity, these proteins have different modes of action, producing different effects on current generation and biofilm production. More studies are needed to explore the mechanisms of biofilm regulation in *S. oneidensis* MR-1 towards the optimization of processes taking place in BES.

Altogether, this work significantly contributes to the existing knowledge regarding electroactive bacteria, providing relevant information on two key points regarding electron transfer to electrodes: cytochrome *c* maturation and biofilm formation.

Abbreviations

1D – One-dimensional

2D – Two-dimensional

3D – Three-dimensional

Abs - Absorbance

ATP - Adenosine triphosphate

BES – Bioelectrochemical Systems

BLAST – Basic Local Alignment Search Tool

BLASTp – Protein Basic Local Alignment Search Tool

CARA – Computer-aided resonance assignment

CcHL – Cytochrome *c* heme lyase

Ccm – Cytochrome *c* maturation

CD – Circular dichroism

DAP - Diaminopimelic acid

DDM - n-Dodecyl-β-D-maltoside

DNA – Deoxyribonucleic acid

DTT - 1,4-Dithiothreitol

EAB – Electroactive Biofilm

EDTA - Ethylenediamine tetraacetic acid

EET – Extracellular electron transfer

EPS – Extracellular polymeric substances

FAD - Flavin adenine dinucleotide

HCCS – Holocytochrome *c* synthetase

His tag – 6-Histidine tag

HPLC – High pressure liquid chromatography

HSQC – Heteronuclear Single Quantum Coherence

IDP – Intrinsically disordered protein

IPTG - Isopropyl β-D-1-thiogalactopyranoside

IUPAC-IUB – International union of pure and applied chemistry - International union of biochemistry

LB – Luria Bertani

MALDI - Matrix-assisted laser desorption/ionization

MEC – Microbial Electrolysis cell

MEGA - Molecular Evolutionary Genetics Analysis

MES – Microbial Electrosynthesis

MET – Microbial electrochemical technology

MFC – Microbial Fuel Cell

MHC – Multiheme cytochrome *c*

MLS - Microphthalmia with linear skin defects

NCBI - National Center for Biotechnology Information

NMR – Nuclear magnetic resonance

OD – Optical density

PCR – Polymerase chain reaction

PDB – Protein data bank

qPCR – quantitative polymerase chain reaction

RT-PCR – Reverse transcriptase polymerase chain reaction

RBS – Ribosome binding site

RNA – Ribonucleic acid

SAXS - Small-angle X-ray scattering

SDS-PAGE – Sodium dodecyl sulfate polyacrylamide gel electrophoresis

SEC – Size exclusion chromatography

SHE – Standard hydrogen electrode

STC – Small tetraheme cytochrome

TB – Terrific Broth

Tris – Tris(hydroxymethyl)-aminomethane

TOF – Time of flight

UV – Ultra-violet

WT – Wild type

Table of contents

List of figures

List of tables

Chapter I

General introduction

Parts of this chapter were published as book sections where the author of this thesis is a co-author: Louro et al., 2019 and Paquete et al., 2019

1. *Bioelectrochemical systems*

At the beginning of the 20th century, the ability of microorganisms to produce electricity was reported (Potter, 1911), a concept that was explored in the forthcoming years, leading to the creation of the first Microbial Fuel Cell (MFC) (Davis and Yarbrough, 1962; Sisler, 1962; Davis, 1963). This technology emerged as a highly sustainable and versatile platform for electricity production, wastewater treatment, environmental bioremediation, bioelectrosynthesis, and biosensing. Ever since, the economic, political, and scientific interest in the technology has been increasing, particularly in the last two to three decades, when the global population and energy crisis increased, and the need for a circular economy became a concern in the political and social agendas throughout the world and particularly in Europe (United Nations, 2015; Schröder, Harnisch and Angenent, 2015; Hernandez and Osma, 2020).

With the advances in several domains of research and the development of different types of reactors with distinct applications, diverse terminology and classifications were proposed. In 2015 a standardization of the classification was suggested (Schröder, Harnisch and Angenent, 2015). From here, the term BES (Bioelectrochemical Systems) is proposed to designate these types of technology. Three main BES can be distinguished from the literature (**Figure I-1**):

Microbial Fuel Cell (MFC) – designed for the chemical conversion of organic matter into electricity production, these devices are used for wastewater treatment and sensing of toxic chemicals. In this type of technology, electroactive microorganisms transfer electrons to the anode (Schröder, Harnisch and Angenent, 2015; Logan *et al.*, 2019).

Microbial Electrolysis Cell (MEC) – designed for the electrochemical production of hydrogen (Logan *et al.*, 2019). In these devices, electroactive organisms transfer electrons to the anode in the presence of small input

power. The most commonly used substrate is acetate, glycerol, glucose, and cellulose with wastewater as a substrate. Additionally, electrotrophs in the cathode can receive these electrons from the electrode via an external circuit and generate CH_4 (Azwar *et al.*, 2015; Mallick *et al.*, 2022).

Microbial Electrosynthesis (MES) - MES is the execution of microbially catalysed electrochemical reactions to transform a substance into a desired product (Schröder, Harnisch and Angenent, 2015). In these systems, microorganisms located at the cathodic side, are used to catalyze the production of complex compounds from an organic waste using a power supply (Schröder, Harnisch and Angenent, 2015; Hernandez and Osma, 2020).

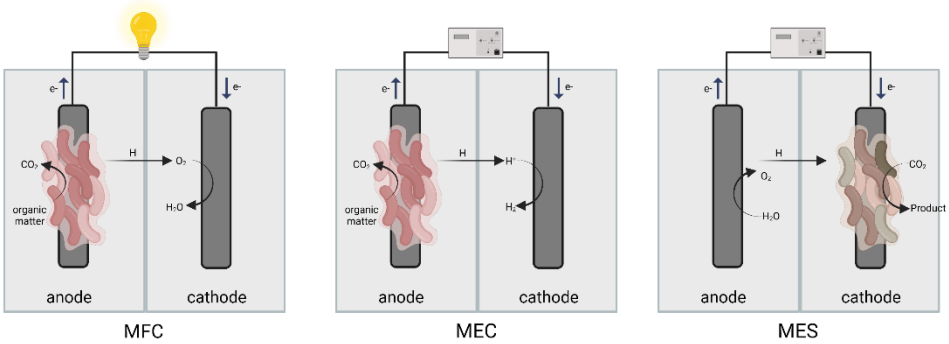

Figure I-1: Schematic representation of the different types of BES.

The central mechanism in these technologies is the innate capability of some microorganisms, known as electroactive organisms, to link their metabolism with the transport of electrons in and out of the cell. The biofilm formed at the electrode surface by electroactive organisms is referred to as electroactive biofilm (EAB) (Chiranjeevi and Patil, 2020) and it is one of the most important biological processes taking place in BES. The primary reason for EAB formation is the use of the electrode as an electron acceptor or donor by microbes to fulfill their respiratory or metabolic needs (Chiranjeevi and Patil, 2020). It has been shown that the increase in biofilm formation by methods such as protein overexpression (Liu *et al.*, 2015), the artificial production of

biofilms by exoelectrogen immobilization (Yu *et al.*, 2011), self-assembled graphene oxide - *S. oneidensis* MR-1 biofilm (Yong *et al.*, 2014) and 3D printing (Zajdel *et al.*, 2018; Freyman *et al.*, 2019) lead to significant increases in current densities, highlighting the potential of EAB study and manipulation for BES optimization.

For most electroactive organisms, extracellular insoluble electron donors or acceptors are typically metallic minerals in their natural environment, or, in BES, electrodes of diverse chemical nature, including carbon (Gralnick and Newman, 2007; Koch and Harnisch, 2016). This process is denominated extracellular electron transfer (EET) (Gralnick and Newman, 2007) and can be found in a broad diversity of organisms in nature, including Gram-positive and Gram-negative bacteria, Archaea, and even some Eukaryotes (Li *et al.*, 2015; Koch and Harnisch, 2016; Lea-Smith *et al.*, 2016). Electroactive organisms can exchange electrons with electrodes through two distinct modes (**Figure I-2**):

1. Indirect electron transfer where soluble electron shuttles mediate electron transfer between microbes and the electrode (Newman and Kolter, 2000; Hernandez, Kappler and Newman, 2004; Marsili *et al.*, 2008; Von Canstein *et al.*, 2008)

2. Direct electron transfer:

- Through cellular appendages, such as pili or nanowires, which enable EET at great distances by forming a physical connection between the microbe and the solid electrode surface (Reguera *et al.*, 2006; Pirbadian *et al.*, 2014)
- Through redox proteins, mainly multiheme cytochromes *c* (MHCs) present at the cell surface (Richardson *et al.*, 2012; Liu *et al.*, 2014)

Microorganisms may employ one or more of the above mechanisms to perform EET. Indeed, it was shown that the combination of different EET

pathways enhances electron transfer rates in BES (Rabaey *et al.*, 2004; Lies *et al.*, 2005; Fredrickson *et al.*, 2008). Despite the different mechanisms for electron transfer, it is now well recognized that MHCs are the key players in EET pathways of electroactive organisms belonging to nearly all phyla (Carlson *et al.*, 2012; Richardson, Fredrickson and Zachara, 2012; Sydow *et al.*, 2014; Shi *et al.*, 2016; White *et al.*, 2016).

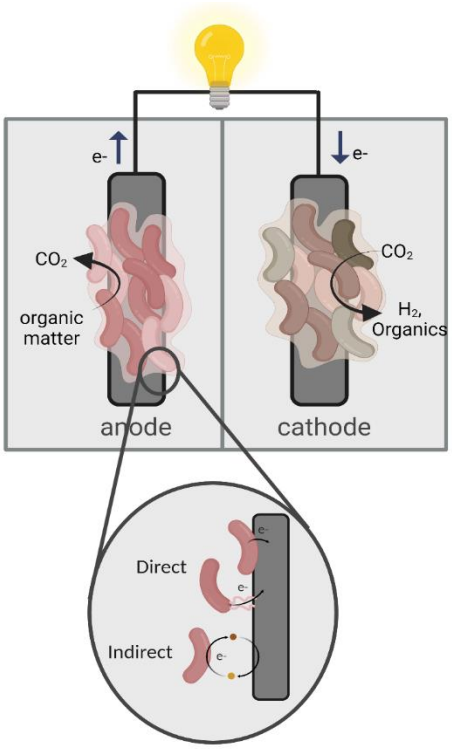

Figure I-2: Schematic representation of BES and EET mechanisms.

Despite the interest and importance of developing BES, the real-life application of these technologies is still incipient (Holtmann and Harnisch, 2019; Mohan, Varjani and Pandey, 2019; Hernandez and Osma, 2020; Jadhav *et al.*, 2021; Peñacoba-Antona *et al.*, 2022). This highlights the need for the continuation of the study and optimization of the processes underlying these technologies. This thesis aims to fulfill some of the current knowledge gaps by studying the fundamental process of cytochrome *c* maturation and

addressing the electroactive biofilm formation in the scope of increasing current production. Most of the knowledge obtained so far for EET processes comes from detailed studies on the Gram-negative metal-reducing organisms G*eobacter sulfurreducens* and *Shewanella oneidensis* MR-1 (Shi *et al.*, 2016; White *et al.*, 2016), which are considered the model organisms for the study of BES. The model organism *S. oneidensis* MR-1 was chosen as the focus of this thesis.

Shewanella oneidensis MR-1

The first reports of *Aeromonas putrefaciens MR-1* date to the late 1980s, when the bacteria were first isolated from lake Oneida in NY as a Manganese-reducing bacterium (Myers and Nealson, 1988). The genus was renamed in 1985 as *Shewanella* (MacDonell and Colwell, 1985), and the species *Shewanella oneidensis* was described in 1999 (Venkateswaran *et al.*, 1999). This was also the year when this species was first shown to produce electricity in the absence of exogenous mediators (Kim *et al.*, 1999).

Taxonomically, the *Shewanella* genus is a member of the class Gammaproteobacteria, order Alteromonadales, and family Shewanellaceae. The genus is composed of Gram-negative, motile, and rod-shaped bacterial species (Venkateswaran *et al.*, 1999; Satomi, 2014). These bacteria are ubiquitous in natural environments, occurring mainly in marine environments, iced fish, proteinaceous foods, and occasionally clinical samples (Satomi, 2014).

S. oneidensis is a halotolerant, facultative anaerobe characterized by its pinkish color and optimal growth temperature of around 30 ºC (Venkateswaran *et al.*, 1999). In what regards EET, it has been shown that *Shewanella oneidensis* MR-1 can employ several electron transfer modes. While the presence of outer membrane cytochromes allows direct electron transfer by contact, the presence of electron shuttles improves the rate of electron transfer to an electrode (Marsili *et al.*, 2008; Baron *et al.*, 2009; Ross,

Brantley and Tien, 2009; Coursolle *et al.*, 2010). Moreover, nanowires in conjugation with outer-membrane cytochromes are essential for high levels of current production (Reguera *et al.*, 2005, 2006; Gorby *et al.*, 2006; Pirbadian *et al.*, 2014).

S. oneidensis MR-1 has been extensively studied over the years and it became a model organism for the study of electroactive organisms and the processes underlying BES. It is easy to grow and maintain in laboratory conditions, it is genetically tractable and easy to manipulate, and protocols are available for heterologous and homologous protein expression (Heidelberg *et al.*, 2002; Sydow *et al.*, 2014; Chiranjeevi and Patil, 2020; Zhao *et al.*, 2021). In these studies, two critical processes have been identified for the generation of electrical current: the production of multiheme cytochromes *c* and biofilm formation. These two processes are, therefore, the focus of this thesis.

2. *Cytochromes c*

Initially referred to as “histoaematins”, the observation of cytochromes started in the 1800s, when MacMunn detected the presence of a red cell pigment not related to any decomposition product of hemoglobin in animal heart muscles (MacMunn, 1884). Histoaematins were defined at that time as respiratory pigments. The observations were controversial, as other specialists argued that these pigments were derived from hemoglobin (Hoppe-Seyler, 1890), and eventually the concept was dismissed.

The pigments were rediscovered and the name “cytochrome” was proposed by Keilin in 1925 (Keilin, 1925), as the author felt that the previous names were misleading. The name aimed at meaning just “cellular pigment” as its composition was not determined at the time. Keilin also described that these pigments were more widespread in nature than previously thought, being found also in unicellular organisms, including yeast and bacteria. In this work,

some of the spectroscopic properties of the pigment were also revealed and the presence of the heme was identified (Keilin, 1925).

The heme co-factor is the core catalytic unit of cytochromes. It is a derivative of the tetrapyrrole ring protoporphyrin IX, containing an iron ion centrally coordinated by four Nitrogen atoms in the ring plane (**Figure I-3**). In addition to the square planar coordination, axial ligands can be bound to the heme iron leading to square pyramidal or octahedral coordination (Paquete *et al.*, 2019).

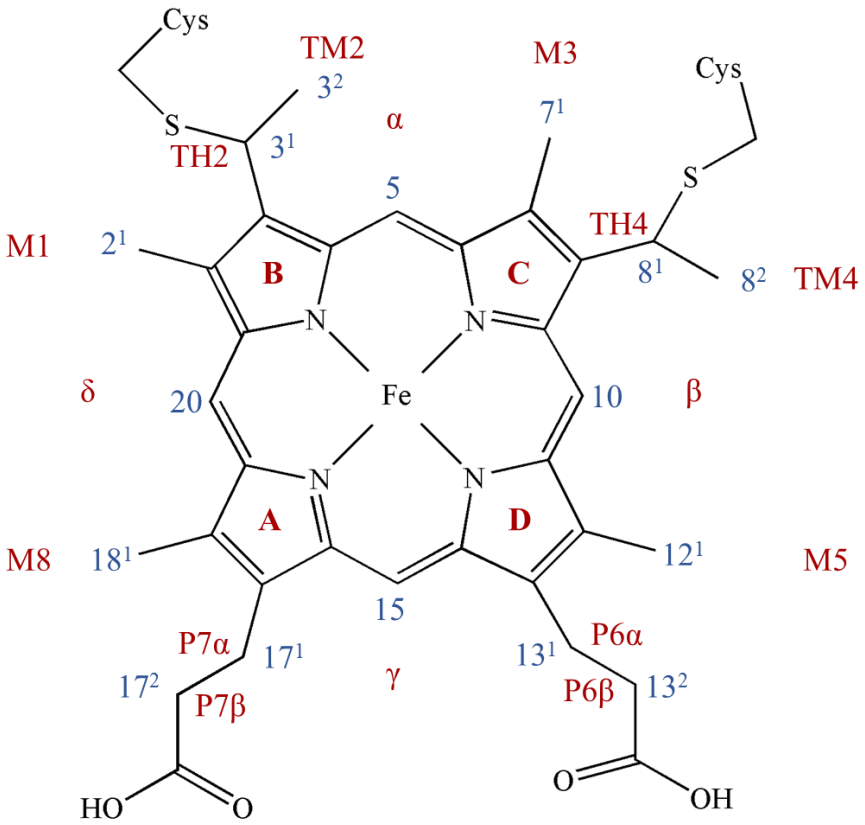

Figure I-3: Representation of a heme *c* with peripheral substituent designated according to the IUPAC (blue) and Fisher nomenclature (red). A-D: Fischer nomenclature of the pirrole rings.

The covalent bond of the heme to the polypeptide chain defines a cytochrome *c*. There are typically two thioether bonds that are formed between the beta pyrrole carbons 3^1 and 8^1 to cysteine side chains (**Figure I-3**). The biological advantages of having a covalently bound heme span from the prevention of heme loss, as the covalent bound is not easily broken, to the single possibility for heme orientation, contrary to what happens in cytochromes-*b* where the heme can be found in different orientations (Paquete *et al.*, 2019). Furthermore, the covalent bond allows for cytochromes *c* to have no constraints in the number of hemes that can be bound to a polypeptide chain, due to the removal of statistical thermodynamic constraints. This feature is partially responsible for the diversity found in this protein family with a single polypeptide chain having up to 113 hemes (Leu *et al.*, 2020).

The diversity of cytochromes *c* led to the need for the division in classes. Surprisingly, the division proposed by Ambler in 1982 (Ambler, 1982) still holds, despite the tremendous advances in genetic and protein analysis tools (**Figure I-4**). This classification divides cytochromes *c* into four classes mainly based on sequence analysis:

Class I – includes cytochromes *c* that contain a single N-terminal heme-binding site originally with a Methionine residue as the sixth ligand, although other coordination options are now known (Costa, Santos and Turner, 1996). Class I was subdivided into 5 subclasses (A-E) according to further sequence characteristics. Generally, cytochromes *c* belonging to this class are globular, soluble, and small, although exceptions may apply. An example of this class of cytochromes is the cytochrome c_2 from *Rhodobacter capsulatus* (**Figure I-4A**).

Class II – defined by the heme binding site located near the C-terminus. These cytochromes *c* form a four-helical bundle fold and can be further divided into two groups. Type IIa displays high-spin cytochromes *c* with histidine ligated heme and an open distal coordination position, while type IIb

cytochromes have hemes with octahedral coordination and low-spin configuration. The cytochrome *c*' from *R. capsulatus* is an example of this class of cytochromes *c* (**Figure I-4B**).

Class III – characterized by the presence of more than one heme-binding site in the polypeptide chain. Originally, also defined by the low redox potential and bis-histidine coordination, although nowadays it is known that a multitude of coordination options and redox potentials can be found in nature (Paquete *et al.*, 2019). An example of this class is the small tetraheme cytochrome *c* (STC) from *Shewanella oneidensis* MR-1 (**Figure I-4C**).

Class IV – identified by the presence of additional co-factors, other than the heme(s) *c*. An example is the FAD cofactor in the case of flavocytochrome *c* from *S. oneidensis* MR-1, which contains four *c*-type hemes and a FAD cofactor (**Figure I-4D**).

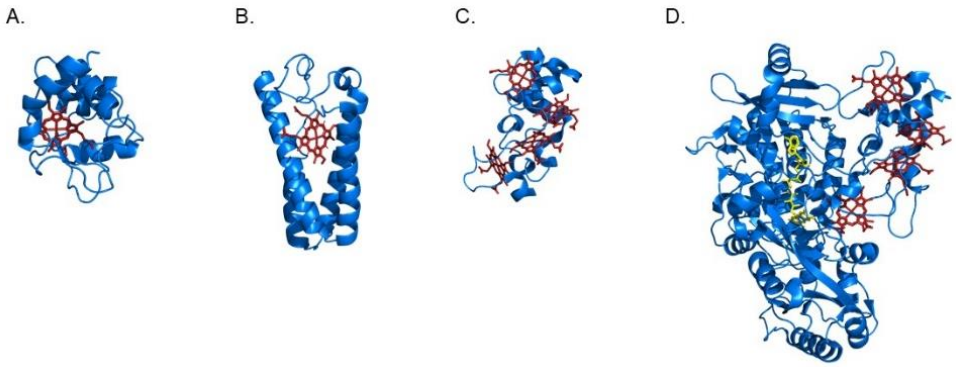

Figure I-4: Examples of *c*-type cytochromes belonging to the different classes. The 3D structure is represented as blue cartoon; hemes are represented as red sticks; FAD is represented as yellow sticks. **A.** cytochrome c_2 from *R. capsulatus* as representation of Class I (PDB: 1C2R), **B.** cytochrome *c*' from *R. capsulatus* as representation of Class II (PDB: 1RCP), **C.** STC from *S. oneidensis* MR-1 as representation of Class III (PDB: 1M1P) and **D.** flavocytochrome *c* from *S. oneidensis* MR-1 as representation of class IV (PDB: 1Y0P).

In terms of BES, Class III and IV cytochromes are the most relevant. Although not all electroactive organisms contain MHCs (Sturm *et al.*, 2012), they were proposed to:

1. create a conductive transport pathway that links intracellular electron carriers (e.g., NADH and quinones) with the bacterial cell surface for electron exchange with electrodes in METs (Carlson *et al.*, 2012; Fonseca *et al.*, 2013; Dantas *et al.*, 2014; Sturm *et al.*, 2015);
2. exchange electrons with the electrode in a direct (Richardson *et al.*, 2012; Liu *et al.*, 2014) or mediated mode (Marsili *et al.*, 2008; Coursolle *et al.*, 2010); and
3. play a crucial role in direct interspecies electron transfer allowing electrochemical communication with other bacterial cells within biofilms (Rotaru *et al.*, 2014; Lee *et al.*, 2017).

MHCs are also involved in catalytic reactions, namely in nitrite and sulfite metabolism (Paquete *et al.*, 2019).

3. *Cytochrome c maturation systems*

The attachment of the heme to the apocytochrome (cytochrome without the heme) does not occur spontaneously in Nature. Due to the covalent bond that characterizes cytochromes *c*, specific enzymatic machinery, known as maturation systems, are necessary for this to occur. Several maturation systems have been described in detail, being Systems I, II, and III the most widely accepted (**Figure I-5**). Other than these, Systems IV, V, and VI, which are mainly variations of the three main systems designed for single cysteine bonds, have also been identified (see Kranz *et al.* 2009; Mavridou, Ferguson, and Stevens 2013 for reviews on maturation systems). Systems I and III are the focus of this work due to their broad prevalence and involvement in health and bioelectrochemistry.

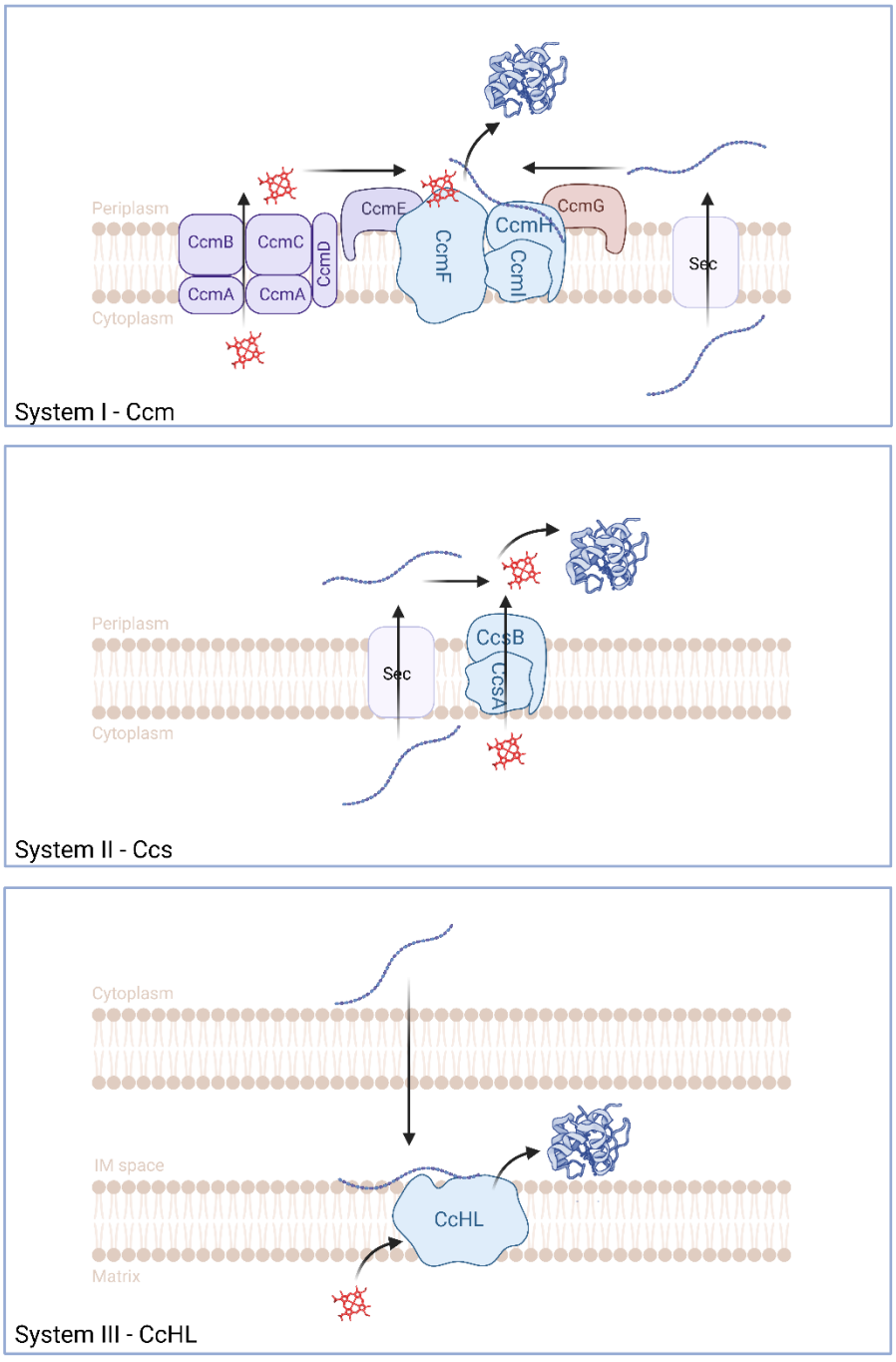

Figure I-5: Schematic representation of cytochrome *c* maturation systems.

System I

System I or Ccm (cytochrome *c* maturation) is the most complex maturation system, involving 8 or 9 membrane-associated proteins, depending on the organism. This system is present in α- and γ-proteobacteria, in Archaea, in deinococci, and in the mitochondria of plants and red algae, as well as in some β- and δ-proteobacteria (Kranz *et al.*, 2009; Verissimo and Daldal, 2014). The components of System I are divided into three functional modules:

(i) Module 1 is responsible for the transport of the heme to the periplasm and loading it to the chaperone CcmE. This module is composed of the complex CcmABCD and CcmE. Of these proteins, only the structure of CcmE is known (Arnesano *et al.*, 2002). In this module, CcmA is the only component of System I located in the cytoplasmic side of the inner membrane and has a typical ATP-binding region (Verissimo and Daldal, 2014; Shevket *et al.*, 2018). CcmB and C are integral membrane proteins that are essential for the membrane location of CcmA. Studies of the transfer of the heme from CcmCD to CcmE (Shevket *et al.*, 2018; Sutherland, Jarodsky, *et al.*, 2018) show that firstly, CcmE binds to CcmCD, facilitating the capture of the heme. Then, CcmAB promotes the detachment of the heme from CcmCD to CcmE. It was also shown that CcmE can only attach the heme covalently when in complex with CcmC.

(ii) Module 2, composed of CcmG and CcmH, is responsible for maintaining the apocytochrome in the reduced state so that it is ready for heme binding. The structures of the soluble parts of these two proteins are available (Edeling *et al.*, 2002; Ouyang *et al.*, 2006; Di Matteo *et al.*, 2007, 2010; San Francisco, Sutherland and Kranz, 2014). From there, it was possible to confirm that these two proteins act as thiol-oxidoreductases to maintain the apocytochrome reduced in the oxidizing environment of the periplasm.

(iii) Module 3 is responsible for the ligation of the heme to the apocytochrome for the final release of the holocytochrome *c* (Verissimo and Daldal, 2014).

This module is composed of the complex CcmFHI, which means that CcmH is part of both modules 2 and 3. Module 3 is responsible for the crucial step of attachment of the heme to the polypeptide chain of the apocytochrome (the lyase activity). In some organisms, like the model enterobacterium *E. coli*, CcmI does not exist as a separate protein but as a subunit of CcmH. When present separately, CcmI is a bipartite protein, with the different subunits performing distinct functions: recognizing and chaperoning the apocytochrome and maintaining it in the proper redox state for ligation (Di Silvio *et al.*, 2013). CcmF is a *b*-type monoheme cytochrome, presumed to be the site where the thioether bonds are formed between the heme and the apocytochrome. Moreover, its heme is proposed to be involved in the reduction of the *c*-type heme in the nascent holocytochrome *c* (San Francisco, Sutherland and Kranz, 2014; Verissimo and Daldal, 2014).

System III

System III is the simplest maturation system, with only one protein essential for the process, CcHL (cytochrome *c* heme lyase) (Dumont *et al.*, 1987; Verissimo *et al.*, 2012), also called HCCS (holocytochrome *c* synthetase) (Babbitt *et al.*, 2017). CcHL is predicted to be a soluble membrane-associated protein with 170 to 289 residues (depending on the organism). System III is present in the mitochondria of most eukaryotic organisms, except in plants (Babbitt *et al.*, 2015). This enzyme, unlike Systems I and II, is only capable of producing Class I cytochromes, defined as mono-heme and low-spin (Ambler 1982, see **Chapter I.1**). This is the least understood maturation system and only recently, the study of CcHL was made possible due to the advances in scientific techniques and a 4 step model for the functioning of the System was proposed (Babbitt *et al.*, 2015). According to this model, the first step is the heme binding to lyase. Then, it binds the apocytochrome *c* (step 2) and the thioether bonds are formed (step 3). The final step of the process is the release of the maturated cytochrome *c*.

Consensus recognition sequences have been identified for both humans (San Francisco, Bretsnyder and Kranz, 2013) and yeast (Verissimo *et al.*, 2012) CcHL. The amino acids in these sequences were shown to be essential for the recognition and subsequent heme attachment by lyase. Despite the acknowledged importance of System III, the enzyme and its recognition mechanisms were never fully characterized.

4. *Biofilm formation*

Biofilms were formally described in the middle 1980s and are defined as aggregates of microorganisms that are attached to each other and/or to interfaces or surfaces (Flemming *et al.*, 2016; Edel, Horn and Gescher, 2019). These cell aggregates are viscoelastic as they are embedded in a matrix of extracellular polymeric substances (EPS) consisting of multiple carbohydrate polymers as well as proteins and nucleic acids that keeps them together (Edel, Horn and Gescher, 2019). Biofilms are one of the most widely distributed and successful modes of life on Earth as microorganisms in biofilms become protected by the matrix, more efficient in capturing resources, differentiated and able to cooperate, and more resistant and tolerant to antibiotics and other antimicrobial agents and to harsh environmental factors and immune response by a host (Chew and Yang, 2016; Flemming *et al.*, 2016).

In most cases, biofilm formation is viewed as a negative process, as it is associated with persistent infections in plants and animals (including humans), the contamination of medical devices and implants, biofouling, water contamination, and corrosion (Flemming *et al.*, 2016). However, in the case of BES, biofilm formation is a key process to enhance current generation, predominantly due to very high biomass concentrations and the possibility to operate the reactors continuously over long periods of time (Edel, Horn and Gescher, 2019). Given the importance of this process in general and for energy production in BESs in particular, it is one of the focuses of this thesis.

Chapter II

Methodology and techniques

1. *Cloning and expression*

Vectors

Successful recombinant protein production always starts with the choice of the vector and host system for expression. In this work, all the vectors utilized were built from constructs that were made available by collaborators. When appropriate, the procedure of site-directed mutagenesis was used to insert mutations in the available plasmids. Detailed information can be found in chapters **III**, **IV**, **V**, and **VI**.

The plasmid pAV6 was available in the Daldal Lab, a collaborator in this project. This plasmid originated from the plasmid pET-3a, where the T7 promoter region was replaced by a DNA fragment encoding LacI and the *tac* promoter region to produce iso-2-cytochrome *c* of *Saccharomyces cerevisiae*. An N-terminal StrepTag II (IBA) was also inserted in the plasmid originating pCS905 (Sanders, Wethkamp and Lill, 2001). This plasmid was later altered to express a Strep-tag II fused GFP (Sanders *et al.*, 2008). This gene is replaceable by cloning any gene of interest in frame into NdeI and BamHI restriction sites, allowing the screening for positive clones by fluorescence (Sanders *et al.*, 2008). The replacement of the GFP by *Rhodobacter capsulatus* cytochrome *c*' originated the plasmid pAV6 (Verissimo, Shroff and Daldal, 2015). This plasmid was used in **Chapter III** for the study of cytochrome *c*' and to produce CcmI.

The plasmid pBTR1 was a kind gift from Dr. Irene Diaz-Moreno. This plasmid originated from pUC18, in which the yeast cytochrome *c* heme lyase (CYC3) and cytochrome *c* (CYC1) were cloned to produce a mitochondrial cytochrome *c* using a bacterial expression system (W. B. Pollock *et al.*, 1998). Later, this construct was used for the expression of isotopically labeled (^{15}N) cytochrome *c*, which allowed the NMR assignment of this protein (Morar *et al.*, 1999). The construct was then used to successfully express horse and human cytochrome *c*, representing an easy and inexpensive way to obtain virtually any mitochondrial cytochrome *c* (Patel, Lind and Pielak, 2001;

Olteanu *et al.*, 2003). In this work, this plasmid was used in **Chapter IV** for the expression of all STC variables using System III. The plasmid pET21a was used to clone the *cctA* gene, encoding for STC (Alves *et al.*, 2017), this plasmid was used for the production of STC mutants using System I.

The plasmid pEC86 represented a breakthrough in the study of cytochromes *c*, as it allows *E. coli* to express the proteins from the Ccm machinery under aerobic conditions (Arslan *et al.*, 1998). The co-transformation with this plasmid allows the heterologous expression of cytochromes *c* with their native system, obtaining high protein yields and reliable expression. This plasmid has been widely used ever since in works that use *E. coli* for bacterial cytochrome *c* expression (see Louro *et al*. 2019 for a detailed review). It is interesting to note that the development of pEC86 was simultaneous to the expression of mitochondrial cytochrome *c* in *E. coli* with pBTR1. This means that from 1998, the scientific community was suddenly able to express both bacterial and mitochondrial cytochrome *c* in *E. coli*, using their native maturation system. The pEC86 plasmid was used for the expression of all cytochromes *c* using System I (**Chapter III** and **Chapter IV**)

Host systems

In all cases mentioned above, the vectors were developed for the use in *E. coli*, as this is the most frequently used microorganism for protein overexpression. The reason for this is the several advantages that this species holds, that range from rapid growth on inexpensive substrates achieving high cell density to fully sequenced genome, characterized metabolic pathways, and availability of mutant host strains (Chen, 2012; Rosano *et al.*, 2014; Rosano, Morales and Ceccarelli, 2019).

Particularly, the strain BL21(DE3) emerged as the preferred host for recombinant protein production (Rosano, Morales and Ceccarelli, 2019). *E. coli* strains belonging to the B line present faster growth rates due to the lack of flagella; produce less acetate which helps to maintain a suitable pH during

growth; lack proteases, which can extend the lifetime of recombinant proteins; and have superior secretion capabilities which can yield better results than having the protein in the cytoplasm (Rosano, Morales and Ceccarelli, 2019). This bacterial strain was used in **Chapter III** and **Chapter IV**.

Although not so common, the *E. coli* strain JM109 (DE3) has also been widely used as an expression system, particularly for cytochromes *c* (Pitts *et al.*, 2003; Echalier *et al.*, 2008; Alferov *et al.*, 2009; Fonseca *et al.*, 2012; Díaz-Moreno *et al.*, 2014; Neto *et al.*, 2014; Paquete *et al.*, 2014; Costa *et al.*, 2015). This strain was developed for high-level gene expression from the T7 promoter and it lacks the *E. coli* K restriction system, which means that there is no undesirable restriction of cloned DNA or recombination with host chromosomal DNA (Promega). Moreover, the endonuclease A– mutation leads to an improved yield and quality of isolated plasmid DNA (Promega). This bacterial strain was used in **Chapter III** and **Chapter IV**.

The bacterial growth conditions were optimized for the needs of each experiment. Based on previous work made with the same combination of strain/vector, conditions like growth medium and temperature or the need for induction were tested. More detailed information can be found in the corresponding chapters.

2. *Protein purification*

Affinity chromatography

Following expression, the choice of the purification method arises. The constructs pAV6, pAS1, and pCP, used in this work, were built for affinity purification. The known advantages of affinity purification include simple purification with usually a maximum of two purification steps, the possible detection of the tag instead of the target protein using antibodies, and the possible increase in protein stability and solubility (Razdan, 2000). However, some setbacks like the tag affecting protein structure, folding and biological

activity may occur and need to be considered. The main properties of the affinity tags used in this study are summarized in **Table II-1**.

Several tags are available, being the most common the 6-histidine tag (hereon referred to as His-tag). Histidine-tagged proteins have a high affinity for Ni^{2+} and other metal ions, that can be immobilized on chromatographic media. Generally, the tagged protein is the strongest binder among all the proteins in a protein extract, although it is common that other histidine-rich proteins also bind to the column with less affinity. The His-tag is small and usually less disruptive than other tags to the properties of the target protein, often eliminating the need for tag removal (detailed information can be found in Razdan 2000). The most common disadvantage of using the His-tag is that often the protein is not eluted with a high degree of purity. This is especially true for metalloproteins, as the metallic center and their ligands may interfere with the purification process (Razdan, 2000).

The Strep-tag®II (heron referred to as Strep-tag) represents a major improvement in what regards protein purity. The basis for the development of the Strep-tag® system is the well-known natural binding of biotin to streptavidin. To take advantage of this very strong interaction, the peptide Trp-Ser-His-Pro-Gln-Phe-Glu-Lys was found as capable of binding to the biotin-binding pocket of streptavidin (IBA, 2020). This peptide was named Strep-tag®II. The properties of streptavidin have also been engineered to optimize the binding of the peptide to the resin being the final product the Strep-Tactin® resin (IBA, 2020). Different resins were also developed for the different applications, using biotin or desthiobiotin as an eluent. The result is a highly robust system for one-step purification of tagged proteins that in most cases does not interfere with structural and functional studies and, therefore, does not have to be removed from the target protein after purification (Razdan, 2000). This purification method was used in **Chapter III**.

Table II-1: Summary of the characteristics of the affinity tags used in this work. Adapted from *Razdan 2000*

Tag-specific characteristics	His-tag	Strep-tag
Compatible expression systems	Any expression system	Any expression system
Metabolic burden to host	Low	Low
Yield after purification	High	High
Purity in a single step	Relatively high purity	Extremely high purity
Effect on solubility of protein	Does not enhance	Does not enhance
Purification scale	Any scale	Any scale
Affinity tag removal	May not need	May not need
Tag detection	Antibodies available	Antibodies available
Elution conditions	Mild	Very mild
Effect on protease action	No effect	No effect
Effect on folding	Minimal effect	Minimal effect
Effect on structure and function	Not likely	Not likely
Suitability for metalloproteins	Not recommended	Yes

Ion exchange chromatography

In the cases where no tag is available on the construct, or in the less common case that the protein, even having the tag, does not bind to the column, the common first step in purification is ion-exchange chromatography. Ion-exchange chromatography separates biomolecules according to differences in their net surface charge. It is one of the most frequently used techniques for the purification of proteins, peptides, nucleic acids, and other charged biomolecules, offering high resolution and group separations with high loading capacity, reason why it is frequently used as a first purification step (Bahadir, 2013; Cytiva, 2021).

The method takes advantage of the fact that the relationship between net surface charge and pH is unique for a specific protein. This promotes reversible interactions between charged molecules and oppositely charged

column resin that are controlled to favor the binding or elution of specific molecules (Cytiva, 2021). At a pH equivalent to its isoelectric point (pI), a protein has no net charge, and will not interact with charged resin. However, at a pH above the pI, the protein will have negative net charge and therefore bind to a positively charged resin (anionic-exchange chromatography). Alternatively, at a pH below the pI, the protein will be positively charged, binding to negatively charged resin (cation-exchange chromatography).

The choice is then based on which type of exchanger and pH give the desired resolution within the constraints of sample stability. The Q-sepharose medium is a strong anion exchanger that uses quaternary ammonium (Q) as functional group ($-CH_2-N^+-(CH_3)_3$) (Bahadir, 2013; Cytiva, 2021). It is the recommended medium for the first purification step of proteins with pI below 7 or unknown and was therefore chosen for the purification of the proteins used in this thesis when affinity tags were not available (**Chapter III** and **Chapter IV**).

Size exclusion chromatography

Typically, as a last step in the purification process, size exclusion chromatography, also called gel filtration, is often used. This is a highly versatile technique, suitable for any type of proteins and a wide variety of conditions. In this case, proteins are separated by size as they pass through the column. This means that contrary to the other types of chromatography, buffer composition does not directly affect peak separation and no elution buffer is used. Consequently, a significant advantage is that conditions can be varied to suit the requirements for further analysis or storage without altering the separation.

To perform the separation, a porous matrix resin composed of chemically and physically stable spherical particles is packed into a column (Cytiva, 2020). These particles have properties to minimize the adsorption of biomolecules. The packed bed is equilibrated with a buffer that fills both the particles and the space between them with liquid. When the sample is applied to the

column, molecules that are larger than the pores in the matrix cannot enter the matrix and pass directly through the column, being the first to elute. Molecules with partial access to the pores of the matrix, such as lower molecular weight proteins, are separated and eluted from the column in order of decreasing size.

The specific volume at which a given protein will be eluted from the column can be predicted according to the size of the column and the matrix being used. The selectivity of a size-exclusion resin is an inherent property of the matrix. The Superdex 75 Increase resin (GE Healthcare) has a particle size of approximately 9 µm and a fractionation range from 3 to 70 KDa (Cytiva, 2020). It was therefore the chosen matrix for this work and was used in **Chapter III** and **Chapter IV**.

3. *NMR spectroscopy*

Nuclear Magnetic Resonance (NMR) Spectroscopy is one of the most powerful techniques for the study of biomolecules. It can be used for a wide range of applications including structural determination, molecular interactions, and metabolomic analysis (Bertini, I.; McGreevy, K. S.; Parigi, 2012). NMR is widely used and particularly relevant for the study of metalloproteins, including cytochromes *c*.

Like any other spectroscopy, NMR takes advantage of the interaction between electromagnetic radiation and matter to obtain information on the sample being analyzed. Based on their nuclear spin, some nuclei will assume a preferential orientation when subjected to an external homogeneous magnetic field (Keeler, 2005). In practical terms, NMR spectroscopy can be performed on nuclei that have an odd number of protons or neutrons. Depending on the chemical nature of the nuclei, the chemical environment, and the strength of the magnetic field, the frequency of radiation absorbed by these nuclei will change, giving rise to the multiple applications of NMR (Trindade and Louro, 2020). The variation of the nuclear resonance

frequencies produces the chemical shift. ^{1}H is the most common element used in NMR experiments, mainly due to its high gyromagnetic ratio and natural abundance that allow simple experiments with optimal resolution and sensitivity.

NMR for intrinsically disordered proteins –protein assignment

Since the early days of the discovery of intrinsically disordered proteins (IDPs), it was clear that X-ray crystallography was not suitable for the study of the structural properties of these proteins and NMR arose as the most suitable alternative. NMR can give important information regarding macromolecular conformations and dynamics both at the very local (to the residue level) to global scales, making it extremely useful for the study of this type of proteins (Barrett *et al.*, 2013). To obtain this information, the protein must be isotopically labeled, using ^{15}N and ^{13}C as these elements occur in very low abundance in nature and are needed for the experiments described below. This is obtained by growing the expression strain in minimal medium containing labeled Nitrogen and/or Carbon sources followed by the regular protein purification method.

The first step to extract useful information from NMR spectra is the protein assignment. The basis of the assignment process is the two-dimensional (2D) $^{1}H^{15}N$ HSQC (Heteronuclear Single Quantum Coherence) spectrum. This experiment, first described by Bodenhausen and Ruben in 1980, is one of the simplest and most useful 2D pulse sequences and relies on the double transfer of polarization between two different nuclei (Bodenhausen and Ruben, 1980). The output spectrum has one peak corresponding to each unique proton attached to the heteronucleus being considered, which is usually ^{15}N or ^{13}C.

Particularly, the ^{1}H ^{15}N HSQC is the most frequently recorded 2D experiment in protein NMR, as it gives a fingerprint of the protein that is being analyzed. This occurs because each residue of the protein (except for proline) has an

amide proton attached to a nitrogen in the peptide bond and will therefore yield a peak in the HSQC spectrum. Most of these peaks are located between 5 and 10 ppm in the ^{1}H dimension and between 105 and 130 ppm in the ^{15}N dimension (**Figure II-1**). Except for the peak of glycine that usually appears around 109 ppm in the ^{15}N dimension. However, in unstructured proteins, such as IDPs, the peak dispersion is smaller, and the peaks are often clustered in the region of 7.5 to 8.5 ppm in the ^{1}H dimension and overlapped, which makes the assignment process more challenging. Sidechains with nitrogen-bound protons also produce peaks, usually in characteristic regions of the spectra (**Figure II-1**). The sidechains of Arginine and Lysine have a nitrogen chemical shift that is usually outside the range of the spectrum (typically around 90 ppm) and their peaks are therefore folded and will appear as negative peaks in a region of the spectrum that does not correspond to their real chemical shifts, which are calculated from the experimentally measured spectral width. The assignment of the HSQC spectrum requires complementation with triple resonance experiments (3D). This need becomes more pressing for IDPs due to the severe peak overlap.

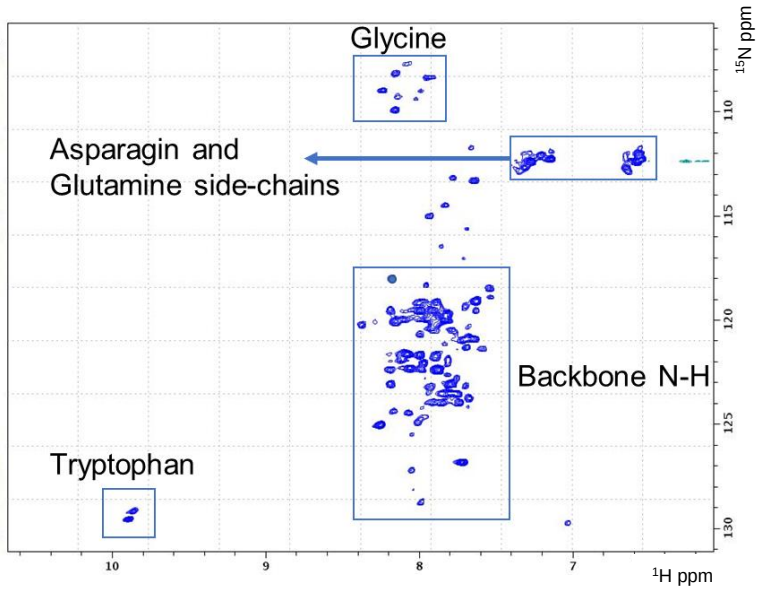

Figure II-1: Typical ^{1}H ^{15}N HSQC spectrum of a highly unstructured protein indicating the typical peak location. Image obtained using the Topspin 4.1.4 software (Bruker).

For the full backbone assignment of the protein, a set of 3D experiments must be conducted. A representation of the sequential peak assignment can be found in **Figure II-2**. The basis for this approach was developed by Kay et al. 1990. In their work, Kay and colleagues developed a set of assignment experiments that included HNCO and HNCA. After the HSQC, the HNCO is the spectrum to be analyzed, as the peaks in the HSQC must correspond to peaks in the HNCO, except for the sidechains. This experiment correlates the amide ^{1}H and ^{15}N shifts with the ^{13}C shift of the carbonyl resonance of the preceding amino acid (Kay *et al.*, 1990). This means that with this correlation we will be able to find the CO group of the amino acid preceding the NH in the HSQC (CO_{i-1}).

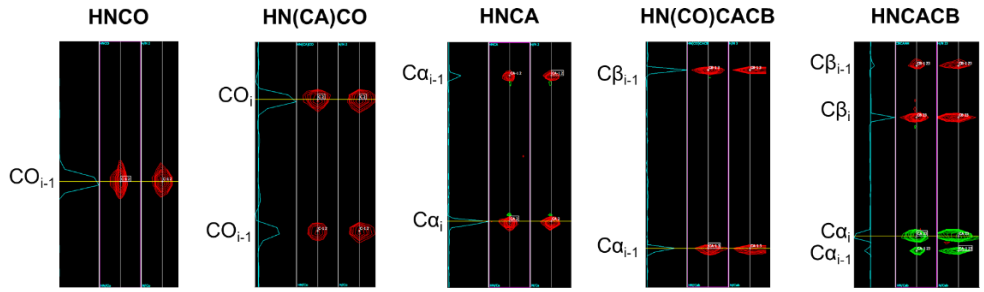

Figure II-2: Representation of sequential peak assignment using a set of 3D NMR experiments. Each panel represents a NH strip for a selected protein peak. Image obtained using CARA software.

The following experiment to look at is the HN(CA)CO. The HN(CA)CO was developed by Clubb, Thanabal, and Wagner in 1992 to improve the protein assignment process. Once again, peaks in the HSQC must correlate to the peaks in this spectrum, except for the sidechains. However, in this case, two peaks are visible in each NH strip. The stronger peak belongs to the carbonyl of the same residue (CO_i) and the weaker one belongs to the carbonyl of the previous residue (CO_{i-1}).

In theory, a set of HNCO and HN(CA)CO could provide a complete sequential assignment of the protein, however, due to spectral overlap, defects, and peak shielding, a more complete and redundant approach is advised. For that, the next spectrum to be analyzed is the HNCA. This spectrum correlates the intra-residue amide ^{1}H and ^{15}N shifts with the Cα chemical shift ($C\alpha_i$). In the same NH strip, this experiment provides a weaker correlation with the Cα of the preceding amino acid ($C\alpha_{i-1}$).

The next spectrum to look at is the HN(CO)CACB (or CBCA(CO)NH). This experiment correlates the amide ^{1}H and ^{15}N resonances of one residue simultaneously with both the $^{13}C\alpha$ and $^{13}C\beta$ resonances of its preceding residue ($C\alpha_{i-1}$ and $C\beta_{i-1}$) (Grzesiek and Bax, 1992b). The correlation with Cβ carbon was a breakthrough in the assignment process as it provides valuable

information by correlating the α with the β Carbons of the amino acid sidechain.

Finally, the last spectrum to analyze in this approach is the CBCANH (or HNCACB). This experiment correlates the amide ^{1}H and ^{15}N signals with both the intra-residue Cα and Cβ signals and with the Cα and Cβ of the preceding residue ($C\alpha_{i-1}$ and $C\beta_{i-1}$) (Grzesiek and Bax, 1992a). This means that in this spectrum, each NH strip contains four peaks and due to the experiment design, Cα peaks have an inverted phase when compared with the Cβ peaks.

These experiments will lead to a sequential correlation of the peaks, leading to the final protein assignment. Different software packages to aid the visualization and analysis of the different spectra and the correlation between them have been developed over the years. CARA (Computer Aided Resonance Assignment) was developed by Rochus Keller (Prof. Kurt Wüthrich's group) as part of his Ph.D. thesis and is a freeware available for all major platforms (Keller, 2004). CARA follows a semi-automatic approach causing a great increase in process efficiency and a decrease in error probability when compared to manual approaches.

The process described was followed for the protein assignment described in **Chapter III**. However, it is important to consider that assignment is not a strict protocol, and several approaches can be used. These approaches can rely on different combinations of spectra and different ways to go through them. However, they all have common features: the protein must be double labelled, the 3D experiments need to be done and the puzzle must be solved.

NMR for protein interactions – Chemical shift perturbation

NMR spectroscopy is again in focus when it comes to protein interactions. This is because this technique can not only detect these interactions but also probe the specific interacting regions and provide the determination of the dissociation constant. In the case of protein interactions, the determination of the binding region relies on the previous assignment of the protein peaks (see

Chapter II.3.i). Interaction studies followed by NMR spectroscopy rely on the fact that the chemical shifts of the nuclei are very sensitive to changes in their chemical environment (Louro *et al.*, 2019). In practical terms, this means that alterations in the spectra of the partners can be observed upon interaction. From these data, a full map of protein-protein or protein-ligand interactions can be obtained.

The main constant characterizing protein interactions is the dissociation constant, K_d. For the reaction of protein *P* binding reversibly to a ligand *L* at a single site:$P + L \leftrightarrow PL$

The dissociation constant *Kd* is equal to:

$$K_d = \frac{[P][L]}{[PL]}$$

Where $[P]$ and $[L]$ correspond to the equilibrium concentration of free protein and ligand, respectively, and $[PL]$ represents the equilibrium concentration of the complex. In practical terms, K_d can be thought of as the concentration of ligand and protein required to saturate half the binding sites (Williamson, 2013).

A key factor in determining NMR interactions is the exchange rate between the free and bound forms, more specifically the off rate k_{off} (Williamson, 2013). This is often referred to as the timescale of the interaction, relative to the NMR time scale. If the interaction is fast, the signals will shift gradually as the ligand is added, with the peak position at any titration point corresponding to the weighted average of free and bound shifts (**Figure II-3**). In contrast, if the interaction is slow, the signal of the unbound form will gradually disappear (lose intensity) as the signal of the bound form appears. The intensity of the two peaks reflects the concentration of free and bound protein (**Figure II-3**) (Williamson, 2013). Interactions in the slow regime are experimentally more challenging as intensity is often hard to determine with enough accuracy.

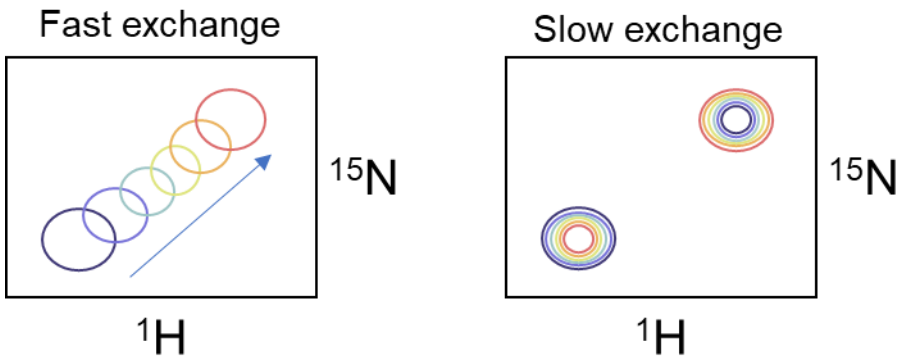

Figure II-3: Representation of ^{1}H ^{15}N HSQC peak change according to the exchange rate of interaction. Left – Fast exchange; Right – Slow exchange. Adapted from Williamson 2013.

The starting point for the protein interaction studies is, again, the ^{1}H ^{15}N HSQC of the target protein. The ligand or partner protein, which will be added to the experiment is not isotopically labelled and will, therefore, be invisible in the spectrum. This means that what the observer will see is the effect of the binding ligand or protein in the target, isotopically labelled, protein. This method is called chemical shift perturbation as it follows changes in the chemical shifts of a protein when a ligand is added and uses them to determine the location of the binding site, the affinity of the ligand, and the time-scale of the exchange regime (Williamson, 2013).

There are essentially two ways of performing these experiments. The most common is to have the target protein in the NMR tube and do a titration by adding increasing amounts of ligand in previously calculated molar ratios. In each addition, a new ^{1}H ^{15}N HSQC spectrum is collected and the peak position and intensity are recorded (Williamson *et al.*, 2006; Sugase, Dyson and Wright, 2007; Williamson, 2013). These data are then plotted, and the dissociation constant can be calculated for each residue by fitting the following equation:

$$\Delta\delta_{obs} = \frac{\Delta\delta_{max}\left\{([P]_t + [L]_t + K_d) - [([P]_t + [L]_t + K_d)^2 - 4[P]_t[L]_t]^{1/2}\right\}}{2[P]_t}$$

Where $\Delta\delta_{obs}$ is the change in the observed chemical shift and $\Delta\delta_{max}$ is the maximum shift change on saturation (often not measurable experimentally and obtained as part of the fitting). $[P]_t$ and $[L]_t$ are the total concentrations of protein and ligand, respectively (sum of the free and bound states). K_d is the dissociation constant (Williamson, 2013).

In 2002, Daltrop *et al*. presented the reconstitution of a cytochrome *c in vitro* using a different way of performing the interactions. In this study, as the interaction proved to be very slow, the authors combined a fixed ratio of protein to ligand and recorded the spectra (in this case UV-vis) at several time points. In this experiment, the kinetics of the reaction are followed instead of the dissociation constant. The same approach was used in a later work for the reconstitution of a different cytochrome *c* (Daltrop and Ferguson, 2003). Although these binding experiments were not conducted using NMR, the authors identify that as a weakness and justify with the instability of the protein at the required concentrations (Daltrop *et al.*, 2002). This means that the experiment could be adapted to be performed using NMR if the target protein is stable enough. In this thesis, interaction studies are presented in **Chapter III**.

4. *Mutant generation*

Predicting the effects of genetic modification is difficult due to the complexity of organisms and their metabolic networks (Wah Tang *et al.*, 2015). Gene deletion or gene knockout (represented with Δ) is a type of mutation that involves the total inactivation of a gene of interest through the loss of genetic material (Garrigues, Martínez-Reyes and de Vries, 2021). The deletion of a target gene, combined with its complementation, is one of the most powerful ways to address its effects *in vivo*. The requirements for the use of this

technique are simply a genetically tractable organism and a target gene. With the huge development of genetic techniques in recent years, the number of genetically tractable organisms is rapidly increasing, making this technique widely applicable. Gene deletion has been widely used for the confirmation of gene roles in different organisms, ranging from bacteria to fungi, plants, and animals, for the last two decades (Saltikov and Newman, 2003; Watanabe and Woodward, 2015; Cai and Xiao, 2021; Edel *et al.*, 2021; Garrigues, Martínez-Reyes and de Vries, 2021; Guzha *et al.*, 2022).

When using this technique, it is of utmost importance to check the effect of this deletion on the growth of the organism, as it can give important hints on viability and interference with the core metabolism which should not be affected. In other words, it is important to confirm that the growth has not been affected by a given deletion. The second key aspect when performing gene deletion assay is to perform a complementation mutant. To complement the Δ strain with the removed gene, usually using a plasmid containing this gene, allows the ultimate confirmation that the observed effect is a consequence of the deleted gene and not of the interference with the genome.

There are several methods described in the literature to perform gene deletion in bacteria. In this work, we used the suicide plasmid-based approach (Saltikov and Newman, 2003). In this technique, the flanking up- and downstream regions of the target gene are amplified and cloned into a suicide vector. The vector is then transformed in the *E. coli* WM3064 strain (a Diaminopimelic acid (DAP) auxotroph) and finally transferred to the target bacterial strain through conjugation. After a plasmid losing step, the mutants without the suicide vector are selected and the mutation is confirmed. Detailed information on the experimental conditions can be found in **Chapter V** and **Chapter VI**.

5. *Biofilm formation investigation*

Biofilm communities have properties that emerge in the biofilm that are not predictable from the study of free-living bacterial cells, making the study of this process of utmost importance (Flemming *et al.*, 2016). Given their importance, several methods have been developed to study biofilm formation. These can be divided into direct methods, mainly different microscopy techniques, and indirect methods, such as the Crystal Violet method, which is the one used in this thesis (**Chapter V** and **Chapter VI**)

The Crystal Violet method was developed in 1985 (Christensen *et al.*, 1985) and has been extensively used ever since. In the process, it suffered several adaptations and alterations until the protocol versions that are used nowadays and that have slight differences according to the microorganism in study (Xu *et al.*, 2016). This is a simple, fast, and inexpensive method that can be applied to microtiter dish assays, allowing for the assessment of biofilm formation on the wall and/or bottom of a microtiter dish. The high throughput nature of the assay makes it useful for genetic screens, as well as testing biofilm formation by multiple strains and/or various growth conditions (O'Toole, 2011). The limitations of the method are mainly the fact that the total biofilm is measured, and not the functional biofilm, as the crystal violet stains for all negatively charged surface molecules and extracellular matrix of polysaccharides (Xu *et al.*, 2016). The other limitation is that the environmental conditions are not mimicked. In the case of BES, the environment that cells are in when in contact with the electrode is not reproduced. For this reason, the complementation with other methods is a requirement, in this case, it is important to complement the biofilm formation assays with the current produced in BES, to confirm the results obtained.

6. *Bioelectrochemical systems*

To address current generation by different organisms and strains, it is important to have an optimized system that allows reproducible results to be obtained over time and across the different organisms in study.

Single chamber systems are simpler in their design and operation, however, they are usually less efficient (Logan *et al.*, 2006). In the case of small-scale, short-term laboratory experiments, they have the advantages of being well reproducible, and easy to set up, maintain and control and manipulate their variables (e.g temperature, working potential, strains, growth media). These characteristics make this system ideal for the study of the fundamental processes of EET.

In this work, the reactor described in Delgado *et al*. 2019 was used. In this setup, a three-electrode single chamber BES is used, containing a graphite felt working electrode (36 cm^2), a platinum counter electrode (1.25 cm^2), and an Ag/AgCl reference electrode (sat. KCl, 0.199 V vs. SHE). This set-up was used in **Chapter V** and **Chapter VI**.

Chapter III

Maturation of Class II cytochromes c does not follow the paradigm proposed for Class I

The author of this dissertation performed all the experiments described in this chapter, except for the SAXS experiments.

Abstract

Cytochromes *c* are ubiquitous proteins defined by the covalent bond between the heme cofactor and the polypeptide that are essential components of several metabolic processes. Four classes of cytochromes *c* have been described in the literature and the maturation of Class I cytochromes *c* has been achieved *in vitro* opening the possibility that *in vitro* maturation can be pursued for any class of cytochromes *c*. To verify this hypothesis, the maturation process of Class II cytochrome *c*' from *Rhodobacter capsulatus* was studied in this work.

The production of cytochrome *c*' in *E. coli* harboring the Ccm machinery allowed the confirmation that the protein is recognized and matured by this system. The interactions of this protein with its physiological binding partners CcmI and hemin were investigated by NMR and UV-visible spectroscopy and the structural features of the apo form were explored by NMR, SAXS, and CD spectroscopies. The results showed that covalent bonds between cysteines and the heme are not spontaneously formed *in vitro*, in the conditions that were reported for Class I cytochromes *c*. This finding, together with the presence of secondary structural elements in the apo form of the protein, highlights the differences in the maturation process of Class I vs Class II cytochromes *c*.

1. Introduction

Cytochromes *c* are ubiquitous proteins that are essential components of several metabolic processes such as respiration (Pettigrew and Moore, 1987; Nicholls and Ferguson, 2013), apoptosis (Jiang and Wang, 2004; Patriarca *et al.*, 2012), and extracellular electron transfer (Paquete *et al.*, 2019; Fonseca *et al.*, 2021). This class of proteins is defined by the covalent bond between the heme cofactor and the polypeptide chain via two (rarely one) thioether bonds to cysteine side chains (Dickerson, 1980; Pettigrew and Moore, 1987).

Four classes of cytochromes *c* have been described in the literature (Ambler, 1982). Briefly, Class I includes cytochromes-*c* that contain a single N-terminal heme-binding site. These are usually globular, soluble, and small (typically up to 15 kDa). Class II

is defined by the heme binding site located near the C-terminus, with the protein forming a four-helical bundle. Class III is characterized by the presence of more than one heme binding site and, finally, Class IV is identified by the presence of additional co-factors, other than the heme(s) *c*.

Cytochromes *c* are not spontaneously formed in nature. Instead, they require specific molecular machinery. To date, three main maturation Systems are described in the literature (Kranz *et al.*, 2009). In the scope of this work, we will only focus on System I. System I or Ccm (cytochrome-*c* maturation) is the most complex maturation system, involving 8 or 9 membrane-associated proteins, depending on the organism. These are divided into three functional modules that are responsible for heme transport to the periplasm (Module 1, composed by the complex CcmABCDE), maintaining the apocytochrome in the reduced state (Module 2, composed by the complex CcmGH), and catalyzing the formation of the covalent bond (Module 3, composed by the complex CcmFHI) (Kranz *et al.*, 2009; Verissimo and Daldal, 2014). This system is present in α- and γ-proteobacteria, in Archaea, in deinococci, and in the mitochondria of plants and red algae, as well as in some β- and δ-proteobacteria (Kranz *et al.*, 2009; Verissimo and Daldal, 2014).

Despite the complexity of System I, it was demonstrated that the covalent attachment of the heme to an apocytochrome could be achieved *in vitro* by the addition of ferrous heme to the apocytochrome under reducing conditions (Daltrop *et al.*, 2002; Daltrop and Ferguson, 2003). These results, achieved for Class I cytochromes *c*, left open the possibility of achieving the *in vitro* maturation for any class of cytochromes *c*. To investigate this possibility, the maturation process of Class II cytochrome *c*' from *Rhodobacter capsulatus* is addressed in the present study.

2. Materials and methods

Protein production

Apocytochrome c*'*

To produce apocytochrome *c*', the plasmid pAV6 (Verissimo, Shroff and Daldal, 2015), harboring the gene for the signal sequence-less and N-terminal Strep II-

tagged apocytochrome *c*' (RCC02682 corresponding to cycP) was transformed in *E. coli* BL21 (DE3) cells. The pre-inoculum was initiated from a single freshly transformed colony and grown overnight at 37 °C with shaking at 150 rpm in Luria–Bertani medium (LB) (Bertani, 2004) supplemented with 100 µg/mL ampicillin. For protein expression, cultures were diluted to an OD_{600} of 0.1 in LB with 100 µg/mL ampicillin and grown aerobically at 37 °C until an OD_{600} of 0.5 with shaking at 150 rpm. Cells were then induced using 1 mM IPTG and grown for 3 h in the same conditions. Cells were harvested by centrifugation at 10,000 x*g* at 4 °C for 10 min and frozen at -20 °C. The same procedure was followed to produce ^{15}N and ^{15}N ^{13}C labeled protein, where the LB media was replaced by ^{15}N and ^{15}N ^{13}C M9 media (Miller, 1972), respectively.

For protein purification, cells were defrosted and resuspended in 100 mM Tris-HCl buffer at pH 8.0, with 150 mM NaCl and 1 mM EDTA (Buffer W), supplemented with protease inhibitor cocktail (Roche, Basel, Switzerland) and DNase I (Sigma-Aldrich, St. Louis, MO, USA). Cell disruption was performed by passing the cells three times in a French Press at 1000 psi. The lysed cells were ultracentrifuged at 210,000 *xg* at 4 °C for 90 min, and the resulting soluble protein extract was purified using a 5 mL pre-packed Strep-Tactin column (IBA Lifesciences GmbH, Göttingen, Germany), previously equilibrated with Buffer W. The protein was then eluted using 100 mM Tris-HCl buffer at pH 8.0, with 150 mM NaCl, 1 mM EDTA, and 2.5 mM desthiobiotin (Buffer E).

Cytochrome c*'*

To produce cytochrome *c*', the *cycP* gene was amplified from the plasmid pAV6 (Verissimo, Shroff and Daldal, 2015) using primers 3 and 4 (Supplementary Table III-1) and fused to the signal peptide of *ompA*, amplified from the genome of *E. coli* BL21 (DE3) using primers 1 and 2 (Supplementary Table III-1). The fusion product was re-inserted in the pAV6 plasmid, previously digested with the restriction enzymes BamHI and NdeI (NZYTech, Lisboa, Portugal), yielding the plasmid pAV6SP. The plasmid was transformed in *E. coli* JM109 harboring the plasmid pEC86 (Arslan *et al.*, 1998) for expression of cytochromes *c*. Pre-inocula were initiated from a single

freshly transformed colony and grown overnight at 37 °C with shaking at 150 rpm in LB supplemented with 100 µg/mL ampicillin and 50 µg/mL chloramphenicol. For protein expression, cultures were diluted to an OD_{600} of 0.1 in Terrific Broth (TB) (Tartoff and Hobbs, 1987) with 100 µg/mL ampicillin and 50 µg/mL chloramphenicol and grown overnight aerobically at 37 °C. Cells were harvested by centrifugation at 10,000 x*g* at 4 °C for 10 min and frozen at -20 °C.

Cell disruption was performed by osmotic shock using a solution containing 20 mM Tris–HCl at pH 8.0, with 20% sucrose, 1 g/L of lysozyme, 0.5 mM EDTA, protease inhibitor cocktail (Roche, Basel, Switzerland), and DNase I (Sigma-Aldrich, St. Louis, MO, USA) according to the previously described protocol (Alves *et al.*, 2017). The lysate was incubated with shaking for 60 min at 4 °C. Cells were then ultracentrifuged at 210,000 *xg* at 4 °C for 90 min and dialyzed overnight against 20 mM Tris at pH 7.6. The resulting protein extract was loaded in a Q-Sepharose™ Fast Flow Column (GE Healthcare, Chicago, IL, USA) previously equilibrated with 20 mM Tris buffer at pH 7.6. The target protein was eluted at 15 mM of NaCl in the same buffer. Fractions containing the target protein were concentrated using centrifugal filter units (Millipore, Burlington, MA, USA) with a 3 kDa cut-off membrane. The same units were used to change the buffer to 20 mM phosphate buffer at pH 7.6 with 100 mM KCl. A second purification step was performed using a Superdex 75 size exclusion column (GE Healthcare, Chicago, IL, USA).

All chromatographic fractions were analyzed in 15% acrylamide SDS-PAGE gels. The gels with cytochrome *c*' were stained using heme staining (Goodhew, Brown and Pettigrew, 1986) and all gels were stained using BlueSafe (NZYTech, Lisboa, Portugal). Fractions containing the target protein were concentrated using centrifugal filter units (Millipore, Burlington, MA, USA) with a 3 kDa cut-off membrane. Protein integrity was verified by UV-visible spectroscopy and 1D ^{1}H NMR spectroscopy.

CcmI

To produce CcmI, the gene encoding the soluble fraction of the protein was inserted in the pCS1302 plasmid. First, the membrane-anchoring sequence was removed and

restriction sites for BamHI and NdeI were inserted in the gene. The gene coding for the soluble fraction of CcmI was then cloned in the pCS1302 plasmid, yielding plasmid pAS1. The plasmid was transformed in *E. coli* BL21 cells. Pre-inocula were initiated from a single freshly transformed colony and grown overnight at 37 °C with shaking at 150 rpm in LB supplemented with 100 µg/mL ampicillin. For protein expression, cultures were diluted to an OD_{600} of 0.1 in LB with 100 µg/mL ampicillin and grown aerobically at 37 °C until an OD_{600} of 0.5 with shaking at 150 rpm. Cells were then induced using 1 mM IPTG and grown overnight in the same conditions. Cells were harvested by centrifugation at 10,000 x*g* at 4 °C for 10 min and frozen at -20 °C.

For protein purification, cells were defrosted and resuspended in Buffer W supplemented with protease inhibitor cocktail (Roche, Basel, Switzerland) and DNase I (Sigma-Aldrich, St. Louis, MO, USA). Cell disruption was performed using a French Press by passing the cells three times at 1000 psi. The lysed cells were ultracentrifuged at 210,000 *xg* at 4 °C for 90 min, and the resulting soluble protein extract was purified using a 5 mL pre-packed Strep-Tactin column (IBA Lifesciences GmbH, Göttingen, Germany), previously equilibrated with Buffer W. The protein was then eluted using Buffer E. To increase protein purity, a second chromatographic step was conducted using a size exclusion chromatography. All chromatographic fractions were analyzed in 12% acrylamide SDS-PAGE gels. The gels were stained using BlueSafe (NZYTech, Lisboa, Portugal). Fractions containing the target protein were concentrated using centrifugal filter units (Millipore, Burlington, MA, USA) with a 5 kDa cut-off membrane. Pure proteins were revealed as a single band in the BlueSafe-stained SDS-PAGE gel (Supplementary Figure III-8).

Cell and membrane extracts

For the cellular extracts, *E. coli* JM109 cells harboring the pEC86 (Arslan *et al.*, 1998) plasmid were grown aerobically overnight at 37 °C in LB medium supplemented with 50 mg/L chloramphenicol. Cells were harvested by centrifugation at 10,000 x*g* at 4 °C for 10 min and frozen at -20 °C. Cells were washed in 50 mM potassium phosphate buffer at pH 7 supplemented with protease inhibitor cocktail (Roche,

Basel, Switzerland), DNase I (Sigma-Aldrich, St. Louis, MO, USA), and 5 mM DTT. Cells were then centrifuged at 10,000 x*g* for 10 min and resuspended in 50 mM potassium phosphate buffer (pH 7.0). From here, 100 µL of cell suspension were collected and used as cell extract. The remaining cell solution was ultracentrifuged at 210,000 *xg* for 60 min to separate the membrane fraction. The supernatant was removed, and the membranes were resuspended in 50 mM potassium phosphate buffer at pH 7.0 supplemented with 2 % DDM. The resulting extract was ultracentrifuged again at 210,000 *xg* for 60 min and the supernatant was used as the membrane fraction.

Stru*ctural characterization of apocytochrome c'*

SAXS

Synchrotron SEC-SAXS data were collected on the B21 Diamond Light Source beamline (Dicot, UK) using an in-line HPLC system (Shimadzu). A 45 µL sample with 10.0 mg/ml of apocytochrome *c*' was injected into a 4.6 ml Shodex 402.5-4F (Shodex) size exclusion column at a flow rate of 0.16 mL min^{-1}. The SEC mobile phase consisted of 20 mM potassium phosphate buffer at pH 7.4 with 200 mM NaCl at 20 °C. Two-second frames were acquired using a Pilatus 1M pixel detector (DECTRIS) at a sample-detector distance of 2.7 m and a wavelength of λ = 0.95 Å, covering a momentum of transfer range of $0.0032 < s < 0.44$ $Å^{-1}$. The scattering intensities from apocytochrome *c*' elution peak region (168-frames) were integrated, buffer subtracted, and averaged using the ScÅtter software (Didcot, UK) to produce the averaged SEC-SAXS profile. From this profile, the pair-wise distance distribution function, *P(r)*, was obtained by indirect Fourier Transform with GNOM using a momentum transfer range of $0.014 < s < 0.40$ $Å^{-1}$. The R_g values were estimated by applying the Guinier approximation in the range $s < 1.3/R_g$.

CD

The Far-UV CD spectrum of an 11 µM apocytochrome *c*' sample was recorded on a Jasco-815 spectrophotometer using a quartz cell with 1 mm path length. The CD spectrum is an averaged spectrum from 3 accumulations recorded at a scan speed of 50 nm/min, with 0.1 nm data pitch and 2 nm bandwidth in 20 mM potassium

phosphate buffer at pH 6.5 at 20 °C before and after a thermal denaturation study in the range of 5 to 95 °C in 5 °C steps.

NMR assignment

A sample of 70 µM uniformly double ^{15}N,^{13}C-labeled apocytochrome *c*' was prepared in 20 mM potassium phosphate buffer at pH 6.5 with 80 mM KCl. with 10 % $^{2}H_2O$ (99.9 atom %) added for locking. Small amounts of solid sodium dithionite were added to the sample in an argon atmosphere to obtain the fully reduced state of the protein. NMR experiments were performed at 15 °C on a Bruker Avance 800 MHz spectrometer equipped with a TCI cryoprobe. A set of double and triple resonance experiments was performed: ^{15}N-HSQC, HNCA, HNCO, HNCACO, HN(CO)CACB, HNCACB, and CBCANH. ^{1}H chemical shifts were calibrated using the water signal as internal reference and both ^{13}C and ^{15}N chemical shifts were calibrated through indirect referencing (Wishart *et al.*, 1995). All NMR spectra were processed using Topspin 4.1.1 software (Bruker Biospin, Karlsruhe, Germany). The software CARA (Keller, 2004) was used for the backbone assignment.

Protein interaction studies

NMR spectroscopy

The 2D ^{1}H,^{15}N HSQC NMR interaction studies were performed at 15 °C on a Bruker Avance 800 MHz spectrometer equipped with a TXI probe. ^{15}N apocytochrome *c*' and unlabelled Zn porphyrin, hemin, and CcmI samples were prepared in 20 mM potassium phosphate buffer (pH 6.5) with 80 mM KCl with the addition of 10 % $^{2}H_2O$ (99.9 atom %). Small amounts of solid sodium dithionite in an argon atmosphere were added to the samples to obtain the fully reduced state of the protein when stated. ^{15}N apocytochrome *c*' sample was titrated with CcmI to a final molar ratio of 0.6, and Zn porphyrin to a final molar ratio of 0.8. For the interactions with hemin, a fixed molar ratio of 2 was used. 2D ^{1}H,^{15}N HSQC NMR spectra were recorded with a sweep width of 13 kHz in F2 and 28 kHz for CcmI interactions, 36 kHz for Zn porphyrin interactions, and 26 kHz for hemin interactions in F1. 2048, 4096, and 1024 data points were collected in F2 for CcmI, Zn porphyrin, and hemin interactions, respectively. 128, 256, and 128 data points were collected in F1. 8 scans were

collected for CcmI, and hemin interactions, and 120 scans for Zn porphyrin interactions. The spectra were processed and analyzed using the Topspin 4.1.1 software from Bruker.

UV-visible spectroscopy under anaerobic conditions

The interaction between the apocytochrome *c*', hemin, CcmI, and cell extract containing the Ccm machinery were performed inside an anaerobic glove box (Coy Laboratory, model type B), using a UV–visible spectrophotometer (Shimadzu model UV-1800) to collect spectra in the range of 250–800 nm. A 1 mL cuvette was prepared using 50 mM potassium phosphate buffer (pH 7.0) with the target proteins and hemin at an approximate concentration of 10 µM. The components were kept in the reduced state by adding 5 mM DTT or sodium dithionite in the case of hemin. Experiments were performed with constant stirring and the temperature was kept at 15 °C using an external thermostatic bath.

3. Results and Discussion

Cytochrome c' is matured by System I

The production of cytochrome *c*' in *E. coli* cells harboring the Ccm machinery confirmed that this protein is recognized and matured by System I. UV-visible and NMR spectroscopy of the produced protein, show the typical features of a high spin monoheme cytochrome, as expected **Figure III-1** (Banci *et al.*, 1992; Monkara *et al.*, 1992; Caffrey *et al.*, 1995; Bertini *et al.*, 1998).

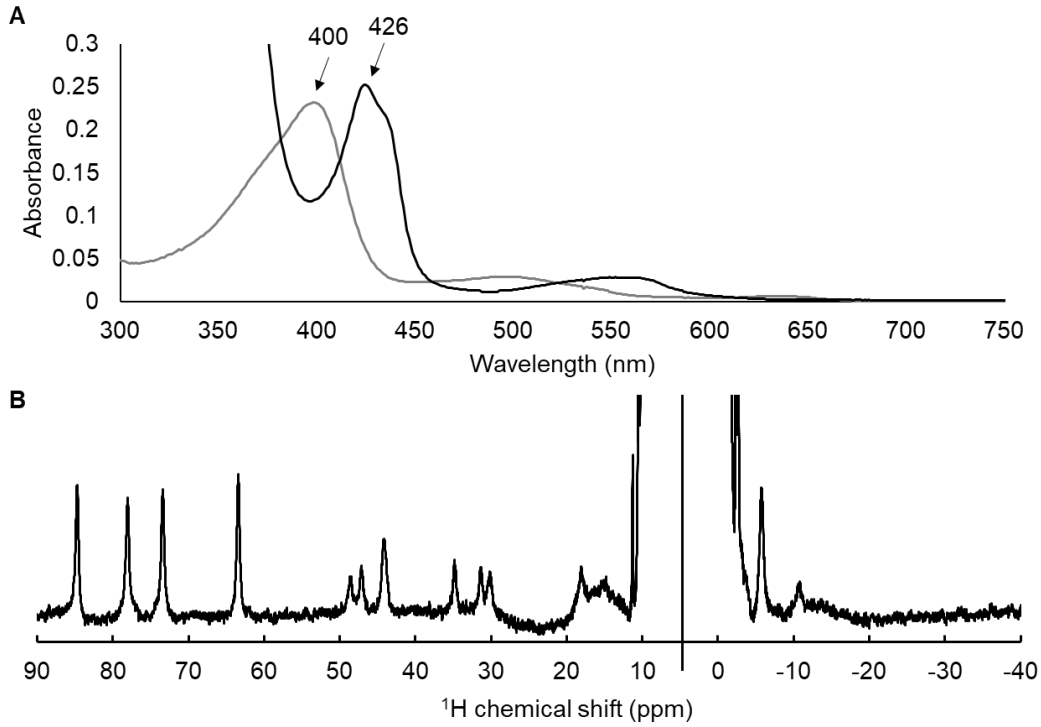

Figure III-1: Spectroscopic analysis of holocytochrome *c*'. **A.** Uv-visible spectra of reduced (black) and oxidized (grey) cytochrome *c*'. **B.** ^{1}H NMR spectrum of cytochrome *c*'.

Maturation of apocytochrome c' does not fit the paradigm established for Class I cytochromes c

To study the interaction process between apocytochrome *c*' and CcmI, 2D NMR spectroscopy was used. With the use of chemical shift perturbation, it is possible to follow changes in the chemical shifts of specific residues in a protein when a binding partner is added. With this information it is possible to determine the affinity and the location of the binding site, making NMR one of the more powerful techniques to study protein-protein or protein-ligand interactions (Williamson, 2013).

To address the *in vitro* maturation of apocytochrome *c*', the interaction with hemin was explored using the experimental conditions described in the literature (Daltrop

and Ferguson, 2003). Briefly, reduced hemin was added to reduced apocytochrome *c*' in a fixed ratio of 0.5 hemin to apocytochrome *c*'. The reaction was then monitored for 72 hours. **Figure III-2**, shows that no spectral changes were detected, indicating that an interaction between hemin and apocytochrome *c*' did not occur.

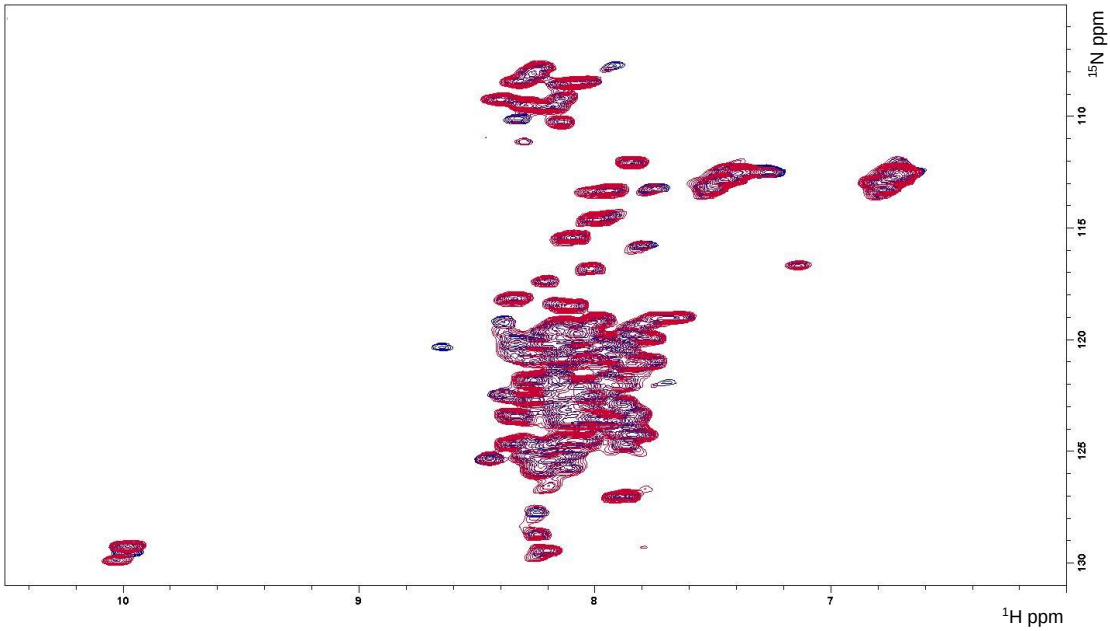

Figure III-2: ^{1}H-^{15}N-HSQC of apocytochrome *c*' in the absence (blue) and the presence (red) of hemin, in a ratio of 0.5 hemin to apocytochrome *c*' after 72 h of incubation.

To eliminate the paramagnetic effect of Iron on the NMR spectrum of the apocytochrome (Trindade *et al.*, 2022), Zn porphyrin was used instead of hemin. Different conditions were also tested, where increasing amounts of Zn porphyrin were added to apocytochrome *c*' to a final molar ratio of 0.8. Again, no interaction could be observed between the protein and the ligand (**Figure III-3**).

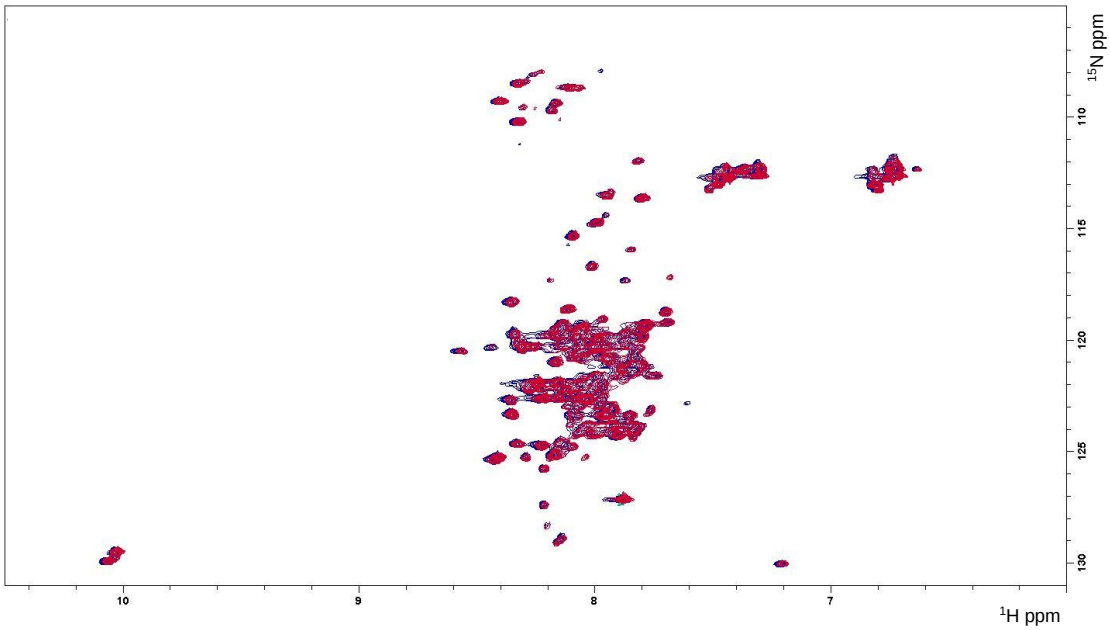

Figure III-3: ^{1}H-^{15}N-BEST-HSQC of apocytochrome *c*' in the absence (blue) and the presence (red) of Zn-porphyrin in a ratio of 0.8.

Following the mode of action of Ccm, the apocytochrome interacts with the enzymes from the functional module 3, to then receive the heme substrate (Verissimo and Daldal, 2014). To address this interaction, apocytochrome *c*' was titrated with increasing amounts of CcmI, and its NMR spectra were recorded after each addition (Figure III-4). It is possible to observe that some peaks broaden or shift after the addition of CcmI, with some of them disappearing from the spectrum. This indicates that an interaction occurs between the proteins. This is in accordance with the proposed role of CcmI as an apocytochrome chaperone (Verissimo *et al.*, 2011). However, no sign of induced folding is observed, since the peak dispersion is maintained throughout the experiment. The preliminary assignment of cytochrome *c*' (Supplementary **Table III-2**) allowed the identification of two interacting regions with CcmI in the protein. These regions are located in the first and second alpha helixes and in the same face of the protein (**Figure III-4**).

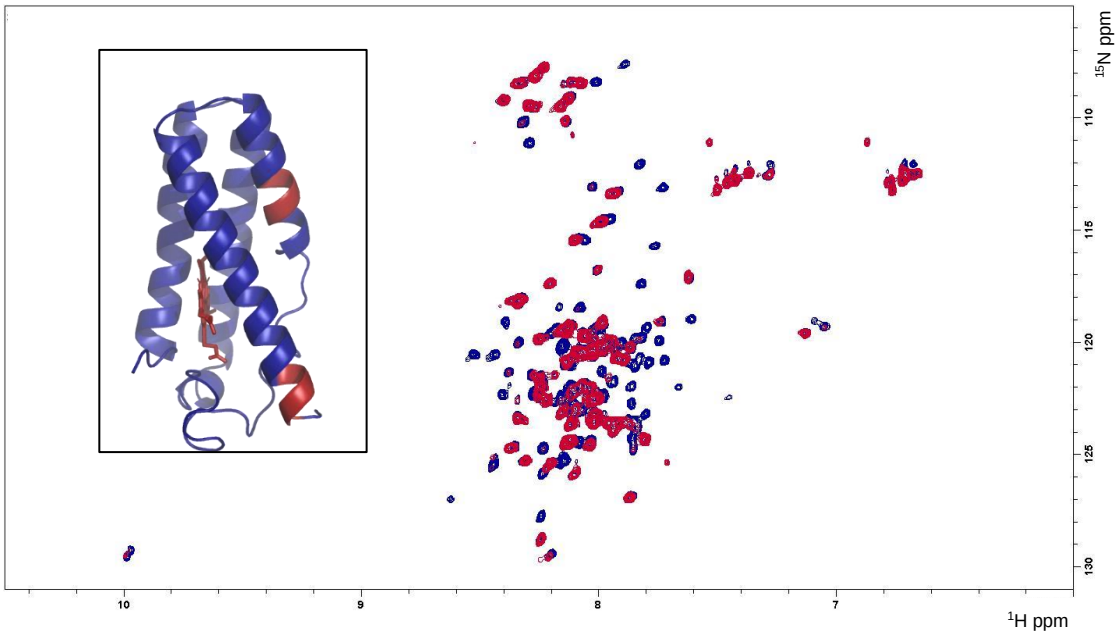

Figure III-4: ^{1}H-^{15}N-BEST-HSQC of apocytochrome *c*' in the absence (blue) and the presence (red) of CcmI in a ratio of 0.5. Inset: Map of the interacting residues (red) in the cytochrome *c*' crystal structure.

Given these results, the need for the presence of Ccm in the interaction process between the apocytochrome and hemin was explored. For this, the interactions were addressed using UV-visible spectroscopy inside an anaerobic glovebox to maintain reducing conditions. First, reduced hemin was added to the reduced apocytochrome. The reaction was monitored for 35 minutes, however, no change was observed in the region of the alpha, beta, and Soret peaks. The subsequent addition of cell extract, membrane extract (data not shown), and/or dithionite to the reaction did not yield any spectral changes (**Figure III-5**). This indicates that the formation of a cytochrome-*c* or its *b*-type intermediate did not take place, as would be expected from the literature (Daltrop *et al.*, 2002; Daltrop and Ferguson, 2003).

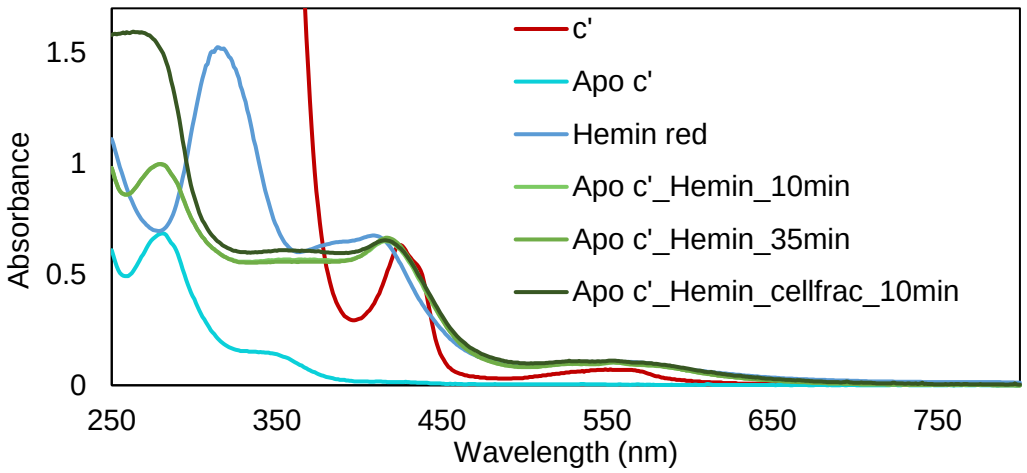

Figure III-5: Absorption spectra of cytochrome c' (red) apocytochrome *c*' (light blue), hemin (blue) and their interaction at different time points and with the addition of cell fraction and dithionite (green).

Apocytochrome c' presents secondary structure elements

Class I cytochromes *c* acquire their secondary and tertiary structural elements upon the covalent binding of the heme (Verissimo and Daldal, 2014). The structural features of apocytochrome *c*' were explored by SAXS (**Figure III-6** and **Figure III-9**). It is possible to observe that, in contrast to Class I apocytochromes *c*, apocytochrome *c*' shows a mixed structured-disordered profile. Although this is not a stably folded protein with homogeneous structure, it is also not a random coil, as evidenced by the shape of the SAXS Kratky plot (**Figure III-6**).

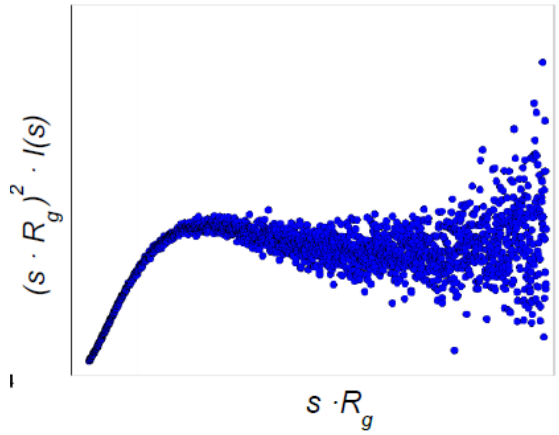

Figure III-6: Kratky plot resulting from SAXS analysis of apocytochrome *c*'.

To complement these data, the CD profile of apocytochrome *c*' was recorded. Previous works assessing cytochrome *c* maturation *in vitro* have shown no evidence of structural elements in the CD spectra of the Class I apocytochromes *c* (Daltrop *et al.*, 2002; Daltrop and Ferguson, 2003). In the case of apocytochrome *c*', it is clear that structural elements are present, with the CD spectra displaying mixed α-helical and random coil components of the structure. The presence of a negative band at 222 nm and the positive band under 200 nm are characteristic of the α-helical structure, while the band at 208 nm indicates the mixing of α-helical and random coil characteristic bands (**Figure III-7**).

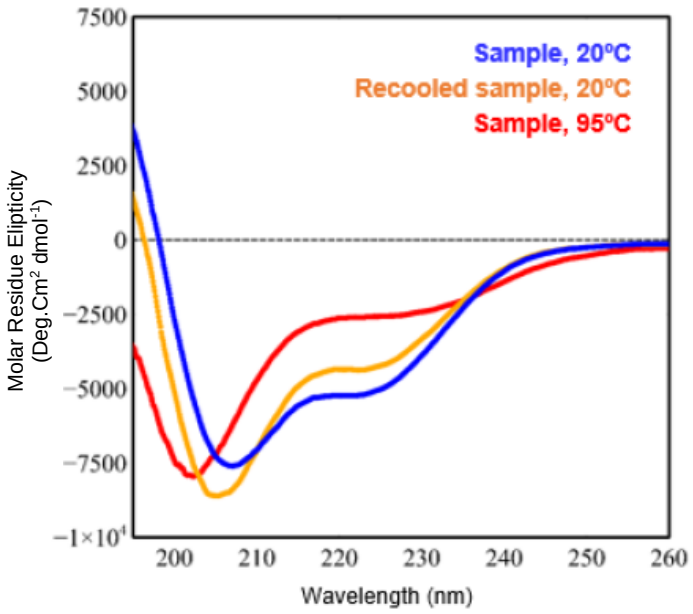

Figure III-7: CD spectrum of apocytochrome *c*' at 20 °C (blue), 95 °C (red) and re-cooled to 20 °C (orange).

The temperature dependence of the CD spectra shows that the apocytochrome *c'* has a melting temperature at 25 °C in the conditions tested (supplementary **Figure III-10**) and that the process is not fully reversible as seen by the difference in the spectra between the starting spectrum at 20 °C and the recooled spectrum after heating to 95 °C (**Figure III-7**).

4. Conclusions

Although Ccm can maturate all classes of cytochromes (Verissimo and Daldal, 2014), our data show that this process occurs differently for Class I and Class II cytochromes. While Class I cytochromes *c* have no defined structural elements without the presence of the heme (Daltrop and Ferguson, 2003), both CD and SAXS revealed that in the case of apocytochrome *c*', some propensity for structural elements are already present before insertion of the heme. Moreover, the lack of spontaneous formation of a *b*-type intermediate or the final covalently bound cytochrome *c in vitro*, even in the presence of the maturation proteins, indicates fundamental differences in the maturation process of these different classes of

cytochromes. The presence of structural elements indicates the need for the alteration of these elements for the insertion of the heme, that in the formed cytochrome *c*' is located inside the four-helix bundle (Tahirov *et al.*, 1996). This hypothesis is corroborated by the location of the identified interacting regions, which indicates the interaction of CcmI with defined regions in two of these helixes. These differences highlight that the classification proposed more than 30 years ago (Ambler, 1982) still stands and new data available corroborate the observations made at the time.

This finding can be an indication of the need for the presence of a complex of 9 proteins for the maturation of cytochromes, evidencing the need for the retention of such a complex system versus the presence of System II (two proteins) and System III (only one protein) (Sutherland, Tran, *et al.*, 2018; Silva *et al.*, 2022). The evolution of the maturation systems has been the subject of debate and our data can add in important arguments to this discussion (Kranz *et al.*, 2009; Paquete *et al.*, 2019; Brausemann *et al.*, 2021). The need for bacteria to thrive in different environments and therefore possess high metabolic diversity, often relying on the differential expression of cytochromes *c* led to the development of metabolic pathways containing cytochromes that belong to different classes (Fonseca *et al.*, 2013; Faustino *et al.*, 2021; Jain *et al.*, 2022). This requirement for the expression of different classes of cytochromes may be the reason behind the evolutionary need for the maintenance of the complex and energy-demanding maturation System I.

5. Supplementary Material

Table III-1: List of primers used in this study and their purpose.

N	Name	Sequence	Purpose
1	pAV6_OmpA_Fw	GAAGGTCGTCATATGAAAAAGACAGCTATCGCGATTGC	Amplify OmpA signal peptide
2	*c*'_OmpA_Rv	TTCTTTGGTATCAGCTGCCTGCGCAACGGTAGCG	
3	*c*'_OmpA_Fw	ACCGTTGCGCAGGCAGCTGATACCAAAGAAGTTCTTGAAGC	Amplify apocytochrome *c*'
4	pAV6_*c*'_Rv	TTAGCAGCCGGATCCTTAGTCTTCTTCGCGATAGTCGTCG	

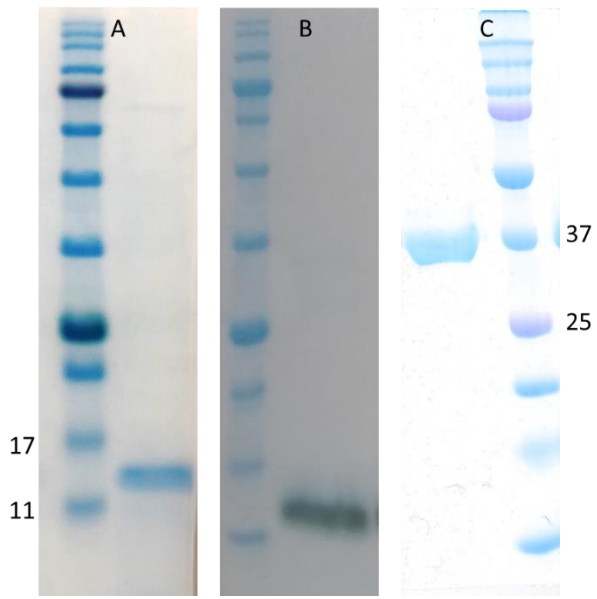

Figure III-8: Blue-safe stained gels revealing the protein purity of A) apocytochrome *c*'; B) cytochrome *c*'; and C) CcmI.

Table III-2: Preliminary assignment data of apocytochrome *c*'. One-third of the amino acid residues were tentatively assigned.

Residue	Amino acid		H	N	Cα	Cβ
18	ALA	A	8.1401	125.1647	49.655	16.2264
19	ASP	D	8.1441	119.9587	51.484	38.5215
20	THR	T	7.7309	113.0574	59.0673	67.4383
21	LYS	K	8.3985	122.2761	55.7767	29.7266
22	GLU	E	8.3829	119.0841		26.5513
23	VAL	V	7.6677	121.8542	62.0086	29.1924
40	ALA	A	8.1174	124.3596	50.1494	16.2533
41	MET	M	8.1223	119.2938	52.9393	29.869
42	THR	T	7.9459	114.3565	59.1656	66.7851
43	GLY	G	8.2834	111.017	42.5174	
44	VAL	V	8.0295	120.322	51.6031	38.2451
50	ALA	A	8.233	128.6125	49.578	16.261
51	GLU	E	8.1078	123.6083	49.6024	
52	ALA	A	8.0116	123.0712		16.141
53	ALA	A	7.8043	123.1339	51.2116	15.4362
54	LYS	K	8.0793	118.429	55.3903	26.3871
55	ALA	A	7.8643	124.1943	51.2645	15.3561
56	GLU	E	8.0071	119.3528	55.2054	26.7616
57	ALA	A	7.864	122.6529	51.1829	15.4681
58	ALA	A	7.7904	120.8519	50.7713	15.5646
59	LYS	K	7.6152	118.915	54.8817	29.8362
60	LEU	L	7.7293	120.8271	53.0799	39.1121
74	ALA	A	8.3429	124.5987	49.8515	16.2373
75	GLY	G	8.2244	107.7401	42.4897	
76	THR	T	7.9295	113.2636	58.9589	67.1318
77	SER	S	8.3324	118.0947	55.3126	60.984
78	SER	S	8.3186	118.0321	56.0532	60.9324
79	THR	T	7.972	114.4545	59.0252	66.6584
80	ASP	D	8.0024	122.435	51.5006	38.2676
81	LEU	L	7.931	120.6049	55.4118	35.6658
101	LYS	K	8.1141	119.3964	53.9851	29.8057
102	GLY	G	8.1193	109.0461	42.5505	
103	LYS	K	7.8913	120.7232	53.5889	30.2126
104	ALA	A	8.0285	124.455	49.7768	16.2417
105	MET	M	8.1997	117.2909		36.0839
106	HIS	H	7.8043	124.1298	52.5212	28.5005

107	GLU	E	8.2477	122.4878	53.6883	27.3563
108	ALA	A	8.2862	124.941	49.979	16.239
109	GLY	G	8.2533	108.0045	42.4397	
110	GLY	G	8.0678	108.3756	42.2363	
111	ALA	A	8.0072	123.5535	49.6837	16.2905
112	VAL	V	7.7282	118.9464	58.6937	35.7775

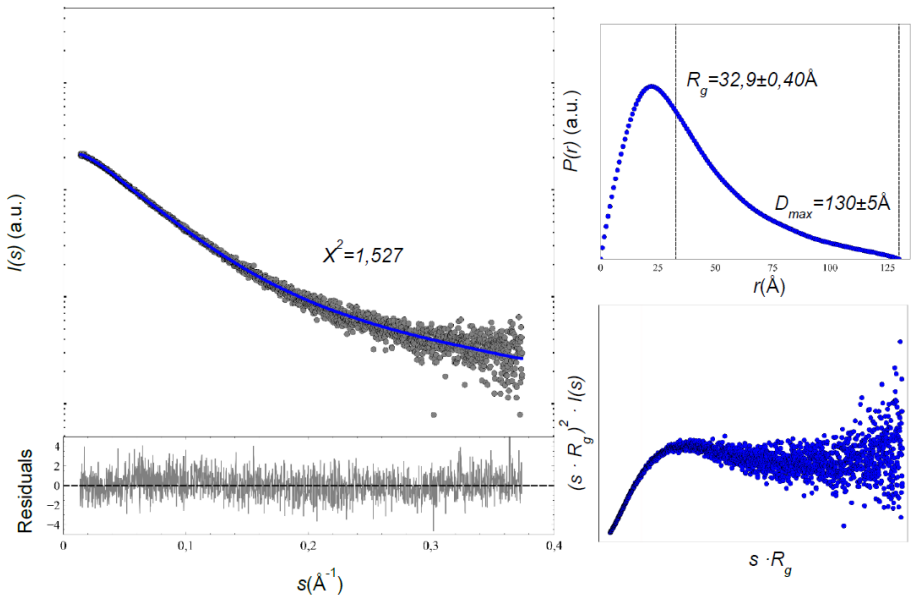

Figure III-9: SAXS analysis of apocytochrome *c*' A) SEC-SAXS B) SAXS intensity (grey circles), I(s), is represented in logarithmic scale as a function of the momentum of transfer, s = (4πsin θ)/λ, where 2 is the scattering angle. The solid line corresponds to the scattering profile (blue line) calculated from the ab initio model that best fitted the experimental data (2=1.5). Point-by-point residuals of the fitting and the absolute intensities are shown at the bottom. B) Pair-wise distance distribution (P(r)) of SEC-purified apocytochrome *c*' calculated from data in the range 0.014 < s < 0.39Å-1 using GNOM. The derived R_g and D_{max} values are displayed in dashed lines. C) Kratky plot.

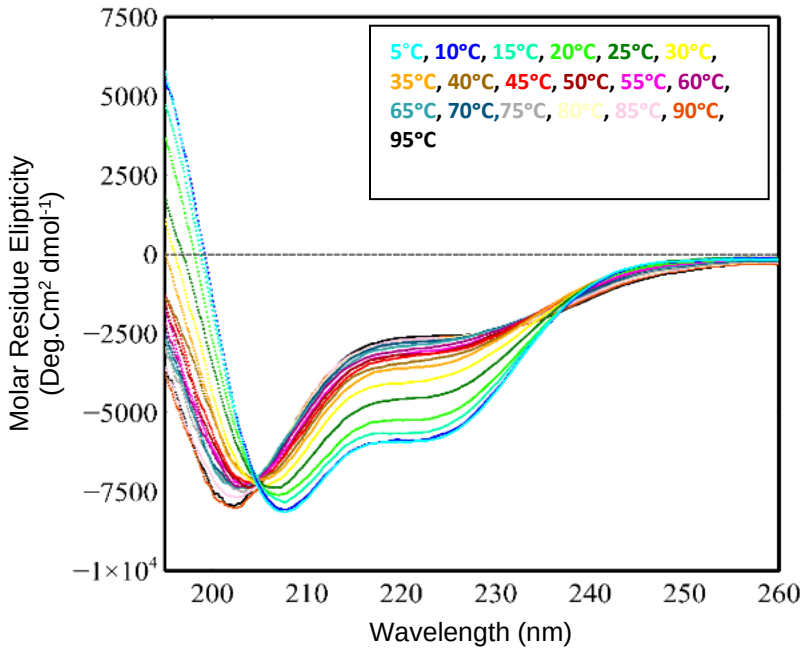

Figure III-10: CD spectrum of apocytochrome c' at 5 °C step intervals from 5 °C to 95 °C.

Chapter IV

Investigation of the Molecular Mechanisms of the Eukaryotic Cytochrome c Maturation System

The author of this dissertation performed all the experiments described in this chapter except for Mass spectrometry and N-terminal sequencing.

This chapter was published as a research article where the author of this thesis is the first author: Silva et al., 2022

Abstract

Cytochromes *c* are ubiquitous heme proteins with enormous impact at the cellular level, being key players in metabolic processes such as electron transfer chains and apoptosis. The assembly of these proteins requires maturation systems that catalyze the formation of the covalent thioether bond between two cysteine residues and the vinyl groups of the heme. System III is the maturation system present in Eukaryotes, designated CcHL or HCCS. This System requires a specific amino acid sequence in the apocytochrome to be recognized as a substrate and for heme insertion. To explore the recognition mechanisms of CcHL, the bacterial tetraheme cytochrome STC from *Shewanella oneidensis* MR-1, which is not a native substrate for System III, was mutated to be identified as a substrate. The results obtained show that it is possible to convert a bacterial cytochrome as a substrate by CcHL, but the presence of the recognition sequence is not the only factor that induces the maturation of a holocytochrome by System III. The location of this sequence in the polypeptide also plays a role in the maturation of the cytochrome *c*. Furthermore, CcHL appears to be able to catalyze the binding of only one heme per polypeptide chain, being unable to assemble multiheme cytochromes *c*, in contrast with bacterial maturation systems.

1. *Introduction*

Cytochromes *c* are essential proteins for living organisms across all domains of life, serving as an essential component of several metabolic processes such as respiration (Pettigrew and Moore, 1987; Nicholls and Ferguson, 2013), apoptosis (Jiang and Wang, 2004; Ow *et al.*, 2008), and extracellular electron transfer (Paquete *et al.*, 2019; Fonseca *et al.*, 2021). This class of proteins is defined by the stereo-specific covalent attachment of the heme cofactor to the polypeptide chain via two (rarely one) thioether bonds to cysteine side chains (Dickerson, 1980; Pettigrew and Moore, 1987). This allows for the unique feature of binding a virtually limitless amount of heme cofactors per polypeptide chain (Paquete *et al.*, 2019). For this covalent

attachment to occur, a dedicated maturation biochemical machinery is required (Sanders *et al.*, 2010). Although three main cytochrome *c* maturation systems have been described (Kranz *et al.*, 2009), together with variations that constitute subsequent numbering (de Vitry and Vitry, 2011; Ferguson, 2012; Mavridou, Ferguson and Stevens, 2013), the most prevalent in nature are Systems I and III. System I is constituted of up to nine membrane-bound components (for a review, see (Verissimo and Daldal, 2014)), and it is present in α-and γ-proteobacteria, in Archaea, and in the mitochondria of plants and red algae. This system is able to mature all classes of cytochromes *c*, including MHCs (Kranz *et al.*, 2009; Verissimo and Daldal, 2014). In contrast, System III involves only one essential protein, designated cytochrome *c* heme lyase (CcHL) (Verissimo *et al.*, 2012) or holocytochrome *c* synthetase (HCCS) (Babbitt *et al.*, 2017). System III is present in the mitochondria of most eukaryotic organisms, except for plants (Babbitt *et al.*, 2015), being, so far, only found in organisms that do not produce multiheme cytochromes. In this work, for historical reasons, we will use the original name of the enzyme, CcHL (Dumont *et al.*, 1987). CcHL is predicted to be a soluble membrane-associated protein with 170 to 289 residues (Babbitt *et al.*, 2015). In contrast to Systems I and II, System III requires not only the presence of the CX_nCH heme-binding motif but also of a consensus recognition sequence that is different for different organisms and that has been identified for both humans and yeast (Verissimo *et al.*, 2012; San Francisco, Bretsnyder and Kranz, 2013). It has been demonstrated that this sequence is responsible for the formation of an alpha helix required for CcHL to recognize and attach its substrate (Sutherland *et al.*, 2021).

In humans, the malfunction of System III has several health implications, being the sole cause of the genetic disease microphthalmia with linear skin defects (MLS) (Wimplinger *et al.*, 2006). This syndrome is lethal in males and leads to several complications in females, including mental retardation (Slavotinek, 2019). Furthermore, System III has also been implicated in a

caspase-independent cell death pathway in injured neurons (Kiryu-Seo *et al.*, 2006), although the mechanisms by which CcHL triggers apoptosis are still to be identified. Despite the acknowledged importance of System III in human health, this is the least understood maturation system as the enzyme was never fully characterized, and its recognition and maturation mechanisms remain incompletely understood. To address the recognition mechanisms of CcHL, in this work, we tested the ability of the yeast heme lyase to produce a Class III multiheme cytochrome, the Small Tetraheme Cytochrome (STC) from *Shewanella oneidensis* MR-1. STC is a fully characterized protein of similar size to the mitochondrial cytochrome *c*, being involved in the extracellular electron transfer pathway of *S. oneidensis* MR-1 (Fonseca *et al.*, 2009; Alves *et al.*, 2017). STC has four CXXCH heme-binding sites, and mutations were made to implement the known recognition sequence for CcHL before the various heme-binding sites (**Figure IV-1**).

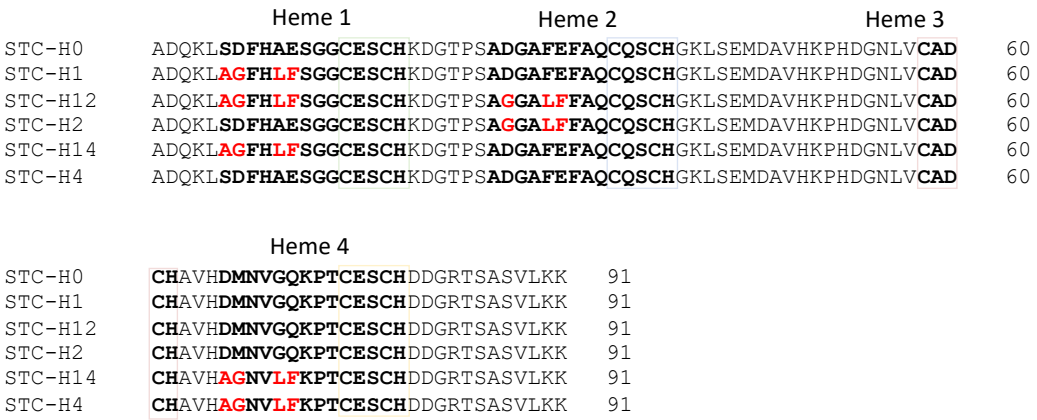

Figure IV-1. Amino acid sequence of the different STC mutants with mutated residues is highlighted in red. Amino acids in bold highlight the recognition sequence and heme-binding motif of the hemes that were mutated.

Here, we demonstrate that CcHL is able to insert only one heme in a multiheme apo-cytochrome and that the distance between the N-terminal and the recognition sequence influences heme attachment. Based on these

results, the four-step model of the CcHL-mediated cytochrome *c* biogenesis, previously proposed by Babbit *et al*. (Babbitt *et al.*, 2015), is updated.

2. *Materials and methods*

Production of STC Mutants with System III

To study System III, we used an expression system that produces the enzyme for the maturation of yeast, horse, and human cytochromes *c* in *E. coli* (W. B. R. Pollock *et al.*, 1998; Morar *et al.*, 1999; Patel, Lind and Pielak, 2001; Olteanu *et al.*, 2003). To produce native STC (hereafter simply referred to as STC) using this system, the *cctA* gene from *S. oneidensis* MR-1, encoding the tetraheme cytochrome STC without its native signal peptide, was cloned in the plasmid pBTR-1 that contains the *S. cerevisiae* CcHL gene (W. B. R. Pollock *et al.*, 1998), using the primers presented in **Table IV-2**. To facilitate the purification procedure, the construct was built to express a 6x Histidine-tag at the C-terminus of the protein. The resulting plasmid was denominated pCPH0. Mutations to insert the consensus sequence for CcHL recognition in the binding region of heme 1 were introduced by site-directed mutagenesis using the primers indicated in **Table IV-2** and using the manufacturers' procedure (NZYTech, Lisboa, Portugal), resulting in the plasmid pCPH1. The same procedure was used to build the plasmids pCPH2 and pCPH4 that contain the consensus CcHL recognition sequence in the binding site for hemes 2 and 4, respectively. Finally, site-directed mutagenesis was performed on pCPH1 to build the plasmids pCPH12 and pCPH14 that contain the consensus sequence inserted in hemes 1 and 2, and 1 and 4, respectively. All constructs were confirmed by DNA sequencing (Eurofins Genomics, Ebersberg, Germany). The resulting plasmids were then transformed into *E. coli* BL21 (DE3) cells. Given that the mutations in the third heme-binding position would affect the second histidine axial ligand of this heme, this experiment was not performed for mutant STC-H13 (see **Figure IV-1**).

Pre-inocula were initiated from a single freshly transformed colony and grown overnight at 37 °C with shaking at 150 rpm in 100 mL of Luria–Bertani medium (LB) (Bertani, 2004) supplemented with 100 µg/mL ampicillin. For protein expression, cultures were diluted to an OD_{600} of 0.1 in Terrific Broth medium (TB) (Tartoff and Hobbs, 1987) with 100 µg/mL ampicillin and grown aerobically at 37 °C for 48 h with shaking at 150 rpm. Cells were harvested by centrifugation at 10,000× *g* at 4 °C for 10 min and frozen at −20 °C.

For protein purification, cells were defrosted and resuspended in 20 mM Tris-HCl buffer at pH 7.6, supplemented with protease inhibitor cocktail (Roche, Basel, Switzerland) and DNase I (Sigma-Aldrich, St. Louis, MO, USA). Cell disruption was performed using a French Press by passing the cells three times at 1000 psi. The lysed cells were ultracentrifuged at 210,000× *g* at 4 °C for 90 min, and the resulting soluble protein extract was purified using a 5 mL pre-packed His-trap column (GE Healthcare, Chicago, IL, USA), previously equilibrated with 20 mM potassium phosphate buffer at pH 7.6 with 300 mM NaCl buffer. A linear gradient from 0 to 100% buffer B (20 mM potassium phosphate buffer at pH 7.6 with 300 mM NaCl and 500 mM Imidazole) in 150 mL was used to elute the target protein. All chromatographic fractions were analyzed in 13% acrylamide SDS-PAGE gels. The gels were stained by both heme stain and BlueSafe (NZYTech, Lisboa, Portugal). The heme stain protocol, which is based on the heme peroxide activity, allows the produced *c*-type cytochrome to be identified on an SDS gel electrophoresis (Goodhew, Brown and Pettigrew, 1986). Fractions containing the target protein were concentrated using centrifugal filter units (Millipore, Burlington, MA, USA) with a 5 kDa cut-off membrane. Pure protein was revealed as a single band in the BlueSafe-stained SDS-PAGE gel (**Figure IV-5**). The same purification procedure was used for all the mutants.

Production of STC Mutants with System I

The production of STC using System I by *E. coli* was performed as previously described (Alves *et al.*, 2017). Mutations to introduce the consensus

sequence for CcHL recognition in the heme-binding sites of heme 1, 2, and 4, to produce STC-H1, STC-H2, and STC-H4 were performed with site-directed mutagenesis using the manufacturers' procedure (NZYTech, Lisboa, Portugal) using the primers listed in **Table IV-2**. Additional site-directed mutagenesis was performed on STC-H1 to build the plasmids STC-H12 and STC-H14, adding the consensus sequence for hemes 2 and 4, respectively. The resulting plasmid was transformed in *E. coli* BL21 (DE3) containing the plasmid pEC86, responsible for the expression of Ccm proteins under aerobic conditions (Arslan *et al.*, 1998). All constructs were confirmed by DNA sequencing (Eurofins Genomics, Ebersberg, Germany).

Pre-inocula were initiated from a single freshly transformed colony and grown overnight at 37 °C with shaking at 150 rpm in 100 mL of LB medium with 100 µg/mL ampicillin and 34 µg/mL chloramphenicol. For protein expression, starter cultures were diluted to an OD_{600} of 0.1 in TB medium with 100 µg/mL ampicillin and 34 µg/mL chloramphenicol and left to grow aerobically at 37 °C for 48 h with shaking at 150 rpm. Cells were then harvested by centrifugation at 10,000× *g* at 4 °C for 10 min and frozen at −20 °C. Disruption was performed by osmotic shock using a solution containing 20 mM Tris–HCl pH 8.0, 20% sucrose, 1 g/L of lysozyme, 0.5 mM EDTA, protease inhibitor cocktail (Roche, Basel, Switzerland), and DNase I (Sigma-Aldrich, St. Louis, MO, USA) according to the previously described protocol (Alves *et al.*, 2017). The lysate was incubated with shaking for 90 min at 4 °C.

For protein purification, the lysed cells were centrifuged at 210,000× *g* at 4 °C for 90 min, and the resulting soluble protein extract was purified using a Q-Sepharose ™ Fast Flow Column (GE Healthcare, Chicago, IL, USA) previously equilibrated with 20mM Tris buffer at pH 7.6. The target protein was eluted at 20 mM of NaCl in the same buffer. When necessary, a second purification step was performed using a Superdex 75 10/300 GL size exclusion column (GE Healthcare, Chicago, IL, USA). All chromatographic fractions were analyzed in 13% acrylamide SDS-PAGE gels. The gels were

stained both by heme stain (Goodhew, Brown and Pettigrew, 1986) and BlueSafe (NZYTech, Lisboa, Portugal). Pure protein was revealed as a single band in the BlueSafe-stained SDS-PAGE gel. The same purification process was used for all the mutants.

Protein Analysis

The identity of the produced proteins was confirmed by N-terminal sequencing (first five amino acid residues) using the Edman degradation method in an ABI Procise Protein Sequencer, an ABI Microgradient Pump System and an ABI Programmable Absorbance Detector.

UV-visible spectra were recorded at room temperature in a Shimadzu UV-1800 spectrophotometer in the range of 250–800 nM. Data were analyzed in the UV-Probe v.2.52 software and MS Excel.

Mass spectrometry analysis was performed in the proteins produced with System III to confirm the number of hemes in the protein. The proteins were applied directly onto the MALDI plate with 1 µL of 5 mg/mL CHCA (alpha-cyano-4-hydroxycinnamic acid, Sigma-Aldrich, St. Louis, MO, USA) in 50% (*v*/*v*) acetonitrile and 5% (*v*/*v*) formic acid. The data were acquired in Linear Low Mass Positive mode using a 4800plus MALDI-TOF/TOF (ABSciex) mass spectrometer and 4000 Series Explorer Software v.3.5.3 (Applied Biosystems) available in the Mass Spectrometry Unit (UniMS), ITQB/iBET, Oeiras, Portugal. External calibration was performed using CalMix5 (Protea).

3. *Results*

Native STC from *S. oneidensis* MR-1 was co-expressed in *E. coli* with yeast CcHL using the pCPH0 plasmid containing both the cytochrome and CcHL genes (construct STC-H0). In this construct, the signal peptide of the STC gene, required for the transport to the periplasm and subsequent maturation by System I, was removed to guarantee that the apo-protein would be maturated by System III in the cytoplasm of *E. coli*. During protein production, aerobic conditions were ensured by shaking the culture at 150 rpm to avoid

the expression of the native cytochrome maturation system (i.e., System I) (Thony-Meyer *et al.*, 1995). By performing an SDS-PAGE gel with the cellular fraction of the *E. coli* culture harboring construct STC-H0, no heme-stained band could be observed around 12 kDa (i.e., MW of native STC), (Lane 1 in **Figure IV-6**), indicating that STC-H0 is not maturated in *E. coli*. This observation is in agreement with the fact that this construct does not contain the consensus recognition sequence required for the maturation process by CcHL (Verissimo *et al.*, 2012). The insertion of the consensus recognition sequence in the first heme-binding position (mutant STC-H1) led to the production of a cytochrome *c* that is visible by heme staining at approximately 10 kDa (Lane 2 in **Figure IV-6**).

The protein produced by CcHL was purified (**Figure IV-5**). It displays characteristic features of a high-spin cytochrome *c*, with a broad Soret peak and the presence of a peak at approximately 660 nm (**Figure IV-2**). This suggests that the heme(s) in the protein produced by this maturation system either lack the distal axial ligand or this has been replaced by a weak-field ligand (e.g., water). Indeed, mass spectrometry revealed that only one heme was inserted in STC-H1 (**Table IV-1**). The lack of the other three hemes offers a rational explanation for the incomplete folding of the protein and lack of coordination of the heme by the distal axial histidine. These results indicate that the recognition sequence prior to the first heme binding position of STC is required for the polypeptide to be recognized as an apocytochrome by CcHL. However, it is not sufficient for the insertion of all four hemes.

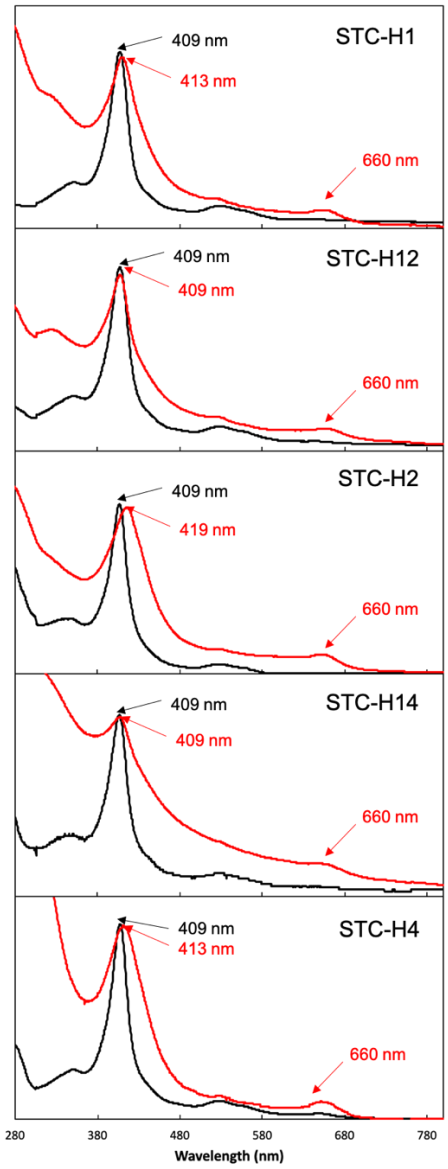

Figure IV-2. UV-visible spectra of STC mutants produced by System III (red) and System I (black).

Table IV-1. Expected molecular weight (kDa) for the different STC mutants, determined from the molecular mass of the total number of residues plus the molecular mass corresponding to the heme group(s) (616.5 Da per heme). Grey shading represents the species detected by mass spectrometry

Mutant	Apo Protein	1 Heme	2 Hemes	3 Hemes	4 Hemes
STC-H1	10.5	11.1	11.7	12.3	12.9
STC-H12	10.4	11.0	11.6	12.2	12.9
STC-H2	10.4	11.0	11.6	12.3	12.9
STC-H14	10.4	11.0	11.7	12.3	12.9
STC-H4	10.4	11.1	11.7	12.3	12.9

To investigate if CcHL is able to insert more than one heme, STC was mutated to contain the consensus recognition sequence prior to the first and second heme-binding positions (mutant STC-H12). This protein was successfully produced in *E. coli* by System III (Lane 3 in **Figure IV-6**) and purified (**Figure IV-5**). The position of the band of this mutant in the gel is, however, slightly higher than that of mutant STC-H1. This, together with the fact that the UV-visible spectrum is also different from that of STC-H1 (**Figure IV-2**), suggests that the produced protein is different from STC-H1. Mass spectrometry revealed that a mixture of the apo-protein (i.e., protein without the insertion of any heme, of ~10.4 kDa) and protein containing one heme

(~11 kDa) exists, being the contribution of both forms very similar (

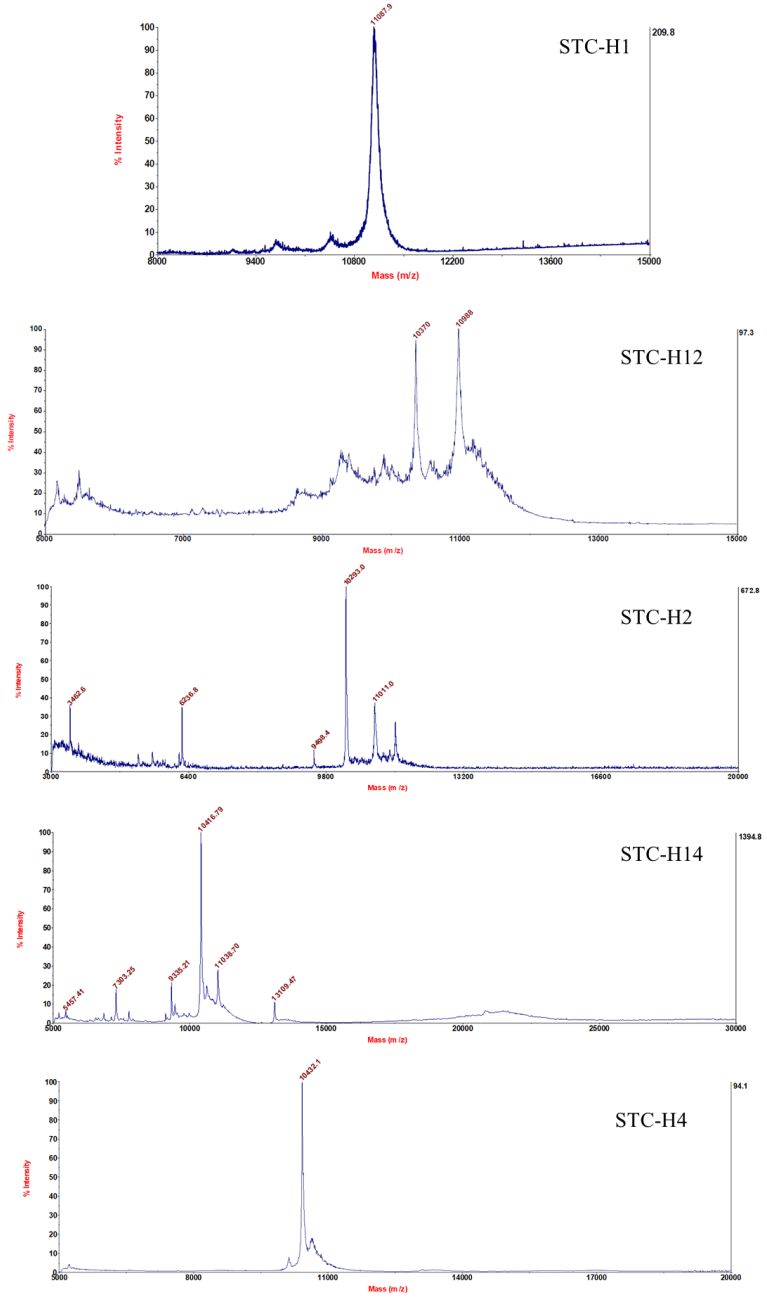

Figure IV-7 and **Table IV-1**). This may explain the different UV-visible spectra and indicates that CcHL was able to insert one heme in this construct but that it was less efficient than insertion in STC-H1.

To investigate why CcHL was not able to insert more than one heme, three different hypotheses were explored: (i) the second consensus sequence is too far from the N-terminus of the protein to be recognized by CcHL; (ii) the distance between the two binding positions is too short, preventing the insertion of the second heme (i.e., the local folding upon the insertion of the first heme impairs the recognition of the second consensus sequence by CcHL), or; (iii) the CcHL can only insert one heme, regardless of the number of consensus sequences in the apo-cytochrome.

To test hypothesis (i), the STC-H2 mutant (insertion of the recognition sequence in the second heme-binding position) was constructed. This protein was successfully produced by CcHL (**Figure IV-5** and Lane 4 in **Figure IV-6**). However, the position of the band of this mutant in the gel (Lane 4 in **Figure IV-6**) is different from the other mutants, showing that the insertion of the heme in this position affected the electrophoretic mobility of the protein in the SDS-PAGE. The UV-visible spectrum corroborates the different properties of this mutant, which displays a shift in the Soret peak from 409 nm to 419 nm (**Figure IV-2**). Mass spectrometry shows a larger contribution of the apo-form

of the protein (~10.4 kDa) versus the form containing one heme (~11 kDa)

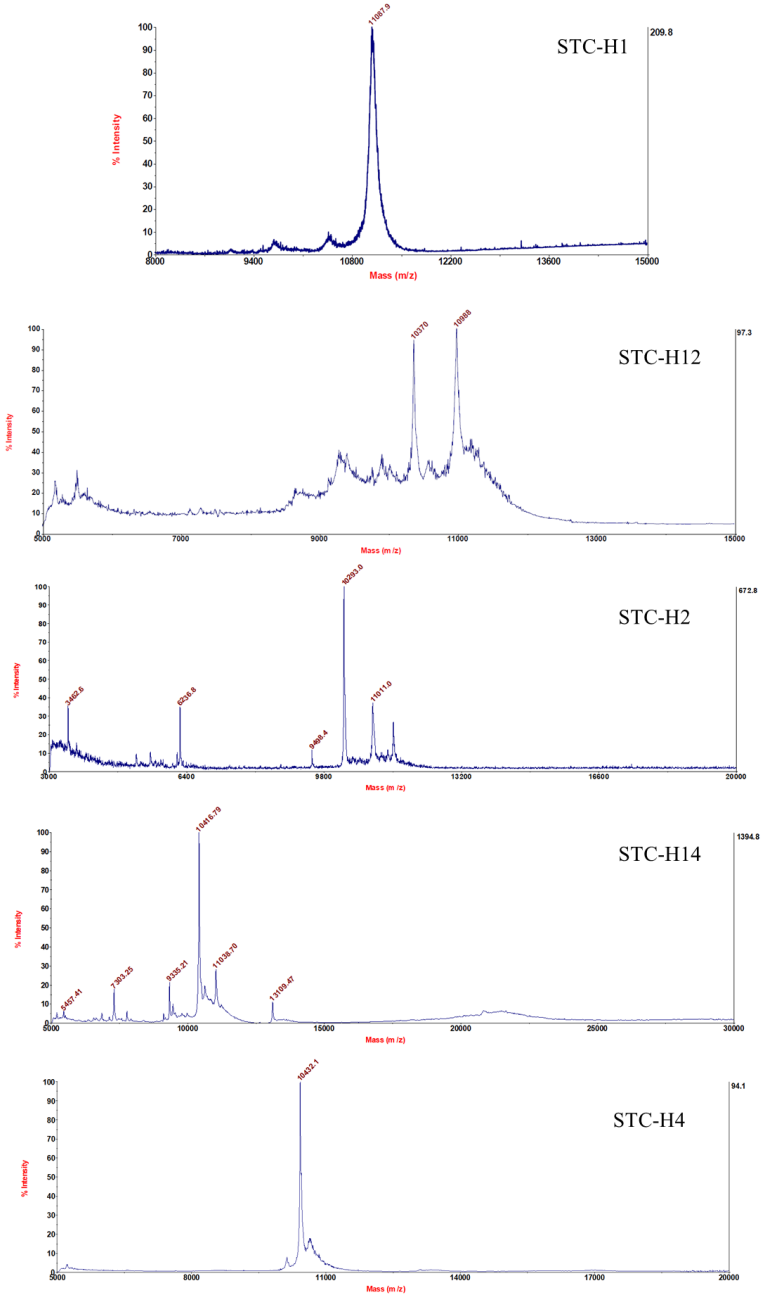

(**Table IV-1** and **Figure IV-7**). These results show that heme binding occurs and that the distance of the recognition sequence from the N-terminus impacts the efficiency of heme insertion by CcHL. These results eliminate hypothesis (i).

To test hypothesis (ii), mutant STC-H14 (insertion of the recognition sequence in the first and fourth heme-binding positions) was built and produced (**Figure IV-5** and Lane 5 in **Figure IV-6**). While the position in the SDS-PAGE gel (Lane 5 in **Figure IV-6**) and UV-visible spectrum of this mutant was similar to that observed for the STC-H12 mutant (**Figure IV-2**), mass spectrometry results showed a larger population of the apo-form of the protein (~10.4 kDa) versus the form with one heme inserted (~11 kDa)

(**Table IV-1** and

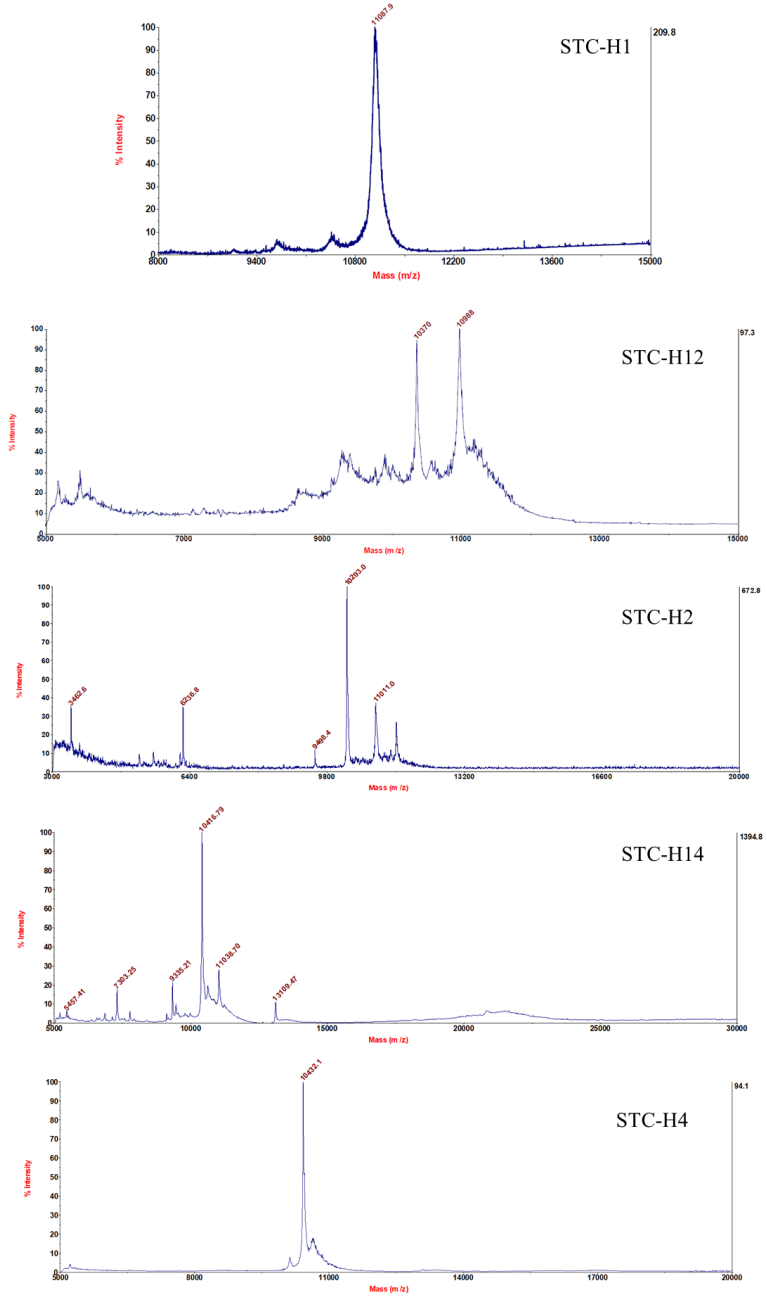

Figure IV-7). For STC-H14, only a small population of the protein form that contains one heme could be observed, with no evidence of protein containing more than one heme. This reveals that the proximity between the two heme-

binding positions was not the reason for the inability of CcHL to place more than one heme, discarding hypothesis (ii).

To investigate if it is the distance from the N-terminus to the last heme-binding position that impairs the second heme insertion in mutant STC-H14, the mutant STC-H4 (insertion of the recognition sequence in the fourth heme-binding position) was built and produced by CcHL (Lane 6 in **Figure IV-6**). The UV-visible spectrum of this mutant is, however, different when compared with the other mutants (**Figure IV-2**), including a modification in the Soret peak shape and relative intensity when compared to the 280 peak. Although this protein presents the characteristic properties of a cytochrome *c*, namely a broad Soret peak at 413 nm in the UV-visible spectrum, and a band that stains for hemes in the SDS-PAGE gel (Lane 6 in **Figure IV-6**), the mass spectrometry signal is dominated by the apo-form of the protein (**Table IV-1**). This is in agreement with the high intensity of the 280 nm peak and suggests that the heme-containing population is of very low abundance and does not emerge from the envelope of the mass spectrometry signal. These results indicate that the distance of the consensus recognition sequence to the N-terminal is important for the efficiency of CcHL in maturating cytochromes *c*.

It has to be mentioned that all the target proteins have been properly assembled by their native cytochrome maturation system (i.e., System I) (**Figure IV-2**). This clearly shows that the lack of insertion of more than one heme is not because of the mutations in the consensus sequence but due to the mode of action of CcHL.

4. *Discussion*

Cytochrome *c* maturation System III has been studied since the 1970s (Korb and Neupert, 1978), and in 1987, the gene responsible for the process was identified in yeast (Dumont *et al.*, 1987). The study of this system has been extremely challenging, mainly due to the fact that this system is composed of only one protein and low amounts of the enzyme present in cells, preventing

its purification (Babbitt *et al.*, 2014). The construct that allowed the purification of this enzyme for the first time was engineered in 2013 when human CcHL was purified from *E. coli* with an N-terminal GST fusion (San Francisco, Bretsnyder and Kranz, 2013). This was fundamental in advancing the understanding of this system, permitting the identification of key residues in CcHL for heme and apo-cytochrome binding, including the consensus recognition sequence for human CcHL (San Francisco, Bretsnyder and Kranz, 2013). At the same time, the recognition sequence for yeast CcHL was also identified, demonstrating that the recognition sequences are distinct in different organisms (Verissimo *et al.*, 2012).

In this study, five genetically engineered variants of the tetraheme cytochrome STC from *S. oneidensis* MR-1 were expressed, purified, and characterized to understand the mechanisms by which CcHL recognizes a polypeptide as an apo-cytochrome that should undergo maturation into a cytochrome *c*. These mutations incorporate the recognition sequence for yeast CcHL located prior to the different heme-binding positions in STC (**Figure IV-3**). The different variants were produced by both System I and III, to ensure that the differences observed were only due to the maturation system and not to alterations in the polypeptide chain that would affect the protein structure.

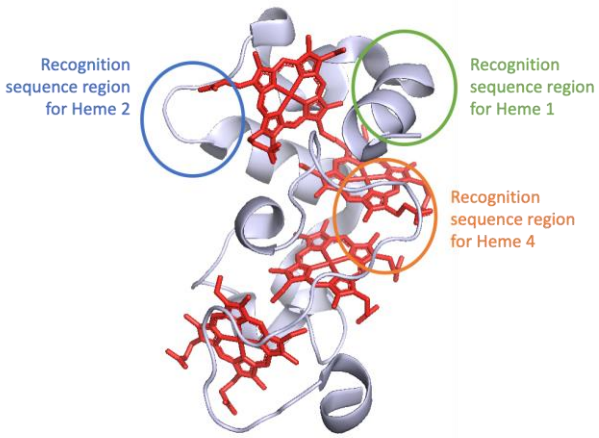

Figure IV-3. Cartoon representation of STC structure (PDB: 1M1Q) with mutated regions highlighted with colored circles.

The production of STC-H0 was performed as a proof of concept, demonstrating that without the recognition sequence, the apo-protein is not recognized by System III and, consequently, no heme cofactor is introduced in the protein, as previously observed (Verissimo *et al.*, 2012). This is in contrast to what has been observed for System I and II, where a specific consensus recognition sequence is not required for cytochrome *c* maturation, and only the heme-binding motif CXXCH is required for recognition and heme binding (San Francisco, Bretsnyder and Kranz, 2013; Mendez *et al.*, 2022). The consensus recognition sequence is part of the alpha helix required for CcHL to recognize the apo-cytochrome and insert the heme (Babbitt, Hsu and Kranz, 2016). In the case of STC, it was crucial for the insertion of one heme, but not sufficient to place all the four hemes. The production of both STC-H12 and STC-H14 demonstrated that the inability of CcHL to place more than one heme was not due to the short distance (15 amino acids) that separates the binding sequence of the two heme-binding sites in STC-H12. The fact that these mutants present similar features between them (i.e., run similarly in the SDS-PAGE gel and present comparable spectroscopic features) that are different from the cytochromes with only one consensus sequence (STC-H1,

STC-H2, and STC-H4), suggests that the produced proteins in STC-H12 and STC-H14 are a mixture of both forms (i.e., heme bound in positions 1 and 2 in STC-H12, and in positions 1 and 4 in STC-H14). These results show that CcHL recognizes the alpha helix, and after binding the heme, the mature cytochrome *c* is released, preventing it from inserting more than one heme in a single polypeptide chain. Furthermore, the efficiency of recognition and binding of the heme to the apo-cytochrome is inversely related to the distance of the position of the recognition sequence to the N-terminus of the polypeptide. This hypothesis correlates well with the amount of mature cytochrome *c* that is obtained for the mutants STC-H1, STC-H2, and STC-H4, where the fraction of apo-protein in the produced protein increases with the distance of the consensus recognition sequence to the N-terminus.

The results obtained with this work complement the four-step model previously proposed for the catalytic mechanism of System III (Babbitt *et al.*, 2015), adding unique information to steps 2 and 4, where the recognition of the apo-protein by the CcHL and release of the mature protein occur, respectively (**Figure IV-4**). Our work demonstrates that the distance of the recognition sequence, and consequently the alpha helix recognized by CcHL to the N-terminus of the apo-cytochrome, plays a key role in the recognition process by CcHL and binding of the heme. When this recognized alpha helix is far from the N-terminus of the apo-protein, the polypeptide chain that precedes it likely causes steric clashes with the CcHL regions surrounding the docking site, disturbing recognition by CcHL and preventing heme binding (see **Figure IV-3**). Furthermore, once the heme is bound, the CcHL releases the cytochrome, being unable to identify further recognition sequences.

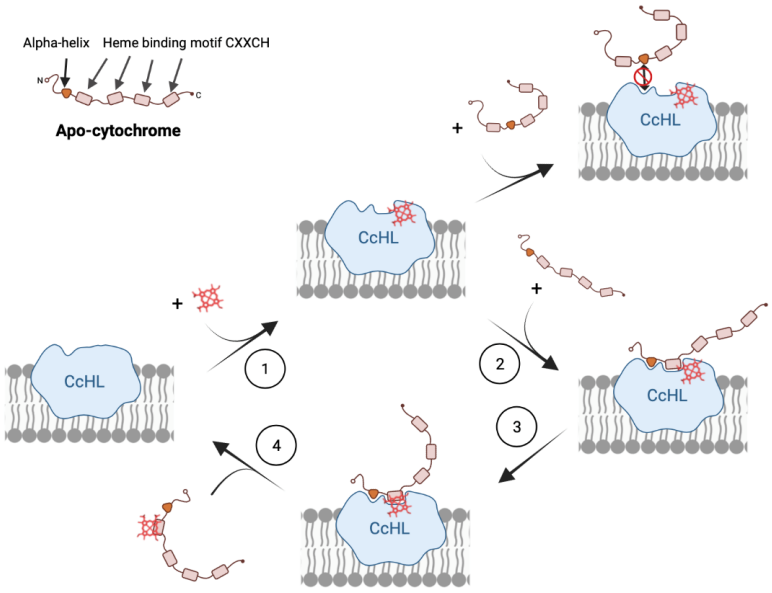

Figure IV-4. Model for the molecular mechanism of cytochrome *c* maturation by System III.

Therefore, the catalytic mechanisms of cytochrome maturation System III comprise: the binding of the heme by CcHL (step 1), enabling CcHL to be ready to recognize and bind the alpha-helix of a polypeptide without stable secondary or tertiary structural elements (step 2). In this step, it is crucial that the consensus sequence in the apo-protein is easily accessible to be recognized by CcHL, to allow the binding of the heme-binding motif. After binding, CcHL recognizes the heme-binding motif and promotes the attachment of the heme to the apo-cytochrome (step 3), allowing the protein to fold. This enables the mature cytochrome *c* to be released from CcHL (step 4).

This process is quite distinct from System I and II, where several hemes are bound to a single polypeptide chain, and therefore, several binding motifs have to be identified, probably sequentially in the apo-protein, and more than one heme has to be inserted. The recent cryo-EM structure of CcsBA from the System II cytochrome *c* maturation system revealed that this complex

changes from an open to a closed conformation, providing the necessary reaction chamber for the stereochemical attachment of the external heme to the CXXCH heme-binding motif in the apo-cytochrome (Mendez *et al.*, 2022). Although the tryptophan-rich loop forming the WWD domain, required to provide assistance to heme binding, attachment, and release of the cytochrome, was shown to be conserved among the different maturation systems (Babbitt *et al.*, 2015; Mendez *et al.*, 2022), structural analysis of the different active sites are quite distinct (**Figure IV-8**). This may explain why System III cannot insert more than one heme, while System I and II are able to mature multiheme cytochromes *c*. In addition to the WWD domain, two conserved periplasmic histidines flanking the WWD domain were shown to be crucial for heme attachment in both Systems I and II (Sutherland *et al.*, 2021). These histidines are absent in CcHL, highlighting the difference between these Systems and CcHL, and may be crucial for the insertion of more than one heme in both Systems I and II. Indeed, the loops around the WWD domain in both the CcsBA complex from System II and CcmC from System I (Sutherland, Tran, *et al.*, 2018) may be important not only for heme motif recognition but also to help in the binding of apo-protein, even after the insertion of a heme and detachment from the active site. This would allow, for example, CcsBA to switch back from the close to an open state with another heme in the external position, necessary to be inserted in the subsequent heme-binding motif of a multiheme cytochrome *c*. In the case of CcHL, once the heme is bound to the apo-protein, the cytochrome is released from the enzyme, becoming ready to uptake another heme and apo-cytochrome (step four in **Figure IV-4**).

5. *Conclusions*

In conclusion, the results obtained with this work unequivocally show that handling of the apo-cytochrome *c* polypeptide chain relies on a different mechanism in System III *versus* System I and II: System III requires the recognition sequence and the heme-binding motif (i.e., CXXCH) to insert a

heme in the apo-cytochrome; the distance between the N-terminal of the apo-protein and the recognition sequence influences heme binding in System III; CcHL can only insert one heme in the apo-protein. This information is relevant to the understanding of how CcHL recognizes its substrates and in finding strategies to manipulate its activity for therapeutic interventions. Further research, including the determination of CcHL structure, and the interaction with its heme and peptide substrates, will be fundamental to fully understand its maturation mechanisms.

6. *Suplementary Material*

Table IV-2: List of primers used in the study and their purpose.

Nº	Primer	Sequence (5' – 3')	Purpose
1	Histag_FW	CGTCTGTTCTGAAGAAGCACCACCACCACCACCACTAACCATGGGCGACGTGGAAAAGG	Histag insertion
2	Histag_RV	CTTCTTCAGAACAGACGCAGAAGTACGGCCATCGTCATGGC	
3	ΔCycI_F	CTTCATCATGAAAGGCTCGCAGGGCCACACGGTGG	CycI removal
4	W ΔCycI_RV	CCACCGTGTGGCCCTGCGAGCCTTTCATGATGAAG	
5	H1_FW	CGGATCAAAAATTAGCAGGCTTCCATCTTTTCTCAGGTGGTTGTGAGAG	Insertion of recognition sequence in Heme 1
6	H1_RV	CTCTCACAACCACCTGAGAAAAGATGGAAGCCTGCTAATTTTTGATCCG	
7	H2_FW	GTACCCCTTCTGCTGGCGGTGCCTTATTTTTTGCACAATGCCAA	Insertion of recognition sequence in Heme 2
8	H2_RV	TTGGCATTGTGCAAAAAATAAGGCACCGCCAGCAGAAGGGGTAC	
9	H4_FW	GCCATGCGGTACATGCTGGGAATGTACTCTTTAAACCTACTTGTG	Insertion of recognition sequence in Heme 4
10	H4_RV	CACAAGTAGGTTTAAAGAGTACATTCCCAGCATGTACCGCATGGC	

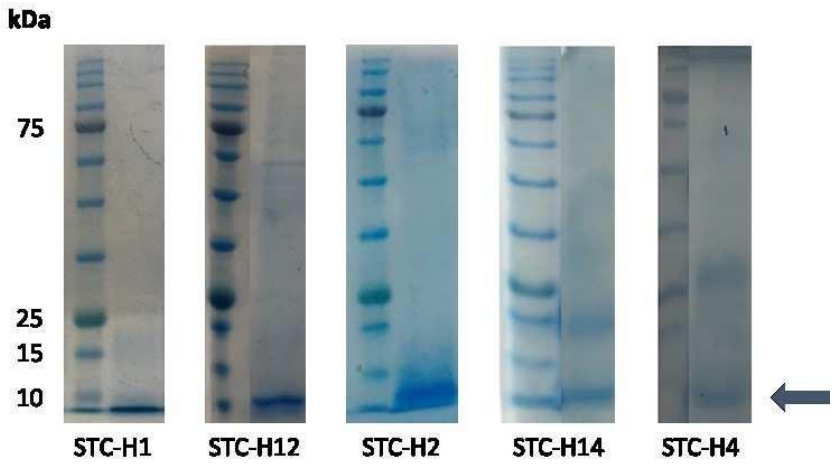

Figure IV-5. Bluesafe SDS-PAGE gel of STC mutants produced by System III

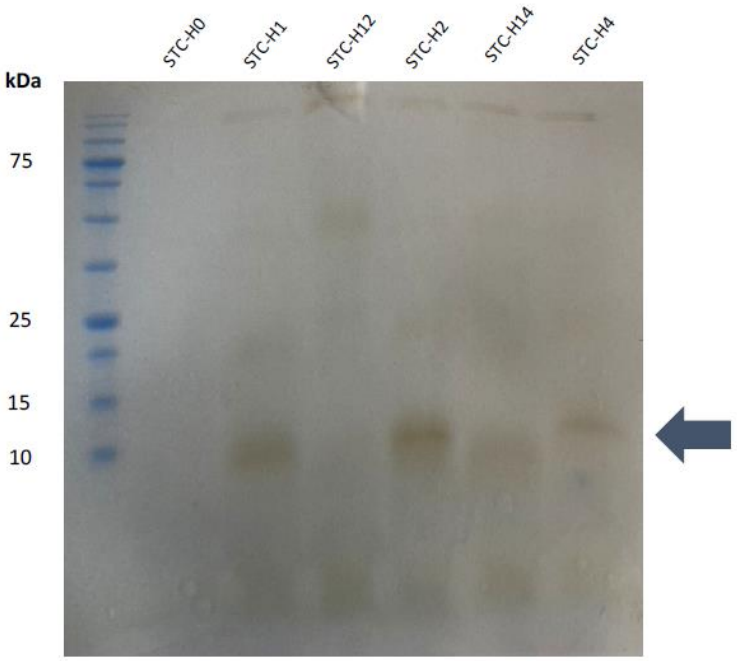

Figure IV-6: Heme-stained SDS-PAGE gel of STC mutants produced by System III

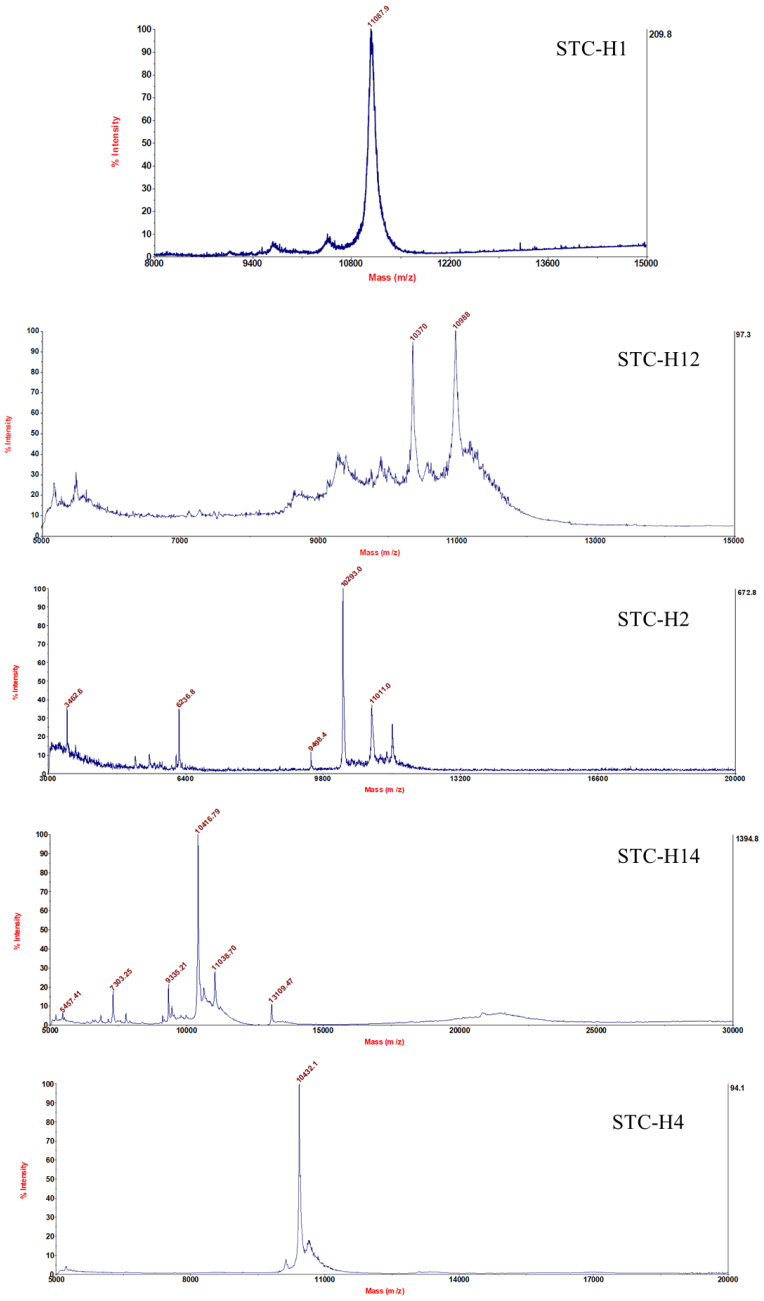

Figure IV-7: Mass spectrometry of the STC mutants produced by System III in *E. coli*. Data obtained by the Mass Spectrometry Unit (UniMS), ITQB/iBET, Oeiras, Portugal.

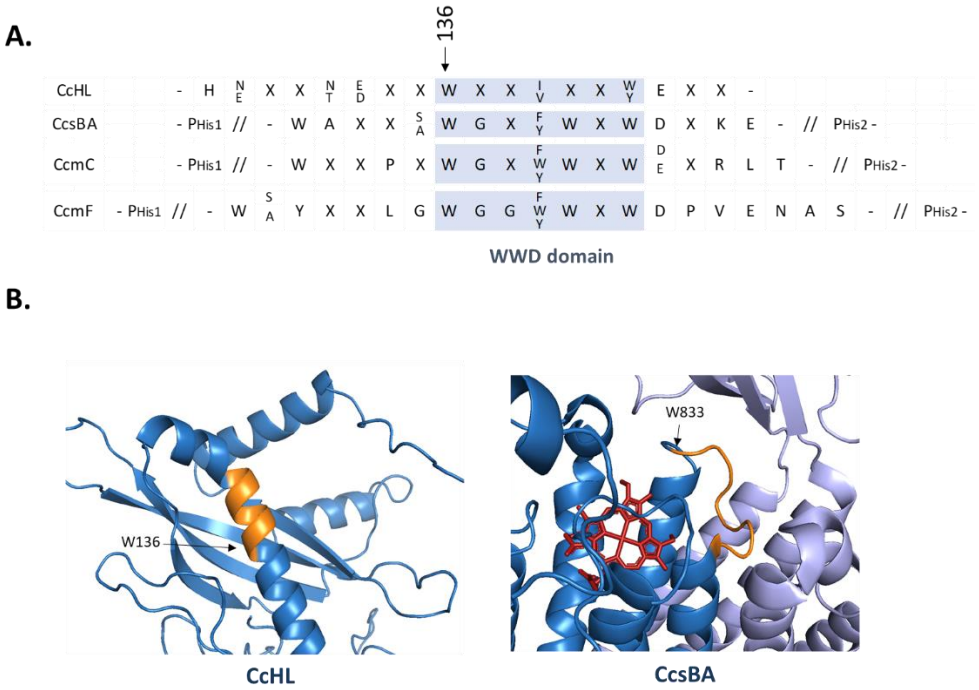

Figure IV-8 A. WWD domain in the cytochrome maturation Systems I (CcmC and CcmF), II (CcsBA), and III (CcHL), proposed to be homologous and important to recognize the heme binding region and insert the heme in the apo-protein (Babbitt *et al.* 2015; Mendez *et al.* 2022). B. Cartoon representation of the active site of CcHL (predicted by alpha-fold: AF-P06182-F1) and CcsBA (PDB: 7S9Y) composed by the WWD domain.

Chapter V

Exploring the Effects of bolA in Biofilm Formation and Current Generation by Shewanella oneidensis MR-1

The author of this dissertation performed all the experiments described in this chapter except for the qPCR analysis.

This chapter was published as a research article where the author of this thesis is the first author: Silva et al., 2020

Abstract

Microbial electrochemical technologies (METs) have emerged in recent years as promising alternative green sources of energy, with microbes consuming organic matter to produce energy or valuable by-products. It is the ability to perform extracellular electron transfer that allows these microbes to exchange electrons with an electrode in these systems. The low levels of current achieved have been the limiting factor for the large-scale application of METs. *Shewanella oneidensis* MR-1 is one of the most studied electroactive organisms regarding extracellular electron transfer, and it has been shown that biofilm formation is a key factor for current generation. The transcription factor *bolA* has been identified as a central player in biofilm formation in other organisms, with its overexpression leading to increased biofilm. In this work, we explore the effect of this gene on biofilm formation and current production by *S. oneidensis* MR-1. Our results demonstrate that an increased biofilm formation and consequent current generation was achieved by the overexpression of this gene. This information is crucial to optimize electroactive organisms toward their practical application in METs.

1. Introduction

Microorganisms have developed strategies to live in virtually every environment on Earth, being able to scavenge energy from a wide range of organic and inorganic compounds. Among these, electroactive organisms harvest energy by reducing insoluble terminal electron acceptors, such as metal oxides in their natural environment or electrodes in microbial electrochemical technologies (METs) (Richardson, 2000; Kracke, Vassilev and Krömer, 2015). In the last decades, these organisms have received considerable attention due to their promising role as self-regenerating catalysts in bioelectrochemical systems (BES) to convert chemical energy stored in biodegradable substances into electrical current (Logan *et al.*, 2006) and added-value compounds (Rabaey and Rozendal, 2010). Although BES arose as a sustainable platform for electricity production (Logan *et al.*, 2006) nowadays they can also be used for wastewater treatment, environmental bioremediation, biofuel production, bioelectrosynthesis and biosensing (Logan and Regan, 2006; Arends and Verstraete, 2012; Ucar, Zhang and Angelidaki, 2017; Logan *et al.*, 2019; Mohan, Varjani and Pandey, 2019; Simonte *et al.*, 2019). However, their large-scale application has been set back by the low power densities obtained so far, mainly limited by the slow electron transfer rates between electroactive organisms and electrodes (Logan and Rabaey, 2012; Logan *et al.*, 2019). Toward this, numerous efforts have been made in recent years to optimize power

generation in BES, including the characterization and optimization of electroactive organisms, in particular of the model organisms *Shewanella oneidensis* MR-1 and *Geobacter sulfurreducens* (Teravest and Ajo-Franklin, 2015; Yang *et al.*, 2015; Bursac, Gralnick and Gescher, 2017; Min *et al.*, 2017; Ueki *et al.*, 2018; Delgado *et al.*, 2019; Fonseca *et al.*, 2019; Reguera and Kashefi, 2019).

In BES, electroactive organisms interact directly with the electrode, via outer membrane cytochromes, nanowires or pili, or indirectly, using redox mediator molecules (e.g. flavins) (Costa *et al.*, 2018; Edel, Horn and Gescher, 2019). At the electrode, they form electroactive biofilms (EABs) (Kalathil *et al.*, 2013), which can be diverse in terms of thickness, conductivity, and shape. Indeed, the thickness and the composition of the biofilm can significantly increase current generation in BES. The increase in biofilm formation by methods such as protein overexpression (Liu *et al.*, 2015), artificial production of biofilms by exoelectrogen immobilization (Yu *et al.*, 2011), self-assembled graphene oxide - *S. oneidensis* MR-1 biofilm (Yong *et al.*, 2014) and 3D printing (Zajdel *et al.*, 2018; Freyman *et al.*, 2019) lead to significant increases in current densities, highlighting the potential of EAB manipulation to optimize BES.

The *bolA* gene, initially identified as a transcriptional regulator for cell shape in *Escherichia coli* (Aldea et al., 1988), was recently shown to be responsible for promoting biofilm development by targeting several genes encoding proteins related to this process (Dressaire et al., 2015). This gene is present in numerous electroactive organisms (Supplementary Table V-2), including in *S. oneidensis* MR-1. Herein, we report the effect of the *bolA* gene in the development of *S. oneidensis* MR-1 biofilm and the consequences for current density production in BES. We demonstrate that the *bolA* gene increases both current generation in BES and biofilm formation, opening the way for future regulation studies focusing on this gene. This work is a step forward towards a clear understanding of the genes that regulate biofilm formation in *S. oneidensis* MR-1. This knowledge is of great importance for the optimization of current production in BES, paving the way for their commercial application.

2. Materials and Methods

Construction of an S. oneidensis MR-1 bolA knock-out strain:

The *bolA* knock-out strain (Table V-1) was constructed according to what is described in Saltikov and Newman 2003. Briefly, regions of 500 bp up- and downstream of the *bolA* gene (SO_1099) (primers 1-4 Supplementary **Table V-3**) were amplified via polymerase chain

reaction (PCR). The resulting up- and downstream regions were inserted into the BamHI and SalI cleaved suicide vector pMQ150 and transformed into *E. coli* WM3064. This was later transferred to *S. oneidensis* MR-1 by conjugation. *S. oneidensis* MR-1 transconjugants containing the integrated mutagenesis vector were selected on Luria Bertani broth (LB) agar plates supplemented with kanamycin (50 µg/mL). The colonies were grown in the absence of antibiotics and subcultured twice into LB. After overnight growth at 30°C, dilutions were plated on LB agar plates supplemented with 10% sucrose and incubated overnight at 30°C. Plates were replica printed onto LB plates and LB plates supplemented with kanamycin (50 µg/mL), and kanamycin-sensitive colonies were screened by PCR for the selection of the strains with the deletion of *bolA* gene (primers 5 and 6 Supplementary Table V-3).

Table V-1: Bacterial strains used in this study.

Name	Strain
WT	*S. oneidensis* MR-1 with empty pBBR1MCS-2
WT+	*S. oneidensis* MR-1 harboring pBBR1MCS-2_*bolA*
Δ*bolA*	*S. oneidensis* MR-1 Δ*bolA* with empty pBBR1MCS-2
Δ*bolA* +	*S. oneidensis* MR-1 Δ*bolA* harboring pBBR1MCS-2_*bolA*

Cloning the bolA gene:

DNA fragments containing the *bolA* gene from *S. oneidensis* MR-1 were amplified via PCR from genomic DNA using the primers 9 and 10 listed in Supplementary Table V-3. In order to include a ribosome binding site (RBS), the gene was first amplified with the primers containing the RBS sequence (7 and 8 Supplementary Table V-3**).** The PCR product was then inserted into the pBBR1MCS-2 vector, previously digested with the restriction enzymes EcoRV and BamHI (NZYTech), using NEBuilder HiFi DNA Assembly Cloning kit (New England Biolabs). The vector containing the *bolA* gene was then transformed into the strains *S. oneidensis* MR-1 and *S. oneidensis* MR-1 Δ*bolA*, creating the strains WT+ and Δ*bolA*+, respectively (**Table V-1**). The vector pBBR1MCS-2 was a gift from Kenneth Peterson (Addgene plasmid # 85168) (Kovach *et al.*, 1995).

Bacterial growth conditions:

Bacterial strains were cultivated overnight in LB supplemented with kanamycin (50 µg/mL) at 30ºC with 150 rpm agitation. For the growth curves, cells were diluted in M4 medium (Delgado *et al.*, 2019) supplemented with kanamycin (50 µg/mL) to a starting OD_{600} of 0.07. 200 µL were then transferred to individual wells of a polystyrene flat bottom 96-well plate (Sarstedt) and allowed to grow at 30ºC without stirring. The cell density was measured at 600 nm every 30 min for 46 h using a Multiskan Sky Microplate Spectrophotometer (Thermo Scientific ™). The experiment was conducted using twelve replicates and the mean and standard deviation were calculated using MS Excel.

Microscopic imaging:

Planktonic cells were harvested from the cultures after the growth curves (46 h of growth). Samples were observed in slides coated with 1.5% (wt/vol) agarose film and enclosed with a cover glass. Images were acquired on a Leica DM 6000B upright microscope equipped with an Andor iXon 885 EMCCD camera and controlled with the MetaMorph V5.8 software, using the 100x 1.4 NA oil immersion objective plus a 1.6x optvar. Images were processed using ImageJ software.

Biofilm characterization:

Growth and analysis of static biofilms under microoxic conditions were measured using crystal violet staining on the 96-well plate resulting from the growth curve experiment according to Dressaire *et al.* 2015. Each well was cleaned 3 times with 200 µL water and then treated with 200 µL 0.1% crystal violet for 15 min. The plate was then washed 3 times with water to remove the excess crystal violet and dried at 65ºC for 15 min. To solubilize the crystal violet, 200 µL of 96% ethanol were added to each well and incubated for 15 min at room temperature and the optical density of each well was measured at 570 nm using a Multiskan Sky Microplate Spectrophotometer (Thermo Scientific ™). The ratio of biofilm development to planktonic growth was calculated using the cell density (OD_{570}/OD_{600}). An unpaired t-test was used to determine the significance of the data. The level of significance was set to 5%.

Bioelectrochemical systems (BES):

The bioelectrochemical experiments were conducted in triplicates using a single chamber BES with a working volume of 270 mL (Bursac, Gralnick and Gescher, 2017). Graphite felt (projected area of 36 cm^2, SGL Group, Germany) and platinum mesh (projected area of 1.25

cm^2, chemPUR, Germany) were used as working and counter electrode material, respectively, and an Ag/AgCl electrode (sat. KCl, 0.199 V vs. standard hydrogen electrode (SHE)) (Sensortechnik Meinsberg, Germany) was used as reference electrode. Before use, the working electrode was rinsed with isopropanol, followed by deionized water. The complete bioelectrochemical setup was sterilized by autoclaving.

Before inoculation, cells were harvested from the preculture by centrifugation (7 min, 6000 xg) and washed 3 times with M4 medium containing neither electron donor nor electron acceptor. Cells were then resuspended to a starting OD_{600} of 0.07 in M4 medium containing 70 mM lactate and kanamycin (50 µg/mL).

During chronoamperometric experiments, the working electrode was poised to 0 mV vs. SHE and current was monitored for 46 h. BES were incubated at 30 °C and constantly flushed with N_2 gas in order to ensure anoxic conditions. For constant mixing of the liquid phase, the medium was continuously agitated using a magnetic stirrer. The OD_{600} was measured in the beginning and after the 46h of the BES experiments and showed that the planktonic growth was negligible (OD_{600} < 0.02). An unpaired t-test was used to determine the significance of the data. The level of significance was set to 5%.

DNA Isolation and qPCR:

For DNA Isolation, the innuPREP Stool DNA Kit (Analytic Jena, Germany) was used according to the manufacturers' suggestions with minor modifications. Relative cell quantifications of anode samples are based on three individual MFCs. Anodes from the BES were sliced into small pieces and 5 mL of SLS buffer were added. The samples were vortexed vigorously for 1 min. Thereafter, the samples were incubated at 95 °C for 15 minutes, and vortexed every 5 minutes. DNA isolation proceeded according to the manufacturer's protocol. The quantitative PCR was performed in duplicate for each sample. Considering the triplicates of the BES experiments, the PCR result for each of the strains is based on the analysis of 6 samples. Quantitative PCR was conducted using Primers 11 and 12 (Supplementary Table V-3) according to (Dolch *et al.*, 2014).

For quantitative analysis, a standard curve using biological triplicates of the bacterial strains in six different dilutions was established. Before isolation of the DNA, the cells were counted in two different dilutions (Neubauer chamber improved, Friedrichsdorf, Germany). Based on the standard curves, cell counts of isolated DNA samples were determined. An unpaired t-

test was used to determine the significance of the data. The level of significance was set to 5%.

3. Results

Bacterial growth and cell shape:

Bacterial growth profile of the different strains was monitored for 46 h under microoxic conditions to evaluate the effect of *bolA* (Figure V-1**A**). There were no significant differences detected in the growth of the strains. Furthermore, the microscopic images taken to explore differences in cell shape show that no morphological differences exist between the strains at this scale (Figure V-1**B**).

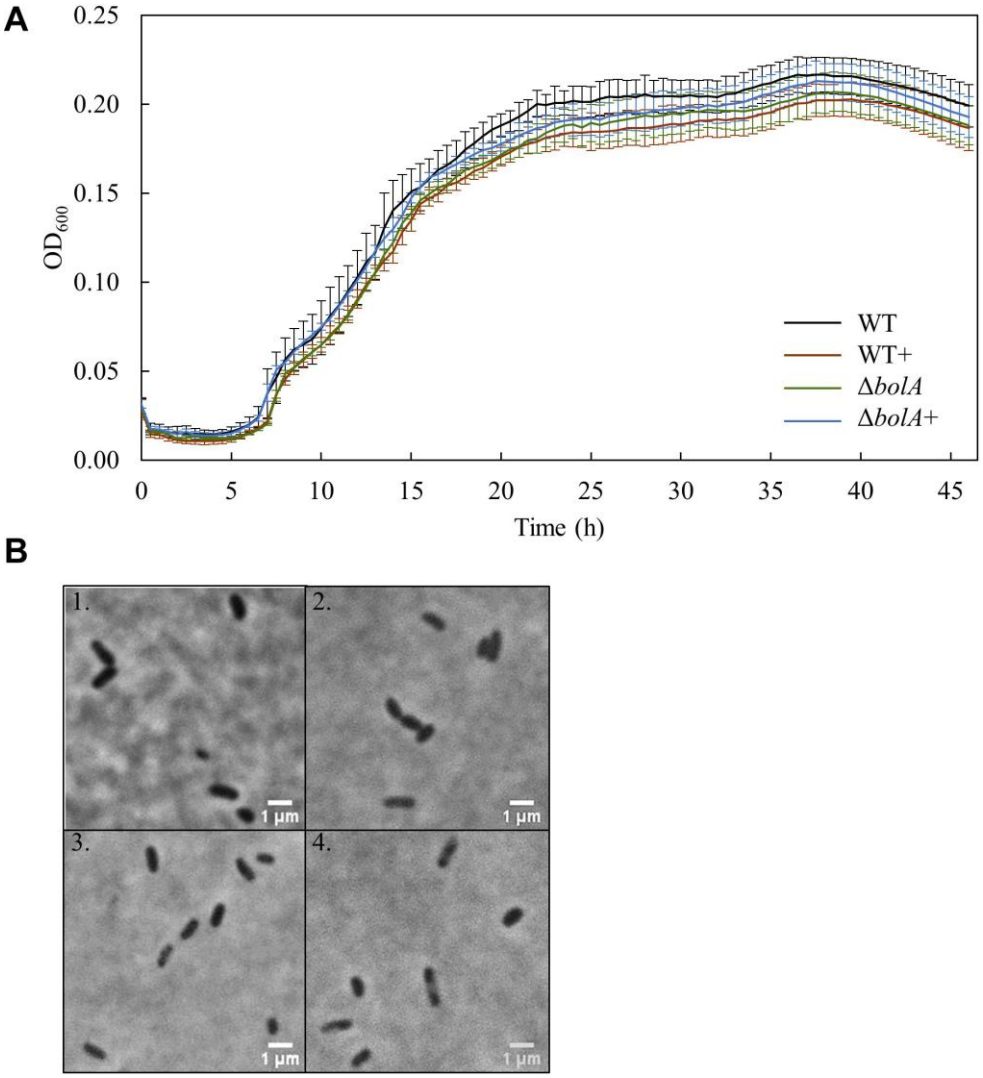

Figure V-1: (A) Growth curves of the different *S. oneidensis* MR-1 strains obtained in the 96 well-plate: Black - WT; Brown - WT+; Green - Δ*bolA*; Blue - Δ*bolA*+. Cells were cultured for

46h under microaerobic conditions in M4 medium and OD600 was measured every 30 min. (B) Phase contrast microscope imaging of the different strains: 1 - WT; 2 - WT+; 3 - Δ*bolA*; 4 - Δ*bolA*+. Pictures were taken using agarose-coated slides and cultures resulting from the growth curves.

Biofilm formation under static conditions

Cultures resulting from the growth curve were used to evaluate biofilm production by crystal violet staining (Figure V-2**A**). The results show that the overexpression of *bolA* leads to an increase in biofilm production, with significant differences (unpaired *t*-test $p<0.05$) found between the WT and both the WT+ and Δ*bolA*+. The strain WT+ produces a 1.24-fold increase in the ratio of planktonic cells to biofilm relative to the WT while the strain Δ*bolA*+ produces a 1.26-fold increase. Although the Δ*bolA* strain presents a slight increase in biofilm formation relative to the WT strain this difference is not significant.

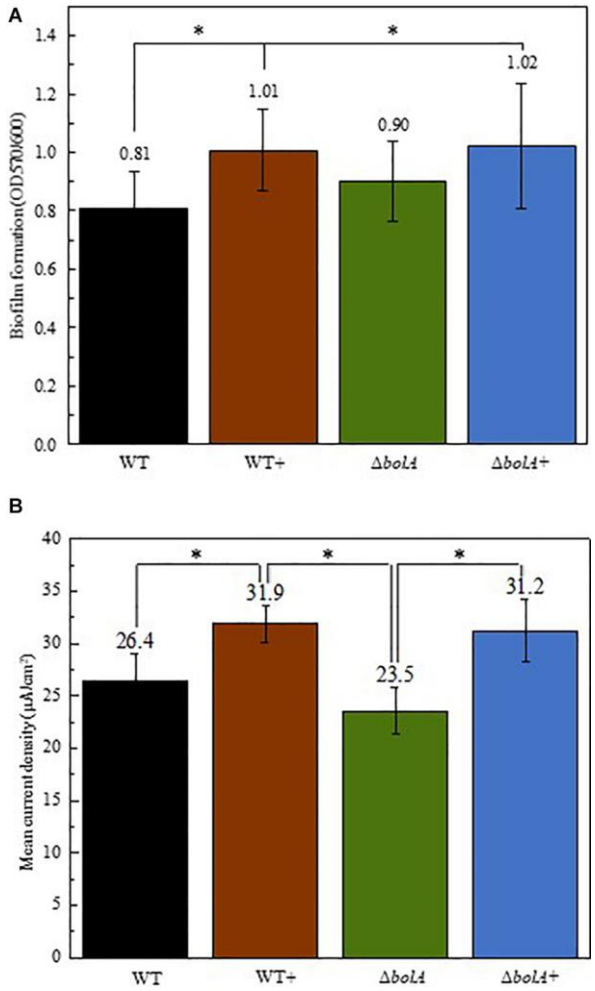

Figure V-2: Representation of the biofilm production by the different strains normalized by OD_{600} of the planktonic cultures (A) and mean current density produced by the different strains in BES (B). Black- WT; Brown- WT+; Green- Δ*bolA*; Blue- Δ*bolA*+. Biofilm formation was measured by crystal violet stain with cell cultures resulting from the growth under microaerobic conditions after 46h incubation. Error bars represent standard deviations. The potential of the anode in BES was poised to 0 vs SHE using an Ag/AgCl reference electrode. Stars represent significant differences (unpaired *t*-test $p<0.05$).

Bioelectrochemical systems (BES)

The effect of the deletion and overexpression of *bolA* in current density was explored in BES. The curves of the current density of the WT and the Δ*bolA*, as well as of the WT+ and the Δ*bolA*+ present very similar profiles (Figure V-5) When comparing the WT with the WT+ and the Δ*bolA* with the Δ*bolA*+, an increase in the produced current density can be observed. Indeed, the mean current density produced for the WT strain upon *bolA* expression (Figure

V-2**B**) shows a significantly higher current generation (unpaired *t*-test $p<0.05$) with a 1.2-fold increase. A very similar effect can be observed in the Δ*bolA*+ strain.

Quantitative PCR (qPCR)

The DNA deposited on the anodes of BES was isolated using qPCR and the DNA content was examined to evaluate if the increased current density of the *bolA* overexpressing strains correlates with cell attachment on the anode. Interestingly, the deletion of *bolA* leads to a 1.8-fold decreased amount of DNA on the anode (**Figure V-3**), while the complementation of the *bolA* deletion shows almost the same amount of DNA on the anode as the WT. No significant difference was observed between the WT and the *bolA* overexpressing strain (WT+).

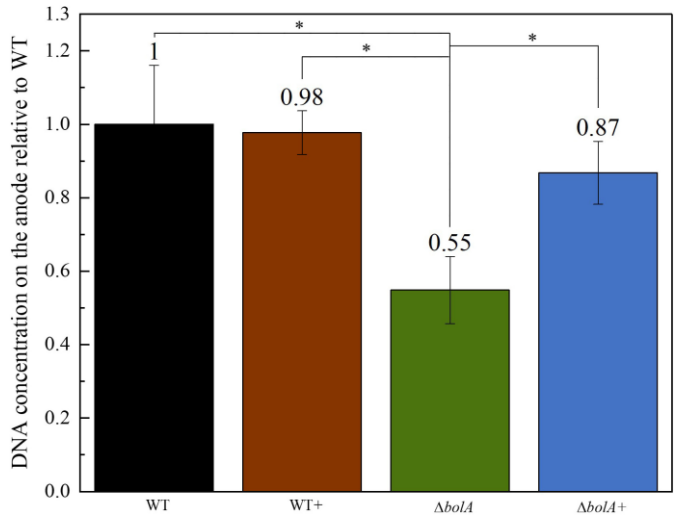

Figure V-3: Amount of DNA on the anode relative to the wildtype determined by qPCR. DNA was isolated from the anodes after BES experiments. Stars represent significant differences (unpaired *t*-test $p<0.05$).

4. *Discussion*

The *bolA* gene was originally identified as a transcriptional regulator for cell shape in *E. coli*, as its overexpression leads to round cell morphology (Aldea *et al.*, 1988). BolA was demonstrated to promote biofilm development by targeting several genes encoding proteins related to this process, being described as a modulator for the switch between planktonic to sessile lifestyles (Vieira, Freire and Arraiano, 2004; Dressaire *et al.*, 2015).

In this work, we addressed the effect of this gene in *S. oneidensis* MR-1, one of the most widely studied microorganisms regarding extracellular electron transfer in BES. It has been

demonstrated that, in these systems, an increase in biofilm thickness leads to an improvement in current generation (Yu *et al.*, 2011; Yong *et al.*, 2014; Liu *et al.*, 2015; Zajdel *et al.*, 2018; Freyman *et al.*, 2019).

At least 10 of the 11 *Shewanella* species described as electroactive (Koch and Harnisch, 2016) contain this gene. The only exception is *S. electrodiphila* for which the genome is not available and, therefore, the presence of the gene could not be confirmed. Among the different electroactive *Shewanella* species, the gene maintains 39.62% identity, with *S. lohica* being the least similar to *S. oneidensis* MR-1 (56.12 % identity) and *Shewanella* sp. ANA-3 the most similar (93.4 % identity) (Figure V-4).

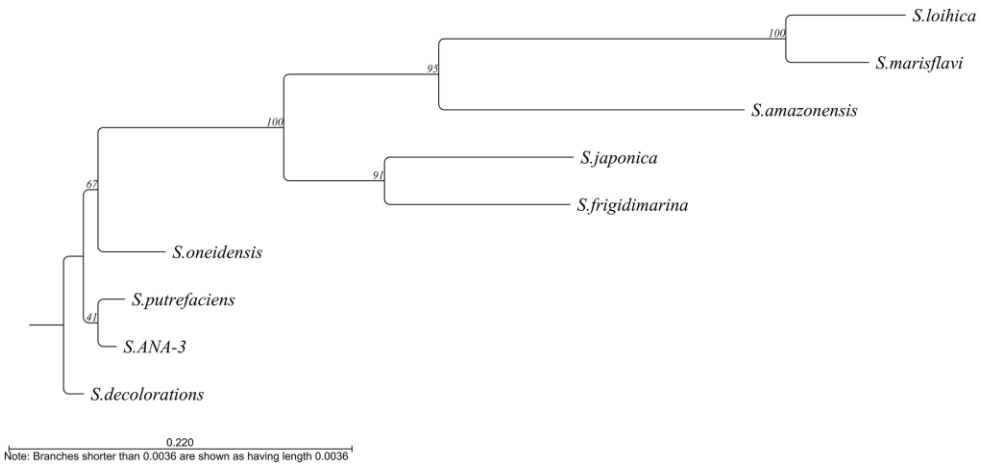

Figure V-4: Phylogenetic tree based on the alignment of the *bolA* sequence from the different electroactive *Shewanella* species. Tree constructed by neighbor-joining using CLC main workbench 8.1 software (Qiagen).

In accordance with what is described for *E. coli* (Dressaire *et al.*, 2015) and *Salmonella enterica* (Mil-homens *et al.*, 2018), the overexpression or deletion of *bolA* does not affect the growth profiles of the different strains. Moreover, contrary to what is described for *E. coli*, we could not detect any cell shape alteration in *S. oneidensis* MR-1 upon *bolA* overexpression (Figure V-1). Although the stress-inducible morphogene *bolA* is widely conserved in all kingdoms of life, leading to a decrease in the surface to volume ratio as an adaptation to harsh conditions (Guinote *et al.*, 2014), it does not affect cell shape in carbon starvation or late stages of growth in all organisms (Koch and Nybroe, 2006). Indeed, no changes in cell morphology could be detected upon *bolA* overexpression in *Pseudomonas fluorescens* (Koch and Nybroe, 2006), a bacterium that is highly homologous to *S. oneidensis* MR-1 (Hau

and Gralnick, 2007). Furthermore, it has been shown that only some homologs of the *bolA* gene have an effect on cell morphology in *E. coli* (Khona *et al.*, 2013).

Differences could also be observed in the biofilm formation, with the overexpression and complemented strains producing an approximate 1.25-fold increase in biofilm production. This result relates very well with the 1.2-fold increase in the mean current density observed upon expression of the *bolA* gene. Although the amount of DNA deposited on the anode in the Δ*bolA*+ strain was higher than that of the Δ*bolA*, this was not observed for the WT strain. As the qPCR detects both intracellular DNA and extracellular DNA, that can be embedded in the biofilm matrix and help in extracellular electron transfer processes, it is difficult to determine if the *bolA* gene promotes biofilm formation by increasing extracellular DNA.

Our data corroborate the hypothesis that an increase in biofilm thickness can lead to higher current generation by electroactive organisms (Yu *et al.*, 2011; Yong *et al.*, 2014; Liu *et al.*, 2015; Zajdel *et al.*, 2018; Edel, Horn and Gescher, 2019; Freyman *et al.*, 2019). The deletion of *bolA*, however, does not interfere with biofilm formation, with the strain producing comparable amounts of biofilm to the WT. This may be a consequence of the fact that the harsh conditions necessary for *S. oneidensis* MR-1 to activate BolA have not been achieved in the WT strain. The same results were reported for *E. coli* but have not been explored further (Dressaire *et al.*, 2015).

The biofilm assay was conducted under microoxic conditions given the inability to detect biofilm formation using this protocol under anoxic conditions. This could be attributed to the low optical densities obtained when growing *S. oneidensis* MR-1 in minimal medium under anoxic conditions in the 96-well plates. Moreover, in the case of oxic or microoxic conditions, the biofilm is formed on the top of the well, at the interface between the culture medium and oxygen, which allows the cells to get both nutrients and the terminal electron acceptor (i.e. oxygen). In contrast, under anoxic conditions, this interface is not present, as the terminal electron acceptor (i.e. fumarate) is soluble in the medium. In BES, the oxygen is absent and the electrode acts as the terminal electron acceptor, promoting biofilm development on its surface.

This work demonstrates that *bolA* is involved in the biofilm formation in *S. oneidensis* MR-1, with its overexpression contributing to an increase in biofilm formation. We could also demonstrate that this increase enhances current production in BES. Further studies are however necessary to characterize the regulatory network of this gene and its protein

product. Indeed, it has been demonstrated that *bolA* interferes with the transition from planktonic lifestyle to biofilm by balancing the intracellular concentration of cyclic-di-GMP (Moreira *et al.*, 2017). Interestingly, this bacterial second messenger was also shown to be an important intracellular regulator for controlling biofilm stability in *S. oneidensis* MR-1 (Thormann *et al.*, 2006). The quantification of cyclic-di-GMP, as well as the understanding of what processes *bolA* regulates would increase our knowledge in enhancing biofilm formation and consequently increase current production in BES.

5. *Supplementary Material*

BolA distribution

Table V-2: List of electroactive organisms (according to Koch and Harnisch 2016) with the indication of the presence or absence of the BolA protein. The presence of BolA was determined by searching each organism's genome in NCBI with the term "BolA" in the corresponding protein list.

Organism	BolA	BolA code
Acidiphilium cryptum	Yes	WP_007423540.1
Acidithiobacillus ferrooxidans	Yes	WP_009560822.1
Acinetobacter calcoaceticus	Yes	WP_133975907.1
Acinetobacter johnsonii	Yes	WP_005401913.1
Actinobacillus succinogenes	Yes	WP_012072352.1
Aeromonas hydrophila	Yes	WP_010673364.1
Anabaena variabilis	Yes	WP_010994972.1
Azospira suillum	Yes*	WP_014236502.1/WP_043799444.1
Bacillus subtilis	Yes	WP_100506968
Branhamella catarrhalis	Yes	WP_120672796.1
Brevundimonas diminuta	Yes	WP_003166945.1

Burkholderia cepacia	Yes	WP_059233936.1
Calditerrivibrio nitroreducens	No	-
Citrobacter freundii	Yes	WP_038638264.1
Citrobacter sp. SX-1	Yes*	WP_042324511.1
Clostridium aceticum	No	-
Clostridium acetobutylicum	No	-
Clostridium butyricum	No	-
Clostridium ljungdahlii	No	-
Clostridium pasteurianum	No	-
Clostridium propionicum	No	-
Clostridium tyrobutyricum	No	-
Comamonas denitrificans	Yes*	WP_043373767.1/WP_003058653.1
Comamonas testosteroni	Yes	WP_034365915.1
Corynebacterium glutamicum (Brevibacterium flavum)	No	-
Corynebacterium sp. MFC03	No*	-
Dechloromonas agitata	Yes	WP_027458058.1
Desulfitobacterium hafniense	No	-
Desulfobulbus propionicus	No	-
Desulfovibrio desulfuricans	No	-
Desulfuromonas acetoxidans	No	-
Enterobacter cloacae (Erwinia dissolvens)	Yes	WP_129362423.1
Escherichia coli	Yes	NP_414969.4

Faecalibacterium prausnitzii	No	-
Geoalkalibacter ferrihydriticus	No	-
Geoalkalibacter subterraneus	No*	-
Geobacillus sp. S2E	No*	-
Geobacter anodireducens	No*	-
Geobacter bemidjiensis	No	-
Geobacter bremensis	No	-
Geobacter chapellei	No*	-
Geobacter humireducens	No*	-
Geobacter hydrogenophilus	No*	-
Geobacter lovleyi	No	-
Geobacter metallireducens	No	-
Geobacter sulfurreducens	No	-
Geobacter uraniireducens	No	-
Geopsychrobacter electrodiphilus	No	-
Geothrix fermentans	No	-
Gluconobacter oxydans	Yes	WP_062449716.1
Kingella denitrificans	Yes	WP_003781876.1
Kingella kingae	Yes	WP_003785498.1
Klebsiella pneumoniae	Yes	WP_048270466.1
Lactobacillus plantarum	No	-
Mariprofundus ferrooxydans	Yes	WP_009849673.1
Methanobacterium palustre	No*	-

Methanococcus maripaludis	No	-
Micrococcus luteus	No	-
Moorella thermoacetica	No	-
Ochrobactrum anthropi	Yes	WP_010657613.1/WP_006466620.1
Propionibacterium freudenreichii	No	-
Proteus mirabilis	Yes	WP_088493680.1
Proteus vulgaris	Yes	WP_072069384.1
Pseudomonas aeruginosa	Yes	WP_009686014.1
Pseudomonas alcaliphila	Yes	WP_074675136.1
Pseudomonas fluorescens	Yes	WP_126365315.1
Raoultella electrica	Yes	WP_041144317.1
Rhodobacter capsulatus	Yes	WP_013066292.1
Rhodobacter sphaeroides	Yes	YP_352030.1
Rhodoferax ferrireducens	Yes	WP_011464683.1
Rhodopseudomonas palustris	Yes	WP_110787197.1
Shewanella amazonensis	Yes	WP_011760654.1
Shewanella decolorationis	Yes	WP_023268362.1
Shewanella electrodiphila	Yes*	WP_144044753.1/WP_144045332.1
Shewanella frigidimarina	Yes	WP_011636419.1
Shewanella japonica	Yes	WP_055023677.1
Shewanella loihica	Yes	WP_011866680.1
Shewanella marisflavi	Yes	WP_088904080.1
Shewanella oneidensis	Yes	NP_716725.2

Shewanella putrefaciens	Yes	WP_011621726.1
Shewanella sp. ANA-3	Yes	WP_011716063.1
Shewanella sp. HN-41	Yes	WP_037458006.1
Shigella flexneri	Yes	NP_706328.3
Spirulina platensis	Yes	WP_006622964.1
Sporomusa ovata	No	-
Sporomusa silvacetica	No	-
Sporomusa sphaeroides	No	-
Staphylococcus carnosus	No	-
Streptococcus lactis	No	-
Synechococcus PCC 6301	Yes	WP_011242716.1
Thermincola ferriacetica	No	-
Thermincola potens	No	-
Tolumonas osonensis	Yes*	TXH65455.1/TXH61899.1
Winogradskyella poriferorum	No*	-

** Genome of the organism could not be found. The indication of the presence of BolA was based on the genus information.*

Primers used

Table V-3: List of primers used in the study and their purpose.

Number	Name	Sequence	Purpose
1	pMQSalI_500up	CAGTGCCAAGCTTGCATGCCTGCAGGTTGCAAAAATTACGCGATAAATTAC	Deletion of *bolA*
2	RevCom_500up	ATTCAAATCTCGACATGGGTAAATC	
3	500up_500dn	AGATTTGAAT TTAACGCGATTTAGGACGG	
4	500dn_pMQBamHI	CGAATTCGAGCTCGGTACCCGGGGATCCGAATACCGCAAAGGCAG	
5	Confirmation_ FW	GTATGGCGACCTAGGATGT	Test deletion of *bolA*
6	Confrimation_Rv	GAGTTTTGCCCTTCCAATAATAGG	
7	RBS_bolA_Forw	TAAGAAGGAGATATACATCCCATGTCCAATACCCAAGAGCAGGGCACAGTG	Insertion of a ribosome binding site
8	RBS_bolA_Rev	ATGAATAATTTTATCAGATCCCATTTAACCGCGGCAATTAGGTGTTTTGGGC	
9	bolA_pBBR_Forw	GTATCGATAAGCTTGATATCGAAGGAGATATACATACCC	Clone *bolA* in pBBR plasmid
10	bolA_pBBR_Rev	CTAGAACTAGTGGATCCTTAACCGCGGCAATTAG	
12	mioC_for_qPCR	TATTCAAGTGCTTCTATTAG	qPCR analysis
13	mioC_rev_qPCR	AAGAACTTCTACTCAACA	

Chronoamperometry curves

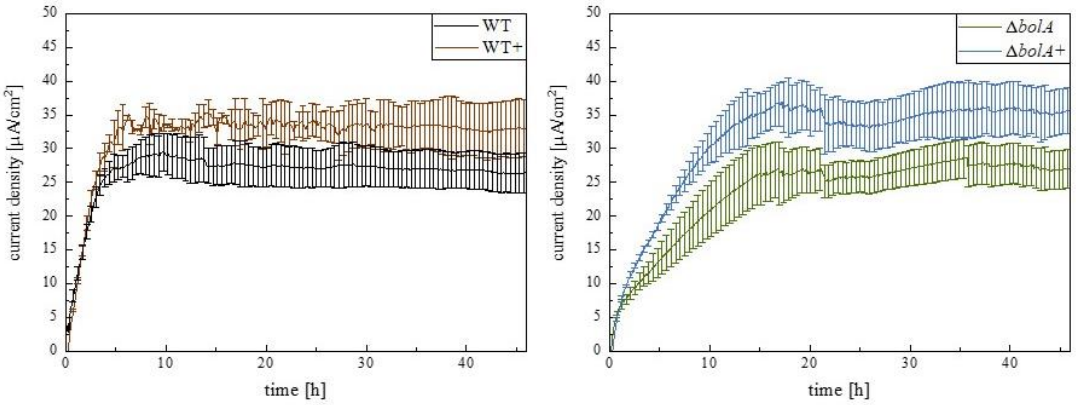

Figure V-5: Current density produced by the different strains. Black- WT; Brown- WT+; Green- Δ*bolA*; Blue- Δ*bolA*+. The potential of the anode in BES was poised to 0 vs SHE using an Ag/AgCl reference electrode.

Chapter VI

Exploring the Effects of ibaG, a bolA homolog, in the Biofilm Formation and Current Generation by Shewanella oneidensis MR-1

The author of this dissertation performed all the experiments described in this chapter except for the genome sequence analyses.

Abstract

Bioelectrochemical systems are emerging as sustainable platforms for the production of energy and valuable products capable of dealing with the increasing problems of overpopulation and energy crises. However, the large-scale application of this technology has been set back mainly by the low power densities obtained. *Shewanella oneidensis* MR-1 is one of the most studied electroactive organisms regarding extracellular electron transfer, and it has been shown that its biofilm formation is a key factor for current generation. Following the work on the transcription factor *bolA*, in this work, its homolog, *ibaG* is addressed and its effects on current generation and biofilm productions are studied. Results indicate that despite their homology and modeled structural similarity, these proteins have different modes of action, producing different effects on current generation and biofilm formation.

1. *Introduction*

Bioelectrochemical systems (BES) emerged as a sustainable platform for energy generation, wastewater treatment, and production of valuable compounds. These technologies offer great promise in the scope of solving the increasing problems of overpopulation and the energy crisis. However, the large-scale application of these systems is still limited mainly due to the low power densities obtained so far (Holtmann and Harnisch, 2019; Mohan, Varjani and Pandey, 2019; Hernandez and Osma, 2020; Jadhav *et al.*, 2021; Peñacoba-Antona *et al.*, 2022).

Over the years, the scientific community has been working towards the optimization of the electron transfer rates between electroactive organisms and electrodes, including the study of electroactive organisms, mainly, of the model organisms *Shewanella oneidensis* MR-1 and *Geobacter sulfurreducens* (Teravest and Ajo-Franklin, 2015; Yang *et al.*, 2015; Bursac, Gralnick and Gescher, 2017; Min *et al.*, 2017; Ueki *et al.*, 2018; Delgado *et al.*, 2019; Fonseca *et al.*, 2019; Reguera and Kashefi, 2019). In BES, electroactive organisms interact directly with the electrode via outer

membrane cytochromes, nanowires or pili, or indirectly, using redox mediator molecules (e.g. flavins) (Costa *et al.*, 2018; Edel, Horn and Gescher, 2019). By growing on the electrode, they form electroactive biofilms (EABs). Bacterial biofilms are communities of cells adhered to each other and to a surface or an interface, which are embedded in a matrix of extracellular polymeric substances (EPS) (Coenye, 2013; Xu *et al.*, 2016). This matrix is composed of proteins, nucleic acids, and polysaccharides that are produced by the cells (Xu *et al.*, 2016).

The *bolA* gene was initially identified as a transcriptional regulator for cell shape in *Escherichia coli* (Aldea *et al.*, 1988), and it was later shown to be responsible for promoting biofilm development in this organism (Dressaire *et al.,* 2015). This gene is present in numerous electroactive organisms, including in *S. oneidensis* MR-1, where we showed that the overexpression of the *bolA* gene can lead to increased biofilm formation and current generation in BES (Silva *et al.*, 2020).

S. oneidensis MR-1, like many other organisms, contains more than one gene encoding BolA family proteins in its genome. In this bacterium, the gene that encodes for IbaG, an 83 aminoacid protein is also found in the genome. Studies regarding IbaG are very scarce and indicate that this protein plays different roles than its homolog, BolA (Takamatsu *et al.*, 1999; Guinote *et al.*, 2012; Dlouhy *et al.*, 2016; Fleurie *et al.*, 2019). However, none of the studies focus on biofilm formation.

No other genes coding for this family of proteins are found in *S. oneidensis* MR-1. Given the homology between *bolA* and *ibaG*, in this work, we investigated the effect of IbaG on the biofilm formation and current generation by *S. oneidensis* MR-1.

2. *Materials and methods*

Bioinformatics analysis of BolA and IbaG

BolA and IbaG homologous amino acid sequences were searched in proteomes from 82 *Shewanella* spp. reference genomes (Supplementary **Table VI-3**) that were gathered from NCBI RefSeq database (O'Leary *et al.*, 2016) using the NCBI Datasets (Beta) tool on January 8th, 2023. BolA and IbaG homologous amino acid sequences were identified using BLASTp 2.13.0+ (Altschul *et al.*, 1990; Camacho *et al.*, 2009). *S. oneidensis* MR-1 BolA (NCBI RefSeq accession code: WP_011071343.1) and IbaG (NCBI RefSeq accession code: WP_011073688.1) were used as query sequences. Matches were considered when having at least 40% identity and 75% query coverage. These threshold conditions were successful to distinguish BolA and IbaG as no matches between the two groups (BolA sequences and IbaG sequences) were found. Amino acid sequence conservation was calculated for the BolA and IbaG sequences using the MEGA 7 platform (Kumar, Stecher and Tamura, 2016): Sequences were aligned using ClustalW (Thompson, Higgins and Gibson, 1994). Overall mean distances were individually computed using the p-distance model (Nei and Kumar, 2000), uniform rates, and pairwise deletion methods. Standard errors were calculated using the Bootstrap method (Efron, 1979) with 1,000 replications.

Construction of S. oneidensis MR-1 strains

All the *IbaG* knock-out and complementary strains (**Table VI-1**) were constructed and cloned according to what is described in (Silva *et al.*, 2020) using primers 1-6 (Supplementary **Table VI-4**). Briefly, regions of 500 bp up- and downstream of the *ibaG* gene (SO_3949) were amplified and inserted in the suicide vector pMQ150. The plasmid was transformed in *E. coli* WM3064 and transferred to *S. oneidensis* MR-1 by conjugation. Transconjugants containing the integrated mutagenesis vector were selected and subsequence medium changes were performed to promote plasmid loss.

Kanamycin-sensitive colonies were screened by PCR for the selection of the strains with the deletion of *ibaG*.

The *ibaG* gene was amplified using primers 7 and 8 (Supplementary **Table VI-4**). The PCR product was then inserted into the pBBR1MCS-2 vector, previously digested with the restriction enzymes EcoRV and BamHI (NZYTech), using NEBuilder HiFi DNA Assembly Cloning kit (New England Biolabs). The resulting plasmid was electroporated in *S. oneidensis* cells for the creation of the WT+ and Δ*ibaG* + strains. The WT, Δ*ibaG,* and Δ*ibaG*Δ*bolA* strains were created by electroporation of the empty pBBR vector in the corresponding strains.

Table VI-1: Bacterial strains used in this study

Name	Strain
WT	*S. oneidensis* MR-1 with empty pBBR1MCS-2
WT+	*S. oneidensis* MR-1 harboring pBBR1MCS-2_*ibaG*
ΔibaG	*S. oneidensis* MR-1 Δ*ibaG* with empty pBBR1MCS-2
Δ*ibaG* +	*S. oneidensis* MR-1 Δ *ibaG* harboring pBBR1MCS-2_ *ibaG*
ΔibaGΔbolA	*S. oneidensis* MR-1 Δ*ibaG*Δ*bolA* with empty pBBR1MCS-2

Bacterial growth conditions

Bacterial strains were cultivated overnight in LB supplemented with kanamycin (50 µg/mL) at 30 ºC with 150 rpm agitation. For the growth curves, cells were diluted in M4 medium supplemented with kanamycin (50 µg/mL) (Delgado *et al.*, 2019). 200 µL were then transferred to individual wells of a polystyrene flat bottom 96-well plate (Sarstedt) and allowed to grow at 30 ºC without stirring. The cell density was measured at 600 nm every 30 min for 46 h using a Multiskan Sky Microplate Spectrophotometer (Thermo Scientific ™). The experiment was conducted using twelve replicates and the mean and standard deviation were calculated using MS Excel.

Microscopic imaging

Planktonic cells were harvested by centrifugation from the cultures after the growth curves experiment (46 h of growth). Samples were observed in slides coated with 1.5% (wt/vol) agarose film and enclosed with a cover glass. Images were acquired on a Leica DM 6000B upright microscope equipped with an Andor iXon 885 EMCCD camera and controlled with the MetaMorph V5.8 software, using the 100x 1.4 NA oil immersion objective plus a 1.6x optvar. Images were treated using ImageJ software.

Biofilm characterization

Growth and analysis of static biofilms under microoxic conditions were measured using crystal violet staining on the 96-well plates (Sarsted) resulting from the growth curve experiment as described in Silva *et al.*, 2020. Briefly, supernatant cultures were removed, and each well was cleaned 2 times with 200 µL water. The wells were then treated with 200 µL 0.1% crystal violet for 15 min. The plate was washed 3 times with water to remove the excess crystal violet and dried at 65 ºC for 1 hour. To solubilize the crystal violet, 200 µL of 96% ethanol were added to each well and incubated for 15 min at room temperature. The optical density of each well was measured at 570 nm using a Multiskan Sky Microplate Spectrophotometer (Thermo Scientific ^{TM}). The ratio of biofilm development to planktonic growth was calculated and plotted using the cell density (OD_{570}/OD_{600}) in MS Excel.

Bioelectrochemical systems (BES)

The bioelectrochemical experiments were conducted in triplicates using a single chamber BES with a working volume of 270 mL (Bursac, Gralnick and Gescher, 2017). Graphite felt (projected area of 36 cm^2, SGL Group, Germany) and platinum mesh (projected area of 1.25 cm^2, chemPUR, Germany) were used as working and counter electrode material, respectively, and an Ag/AgCl electrode (sat. KCl, 0.199 V vs. standard hydrogen electrode (SHE)) (Sensortechnik Meinsberg, Germany) was used as reference electrode. Before use, the working electrode was soaked in isopropanol,

followed by deionized water. The complete bioelectrochemical setup was sterilized by autoclaving.

Pre-cultured cells were harvested by centrifugation (7 min, 6000 g) and washed 3 times with M4 medium containing neither electron donor nor electron acceptor. Cells were then resuspended in M4 medium supplemented with 70 mM lactate and 50 µg/mL kanamycin to a starting OD_{600} of 0.07.

During chronoamperometric experiments, the working electrode was poised to 0 mV vs. SHE, and the current was monitored for 46 h. BES were incubated at 30 °C with constant stirring and N_2 gas purging.

3. *Results:*

Comparison between BolA and IbaG

The sequence alignment of the two proteins allowed the confirmation that BolA and IbaG are homologs (**Figure VI-1A**). The proteins share 22.4 % identity and 44.9 % similarity. Alpha fold models of the proteins show that the predicted structure of the proteins is very similar (**Figure VI-1B**) and that the main structural elements are conserved. The conserved residues between the two proteins are well dispersed in the aminoacid sequence within the overall length of the protein, allowing their structural similarity (**Figure VI-1A** and **C**)

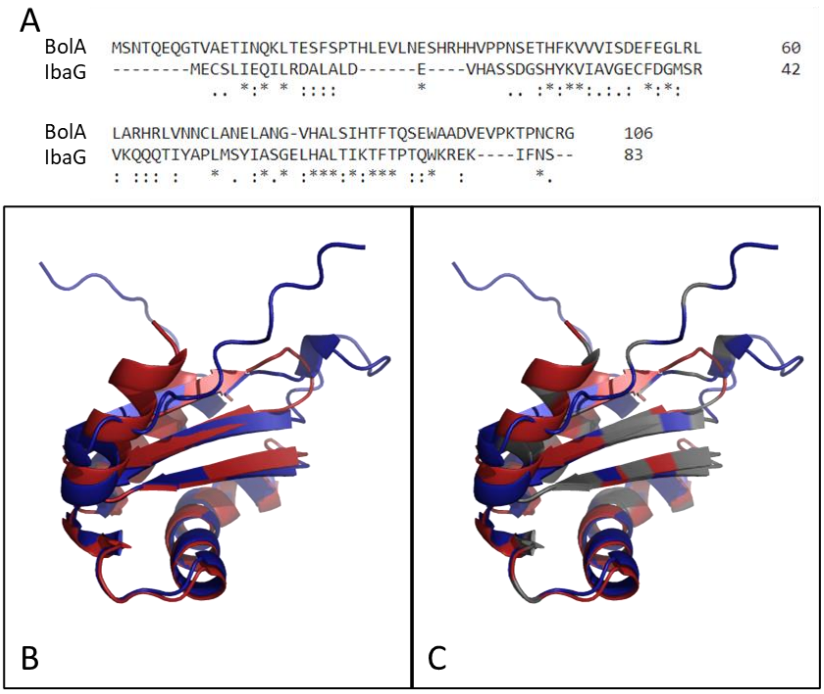

Figure VI-1: A) Sequence alignment of BolA and IbaG; B) Alignment of AlphaFold models of BolA (blue - AF-Q8EHW3) and IbaG (red - AF-A0A2W5E6Q0); C) Distribution of the conserved residues (grey) in the BolA (blue) and IbaG (red) structures.

Conservation of BolA and IbaG in the Shewanella genus

To analyze the conservation of the two proteins the 82 genomes available for *Shewanella* were retrieved and scanned for the two homologs (Supplementary **Table VI-3**). The protein sequences were aligned and the number of amino acid differences per site from averaging over all sequence pairs was calculated for BolA and IbaG (**Table VI-2**). From here, it is possible to observe that IbaG is more conserved than BolA. Fourteen sequences were completely equal for IbaG and only two for BolA.

Table VI-2: Estimates of Average Evolutionary Divergence over all Sequence Pairs.

	BolA	IbaG
d	0.316 ± 0.03	0.251 ± 0.028

The alignment of the protein sequences allowed the identification of conserved residues in both proteins (**Figure VI-2** and **Figure VI-3**).

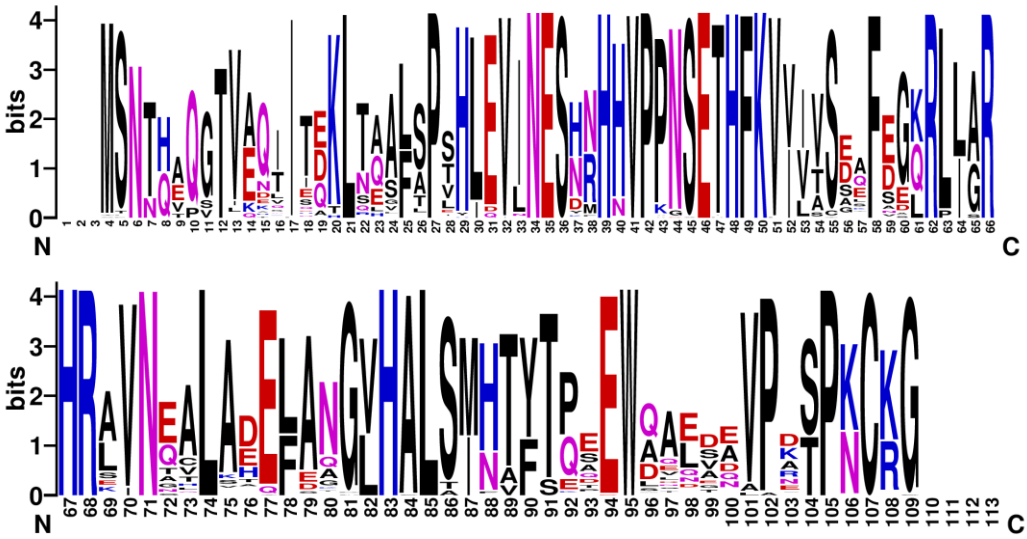

Figure VI-2: WebLogo image of the alignment of the 82 *Shewanella* BolA protein sequences.

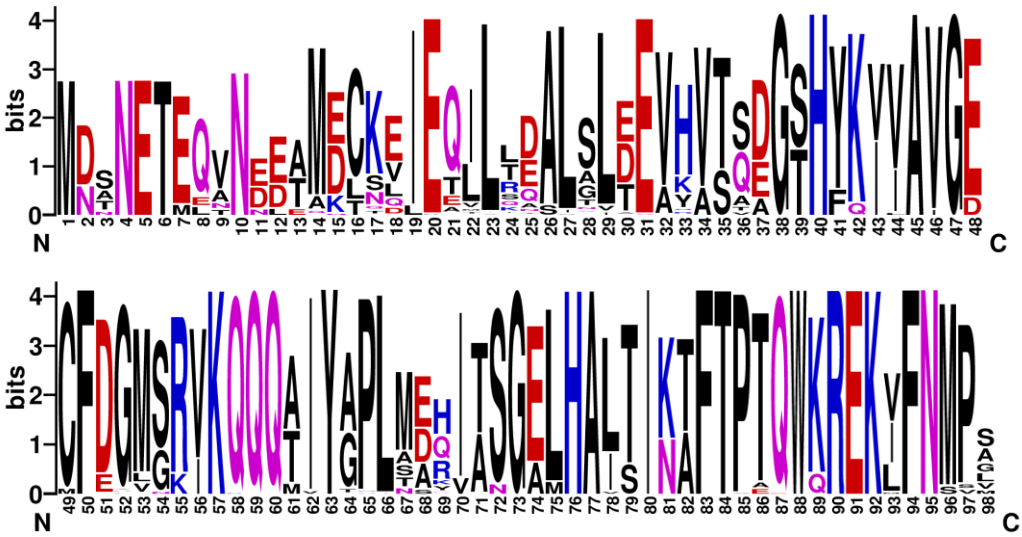

Figure VI-3: WebLogo image of the alignment of the 82 *Shewanella* IbaG protein sequences.

Bacterial growth and cell shape

The effect of IbaG in the bacterial growth profile was addressed by monitoring the growth of the different overexpression and deletion strains (**Table VI-1**) for 46 h under microoxic conditions (Supplementary **Figure VI-7**). There were no significant differences detected in the growth of the strains. The microscopic images taken to explore differences in cell shape show that no morphological differences exist between the strains (Supplementary **Figure VI-8**), indicating that the deletion or overexpression of this gene does not affect the growth or morphology of the *S. oneidensis* cells.

Biofilm formation and current generation

The effect of the deletion and overexpression of IbaG in current density was explored in BES. When comparing the mean current density produced for the strains, no significant differences could be observed between the WT (data from Silva *et al.*, 2020) and any of the mutant strains after 46 h of growth (**Figure VI-4**) using the same BES setup. However, from the chronoamperometry data (Supplementary **Figure VI-9**) it is possible to

observe that the maximum current production between the strains is quite distinct. This data demonstrated that similar profiles exist between WT, WT+, and Δ*ibaG*, while the Δ*ibaG*+ and Δ*ibaG*Δ*bolA* strains present different profiles, with lower current density maximum values.

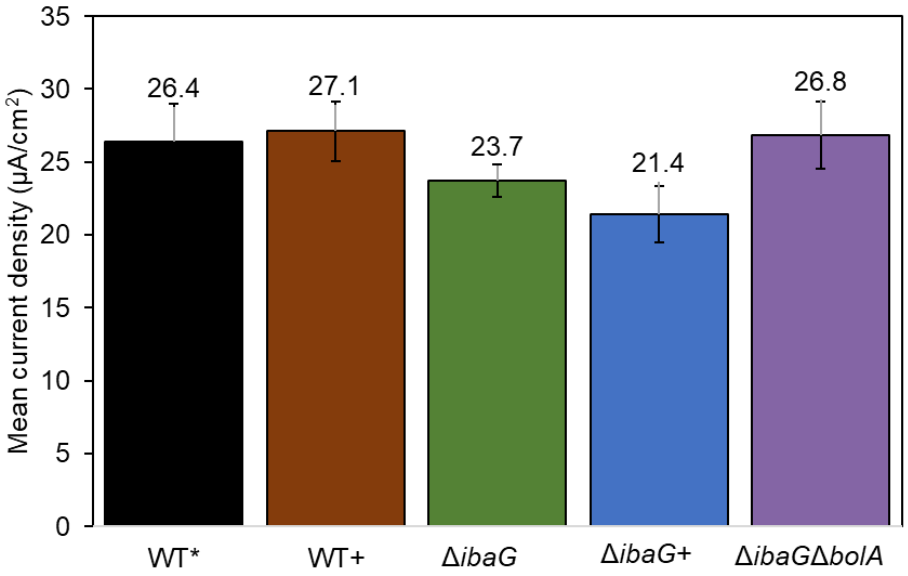

Figure VI-4: Mean current density produced by the different strains in BES. Black – WT; Brown – WT+; Green – Δ*ibaG*; Blue – Δ*ibaG*+; Purple - Δ*ibaG*Δ*bolA*. Error bars represent standard deviations. WT values from Silva *et al.*, 2020.

Cultures resulting from the growth curve were used to evaluate biofilm production by crystal violet staining (**Figure VI-5**). The results show that the overexpression of IbaG does not influence biofilm formation. However, an effect caused by the deletion of the gene that is not completely restored by its expression (Δ+) has been observed. Furthermore, when both *bolA* and *ibaG* are deleted a large effect on the biofilm formation occurs. Visual analysis of the biofilm (Supplementary **Figure VI-10**) shows that the morphology of the biofilm seems to be affected, rather than the amount of biofilm produced.

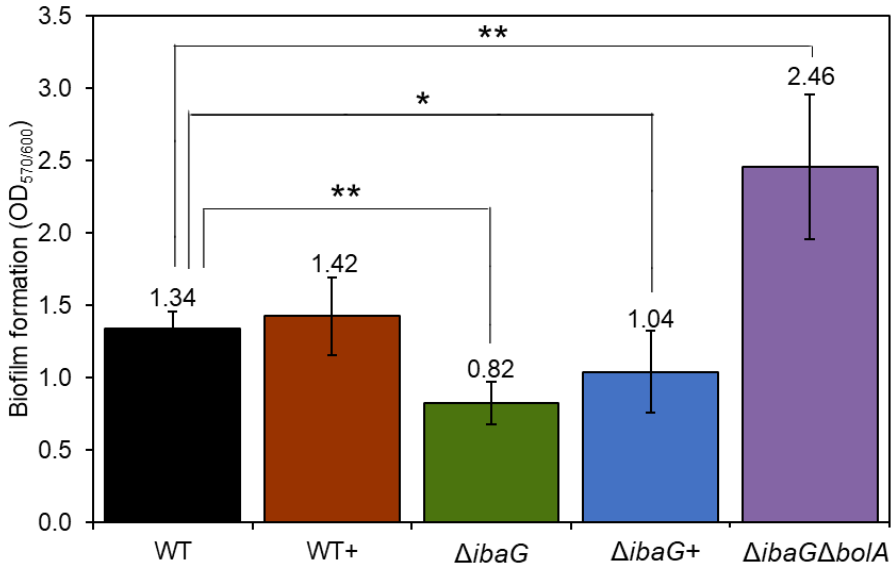

Figure VI-5: Representation of the biofilm production by the different strains normalized by OD_{600} of the planktonic cultures. Black – WT; Brown – WT+; Green – Δ*ibaG*; Blue – Δ*ibaG*+; Purple - Δ*ibaG*Δ*bolA*. Error bars represent standard deviations. Stars represent significant differences (unpaired *t*-test * - $p < 0.05$; ** - $p < 0.01$).

4. *Discussion*

The *ibaG* (named *induced by acid gene*) was first described as an acid response gene (Guinote *et al.*, 2012). Despite belonging to the same family as *bolA*, it was shown that this gene does not interact with the same DNA regions or produce the same phenotypes (cell morphology and growth profile) as its homolog, in *E. coli* (Guinote *et al.*, 2012). It has also been proposed that IbaG may function in Fe−S cluster assembly and trafficking in this organism (Dlouhy *et al.*, 2016). Studies on this gene in other organisms identified it as important for cell morphology and cell envelope integrity in *Vibrio cholera* (Fleurie *et al.*, 2019), and involved in resistance and germination of spores in *Bacillus subtilis* (Takamatsu *et al.*, 1999). To our knowledge, this gene was never studied in *S. oneidensis* MR-1, and the influence of this gene in biofilm formation and/or current generation has never been addressed.

Sequence analysis of the two proteins in *S. oneidensis* MR-1 allowed the confirmation that the proteins are homologs, sharing 44.9 % similarity and conserving their overall structure. However, studies on these proteins indicate that, despite being homologs, the function of BolA family proteins is not related (Takamatsu *et al.*, 1999; Guinote *et al.*, 2012; Dlouhy *et al.*, 2016; Fleurie *et al.*, 2019). Looking at the genomes within the *Shewanella* genus, it is possible to conclude that all the species only contain one copy of *bolA* and one copy of *ibaG*, indicating the importance of the genes in this genus.

Unlike what was observed for *bolA* (Silva *et al.*, 2020), neither the overexpression nor the deletion of *ibaG* had an effect on the mean current densities produced by *S. oneidensis* MR-1 compared to the WT strain. When looking at chronoamperometry curves, however, differences could be observed. In this case, results suggest that these genes may work in a regulatory chain that affects current and biofilm production (**Figure VI-6**). Our hypothesis is that both genes are important to control biofilm and current production, with the presence of IbaG repressing the expression of BolA. When *ibaG* is deleted from the genome (Δ*ibaG*), the presence of *bolA* in the genome mitigates the effect of the deletion. In this situation, and as in the WT and WT+, the current generation has the same profile. However, in the complementary strain (Δ*ibaG*+*ibaG*), the maximum current density is lower and the current generation profile is different. One explanation for this is the fact that *ibaG* is being constitutively expressed by the presence of the plasmid containing the gene, inhibiting the expression of BolA. This would make a strain that behaves like the double mutant (Δ*ibaG*Δ*bolA*) in terms of current generation. This effect is not observed in WT+, because when IbaG inhibits *bolA*, it still contains an active *ibaG* gene, mitigating the effects of this repression. This observation is sustained by the fact that the deletion of *bolA* does not produce an effect on current generation or biofilm formation (Silva *et al.*, 2020).

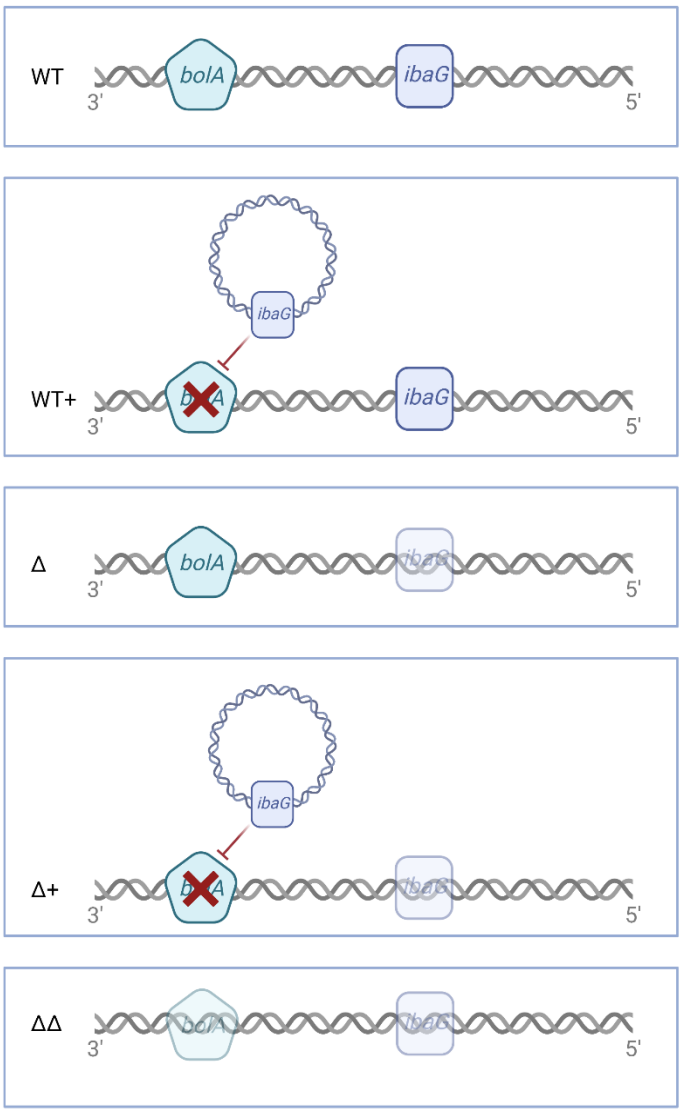

Figure VI-6: Schematic representation of the proposed mechanism of regulation of *bolA* by *ibaG*.

Differences could be observed in biofilm formation when the deletion strains are compared with the WT, suggesting that IbaG is important for biofilm formation in *S. oneidensis*. These differences, however, are not meaningful as the phenotype is not completely restored by the expression of the gene in the delta strain. This is an indication that a secondary effect is caused by

interference with the genome. Interestingly, the deletion of both *bolA* and *ibaG* had a significant impact on biofilm production, with the ΔΔ strain displaying a 1.8-fold increase in biofilm formation, which is not translated in current generation. This is probably a result of the lack of regulation in both genes, affecting both current generation and biofilm production. A closer look at the biofilm produced by this strain allowed the observation that the morphology and the behavior of the biofilm in the 96-well plate was different from the remaining strains. Further analysis of the biofilm, mainly on the composition of the EPS is needed in order to better understand the observed changes. Specifically, it is important to address the conductivity of the EPS, as this difference could justify an increase in biofilm formation that is not translated into current generation.

Overall, results show that despite their homology and modeled structural similarity, these proteins have different modes of action. Although both *bolA* and *ibaG* influence biofilm production and current generation, the phenotypes observed are very distinct. In the case of *ibaG*, there is an effect on biofilm formation, however, this change is not directly correlated to a change in current generation. This suggests that an alteration at the level of the morphology of the biofilm is taking place, probably related to differences in the EPS substances. More studies are needed to explore the mechanisms of biofilm regulation in *S. oneidensis* MR-1, an essential process for the electroactivity in BES. A better understanding of these processes will have a great impact on the improvement of electroactive organisms towards the practical application of these systems.

5. *Supplementary Materials*

Table VI-3: Summary of the type strain *Shewanella* genomes retrieved for genomic analysis.

Organism Scientific Name	Organism Qualifier	Level	Size	Gene Count
Shewanella abyssi	strain: DSM 17171	Contig	5030675	4422
Shewanella aestuarii	strain: JCM 17801	Contig	3883996	3412
Shewanella algae	strain: RQs-106	Complete Genome	4990025	4451
Shewanella algicola	strain: JCM 31091	Contig	4938240	4478
Shewanella algidipiscicola	isolate: 1 *Shewanella algidipiscicola* H1	Contig	4138380	3698
Shewanella amazonensis	strain: SB2B	Complete Genome	4306142	3806
Shewanella aquimarina	strain: JCM 12193	Contig	4412182	3903
Shewanella atlantica	strain: HAW-EB5	Scaffold	5392127	4637
Shewanella avicenniae	strain: FJAT-51800	Complete Genome	4201682	3735
Shewanella baltica	strain: OS678	Complete Genome	5368767	4656
Shewanella basaltis	strain: KCTC 22121	Contig	4347716	3787
Shewanella benthica	strain: DSM 8812	Scaffold	4034511	3435
Shewanella canadensis	strain: HAW-EB2	Contig	5676915	4942
Shewanella carassii	strain: TUM17387	Complete Genome	4454556	3998
Shewanella chilikensis	strain: JC5	Scaffold	4399136	3954
Shewanella colwelliana	strain: CSB03KR	Scaffold	4642543	4135
Shewanella corallii	strain: DSM 21332	Contig	5126954	4632
Shewanella cyperi	strain: FJAT-53726	Complete Genome	4136074	3691
Shewanella decolorationis	strain: sesselensis	Chromosome	4719362	4199

Shewanella denitrificans	strain: OS217	Complete Genome	4545906	3966
Shewanella dokdonensis	strain: CCUG 58667	Contig	4075970	3776
Shewanella donghaensis	strain: LT17	Complete Genome	4912773	4181
Shewanella electrodiphila	strain: DSM 24955	Contig	5228065	4456
Shewanella eurypsychrophilus	strain: YLB-08	Complete Genome	5851320	5049
Shewanella fidelis	strain: ATCC BAA-318	Scaffold	4798688	4166
Shewanella fodinae	strain: 74A	Scaffold	4034972	3708
Shewanella frigidimarina	strain: NCIMB 400	Complete Genome	4845257	4176
Shewanella gaetbuli	strain: DSM 16422	Contig	4038747	3451
Shewanella gelidii	strain: JCM 30804	Scaffold	3904844	3477
Shewanella gelidimarina	strain: ATCC 700752	Contig	5033801	4317
Shewanella glacialimarina	strain: TZS-4	Complete Genome	4456447	3919
Shewanella glacialipiscicola	strain: LMG 23744	Contig	4133602	3623
Shewanella hafniensis	strain: ATCC BAA-1207	Contig	4965338	4501
Shewanella halifaxensis	strain: HAW-EB4	Complete Genome	5226917	4520
Shewanella hanedai	strain: JCM 20706	Contig	5939027	5083
Shewanella indica	strain: CNZ-1	Scaffold	4565217	4099
Shewanella insulae	strain: M14-00200	Contig	4431966	3953
Shewanella intestini	strain: MCCC 1A01895	Scaffold	4004822	3441
Shewanella inventionis	strain: D1489	Complete Genome	4831636	4326
Shewanella japonica	strain: KCTC 22435	Complete Genome	4975677	4270
Shewanella jiangmenensis	strain: JM162201	Contig	4436316	3882
Shewanella kaireitica	strain: DSM 17170	Contig	5071067	4379
Shewanella khirikhana	strain: TH2012	Complete Genome	4858998	4288

Shewanella litoralis	strain: JCM 32306	Scaffold	4601512	4048
Shewanella litorisediminis	strain: SMK1-12	Complete Genome	4237767	3778
Shewanella livingstonensis	strain: LMG 19866	Complete Genome	4839879	4243
Shewanella loihica	strain: PV-4	Complete Genome	4602594	4042
Shewanella mangrovi	strain: YQH10	Contig	4215794	3804
Shewanella marina	strain: JCM 15074	Contig	4424648	4071
Shewanella marinintestina	strain: LMG 21403	Contig	4879403	4276
Shewanella marisflavi	strain: EP1	Complete Genome	4321452	3803
Shewanella maritima	strain: D4-2	Complete Genome	4718011	4059
Shewanella morhuae	strain: CW7	Contig	4285700	3743
Shewanella nanhaiensis	strain: NR704-98	Scaffold	5683156	4911
Shewanella olleyana	strain: LMG 21437	Contig	4654310	3989
Shewanella oncorhynchi	strain: S-1	Scaffold	5035993	4435
Shewanella oneidensis	strain: MR-1	Complete Genome	5131424	4602
Shewanella pealeana	strain: ATCC 700345	Complete Genome	5174581	4463
Shewanella piezotolerans	strain: WP3	Complete Genome	5396476	4637
Shewanella pneumatophori	strain: KCTC 23973	Contig	4885725	4286
Shewanella polaris	strain: SM1901	Complete Genome	4648537	4061
Shewanella profunda	strain: DSM 15900	Contig	4741450	4305
Shewanella psychromarinicola	strain: M2	Chromosome	5134949	4464
Shewanella psychrophila	strain: WP2	Complete Genome	6353406	5582
Shewanella psychropiezotolerans	strain: YLB-06	Complete Genome	6449204	5775

Shewanella putrefaciens	strain: 4H	Complete Genome	4631110	4104
Shewanella sairae	strain: JCM 11563	Contig	5559731	5279
Shewanella salipaludis	strain: SHSM-M6	Contig	4245197	3787
Shewanella saliphila	strain: JCM 32304	Scaffold	4621349	4094
Shewanella schlegeliana	strain: LMG 21406	Contig	4865223	4214
Shewanella sedimentimangrovi	strain: FJAT-52962	Complete Genome	4242357	3791
Shewanella sediminis	strain: HAW-EB3	Complete Genome	5517674	4741
Shewanella seohaensis	strain: CCUG 60900	Contig	4662612	4098
Shewanella submarina	strain: CCUG 71370	Contig	5171589	4677
Shewanella surugensis	strain: DSM 17177	Contig	6083073	5526
Shewanella ulleungensis	strain: JCM 32305	Contig	4637519	4041
Shewanella vesiculosa	strain: LMG 24424	Scaffold	4722637	4068
Shewanella violacea	strain: DSS12	Complete Genome	4962103	4168
Shewanella waksmanii	strain: ATCC BAA-643	Scaffold	4971480	4436
Shewanella woodyi	strain: ATCC 51908	Complete Genome	5935403	5100
Shewanella xiamenensis	strain: HD6416	Complete Genome	5041619	4477
Shewanella yunxiaonensis	strain: FJAT-54481	Complete Genome	3812587	3491

Table VI-4: List of primers used in the study and their purpose.

N	Name	Sequence	Purpose
1	pMQSalI_500up	CAGTGCCAAGCTTGCATGCCTGCAGGGACCATATCCATAAAAATATGGGC	Deletion of *ibaG*
2	RevCom_500up	GTGAGGAAAAGTGGATAAATTAGC	
3	500up_500dn	CTTTTCCTCAC GAAATTCGGTACCTTTTCAATTCG	
4	500dn_pMQBamHI	CGAATTCGAGCTCGGTACCCGGGGATCGTTTAAAGCTCGCCGCC	
5	Confirmation_ FW	GGCCATCAGTAGGTTTTCG	Test deletion of *ibaG*
6	Confirmation_Rv	GTCGTCCGCCGATTAAG	
7	ibaG_pBBR_Forw	GTATCGATAAGCTTGATATCGAAGGAGATATACATACCCATGGAATGCAGCTTAATAGAACA GATTTTACG	Clone *ibaG* in pBBR plasmid
8	ibaG_pBBR_Rev	GGAAACGCGAGAAAATTTTCAACAGCTAGGGATCCACTAGTTCTAGAG	

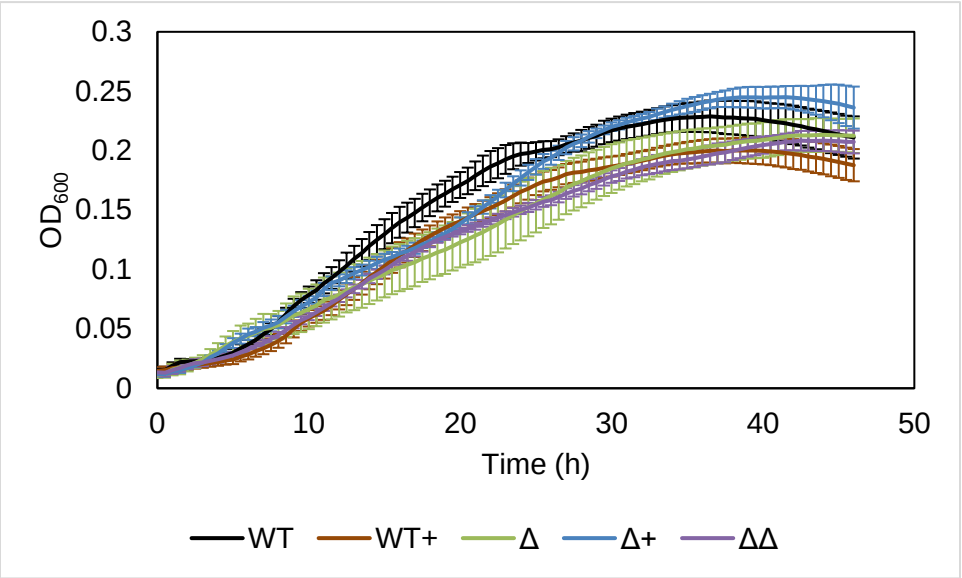

Figure VI-7: Growth curves of the different *S. oneidensis* MR-1 strains: Black - WT; Brown - WT+; Green - Δ*ibaG*; Blue – Δ*ibaG*; Purple - Δ*ibaG*Δ*bolA*.

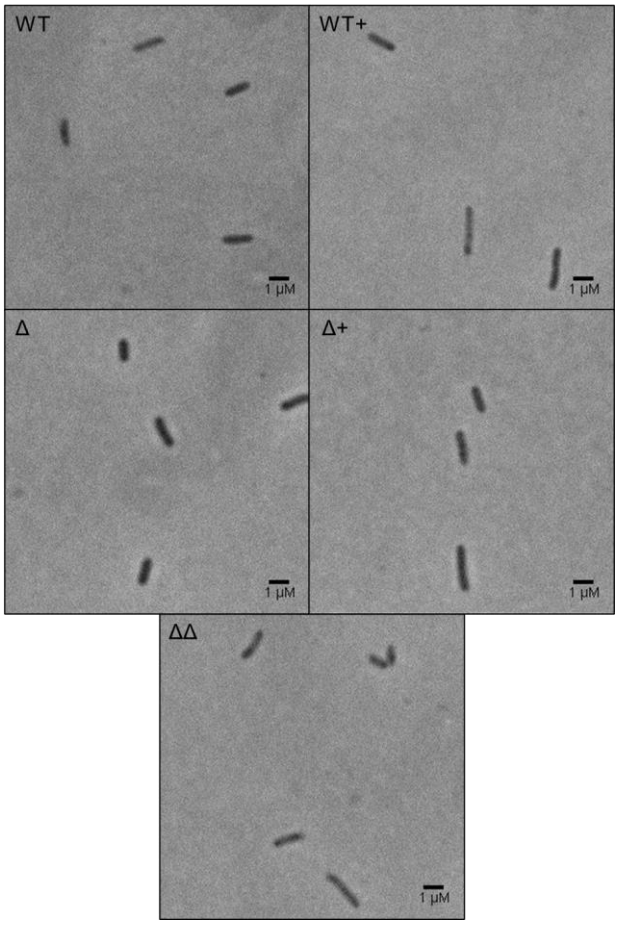

Figure VI-8: Phase contrast microscope imaging of the different strains: WT; WT+*ibaG*; Δ*ibaG*; Δ*ibaG*+*ibaG*; Δ*ibaG*Δ*bolA*.

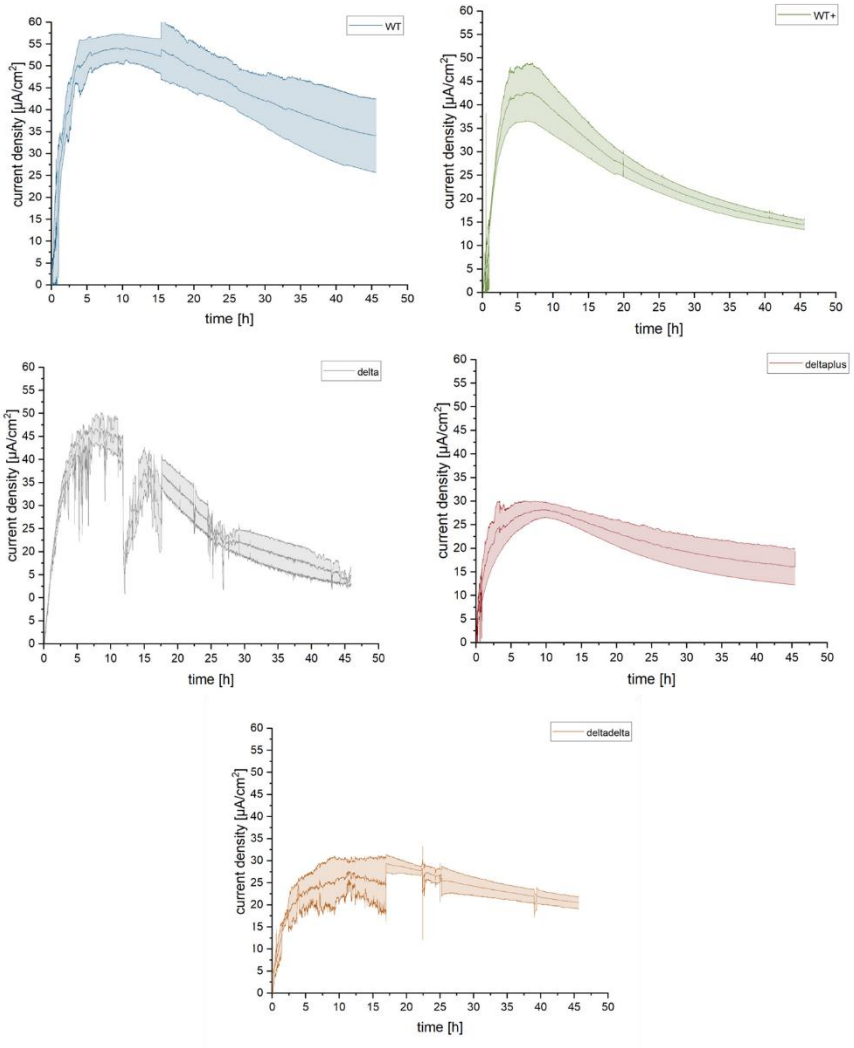

Figure VI-9: Current density curves obtained in single chamber BESs ran for 46h. The mean of three BESs and the standard deviation are represented.

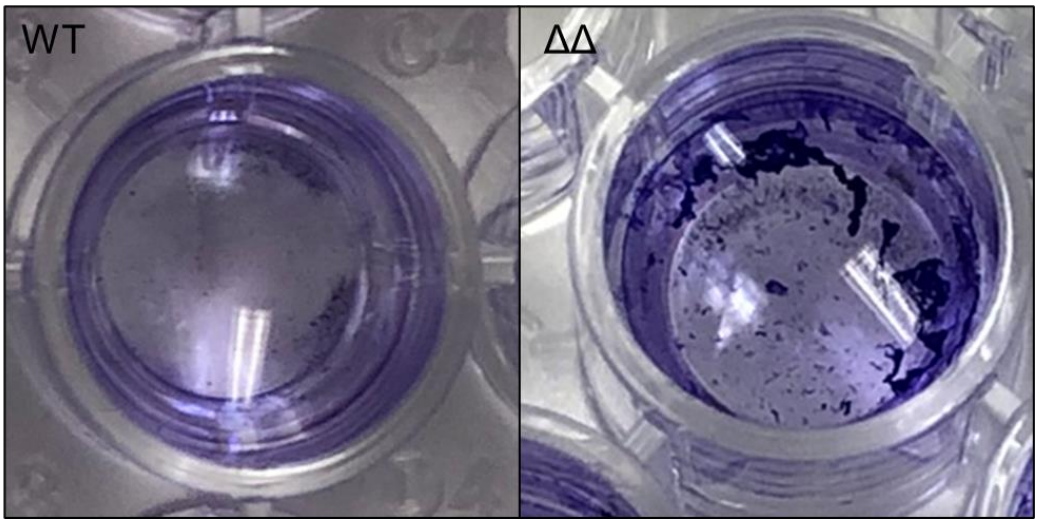

Figure VI-10: Picture of Crystal Violet-stained biofilms of the WT and Δ*ibaG*Δ*bolA* strains.

Chapter VII

Conclusions and future perspectives

BESs are a promising technology with low CO_2 footprint to face the energy crisis and the growing problem of world overpopulation. However, the large-scale application of this technology has been set back by the low power densities obtained (Holtmann and Harnisch, 2019; Mohan, Varjani and Pandey, 2019; Hernandez and Osma, 2020; Jadhav *et al.*, 2021; Peñacoba-Antona *et al.*, 2022). This limitation is mainly caused by the slow electron transfer rates between electroactive organisms and electrodes (Logan and Rabaey, 2012; Logan *et al.*, 2019). In this scope, the study of electroactive organisms is highly relevant and cytochrome *c* maturation and biofilm formation have been identified as two central processes, as they are key for the microbial electron transfer to the electrode.

The first part of this thesis presents important information on the functioning of cytochrome *c* maturation systems I and III (**Chapter III** and **Chapter IV**). In what concerns System I, despite being the most well-known System, it was possible to conclude that there are still important pieces of knowledge to be obtained in what concerns the maturation of the different classes of cytochromes *c*. The fact that the Class II cytochromes follow a different maturation paradigm when compared to Class I, opens the question of the fundamentals for these differences. Moreover, it paves the way for addressing the maturation of Class III and IV cytochromes and adds important arguments for the discussion of the evolution of the maturation systems.

In what concerns System III, results unequivocally show that handling of the apo cytochrome *c* polypeptide chain relies on a different mechanism in System III *versus* System I and II. Although the original aim of producing MHCs with this system was not achieved, as System III is only able to place one heme per polypeptide chain, this information is relevant for the understanding of how CcHL recognizes its substrates. Further research, including the determination of CcHL structure, and the interaction with its heme and peptide substrates, will be fundamental to fully understand its maturation mechanisms.

The second part of the thesis is focused on the study of biofilm formation by *S. oneidensis* MR-1(**Chapter V** and **Chapter VI**). In this scope, the effect of the transcription factor *bolA* in biofilm formation and current generation by this organism was analyzed. This work demonstrated that the overexpression of this gene contributes to an increase in biofilm formation. We could also demonstrate that this increase enhances current production in BES. Further studies are needed for the characterization of the regulatory network of this gene and its protein product. The understanding of what processes *bolA* regulates would increase our knowledge in enhancing biofilm formation and consequently increase current production in BES.

When looking at the *bolA* homolog *ibaG*, results show that despite their homology and predicted structural similarity, these proteins have different modes of action. Although both *bolA* and *ibaG* influence biofilm production and current generation, the phenotypes observed are very distinct. In the case of *ibaG*, there is an effect on biofilm formation, however, this change is not directly correlated to the current generation. This suggests that an alteration at the level of the morphology of the biofilm is taking place, probably related to differences in the EPS substances. More studies are needed to explore the mechanisms of biofilm regulation in *S. oneidensis* MR-1, an essential process for the electroactivity in BES. A better understanding of these processes will have a great impact on the improvement of the practical application of these systems.

In sum, this thesis follows the everlasting paradigm of science: for each question answered, “ten” more are raised, and a multitude of topics were opened for further study. Results on the cytochrome *c* maturation leave the door open for the exploration of the differences in the maturation process of the different classes of cytochromes by System I. An interesting topic of research is if the same Ccm proteins came into play or if there are different chaperones for different classes of cytochromes. Another question to address would be if CcHL can maturate Class II cytochromes, if its recognition

sequence is present, giving the distance from the heme binding motif to the N-terminal in this Class. Regarding the biofilm formation, it would be very relevant to characterize in detail the constituents of the EPS and the differences observed upon the overexpression or deletion of *bolA* and *ibaG*. It would also be interesting to further characterize the regulatory network involved in the biofilm formation of *S. oneidensis* MR-1.

References

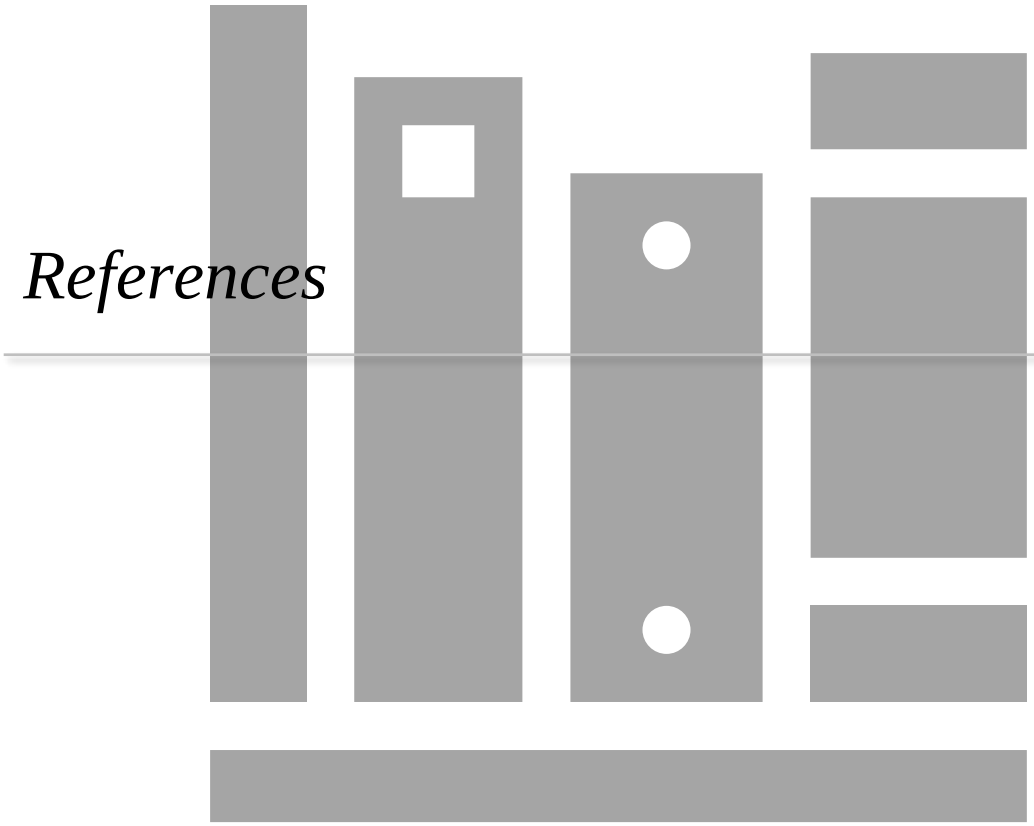

Aldea, M., Hernández-Chico, C., de la Campa, A. G., Kushner, S. R. and Vicente, M. (1988) 'Identification, cloning, and expression of bolA, an ftsZ-dependent morphogene of *Escherichia coli*.', *Journal of bacteriology*, 170(11), pp. 5169–5176. doi: 10.1128/jb.170.11.5169-5176.1988.

Alferov, S., Coman, V., Gustavsson, T., Reshetilov, A., von Wachenfeldt, C., Hägerhäll, C. and Gorton, L. (2009) 'Electrical communication of cytochrome enriched *Escherichia coli* JM109 cells with graphite electrodes', *Electrochimica Acta*, 54(22), pp. 4979–4984. doi: 10.1016/j.electacta.2009.03.090.

Altschul, S. F., Gish, W., Miller, W., Myers, E. W. and Lipman, D. J. (1990) 'Basic local alignment search tool', *Journal of molecular biology*, 215(3), pp. 403–410. doi: 10.1016/S0022-2836(05)80360-2.

Alves, A. S., Costa, N. L., Tien, M., Louro, R. O. and Paquete, C. M. (2017) 'Modulation of the reactivity of multiheme cytochromes by site-directed mutagenesis: moving towards the optimization of microbial electrochemical technologies', *Journal of Biological Inorganic Chemistry*, 22(1), pp. 87–97. doi: 10.1007/s00775-016-1409-0.

Ambler, R. P. (1982) 'The structure and classification of cytochromes *c*', in *From Cyclotrons to Cytochromes*. Elsevier, pp. 263–280. doi: 10.1016/b978-0-12-397580-5.50026-0.

Arends, J. B. A. and Verstraete, W. (2012) '100 years of microbial electricity production: three concepts for the future', *Microbial Biotechnology*, 5(3), pp. 333–346. doi: 10.1111/j.1751-7915.2011.00302.x.

Arnesano, F., Banci, L., Barker, P. D., Bertini, I., Rosato, A., Su, X. C. and Viezzoli, M. S. (2002) 'Solution structure and characterization of the heme chaperone CcmE.', *Biochemistry*, 41(46), pp. 13587–13594. doi: 10.1021/bi026362w.

Arslan, E., Schulz, H., Zufferey, R., Künzler, P. and Thöny-Meyer, L. (1998) 'Overproduction of the *Bradyrhizobium japonicum c*-type cytochrome subunits of the cbb3oxidase in *Escherichia coli*', *Biochemical and Biophysical Research Communications*, 251(3), pp. 744–747. doi: 10.1006/bbrc.1998.9549.

Azwar, M. Y., Hussain, M. A., Abdul Wahab, A. K. and Zanil, M. F. (2015) 'A Comparative study between Neural Networks (NN)-based and Adaptive-PID Controllers for the Optimal Bio-Hydrogen Gas Production in Microbial Electrolysis Cell Reactor', *Computer Aided Chemical Engineering*, 37, pp. 1529–1534. doi: 10.1016/B978-0-444-63577-8.50100-5.

Babbitt, S. E., Francisco, B. S., Mendez, D. L., Lukat-rodgers, G. S., Rodgers, K. R., Bretsnyder, E. C. and Kranz, R. G. (2014) 'Mechanisms of Mitochondrial Holocytochrome *c* Synthase and the Key Roles Played by Cysteines and Histidine of the Heme Attachment Site, Cys-XX-Cys-His', *Journal of Biological Chemistry*, 289(42), pp. 28795–28807. doi: 10.1074/jbc.M114.593509.

Babbitt, S. E., Sutherland, M. C., Francisco, B. S., Mendez, D. L. and Kranz, R. G. (2015) 'Mitochondrial cytochrome *c* biogenesis: no longer an enigma', *Trends in Biochemical Sciences*, 40(8), pp. 1–10. doi: 10.1016/j.tibs.2015.05.006.

Babbitt, S. E., Hsu, J., Mendez, D. L. and Kranz, R. G. (2017) 'Biosynthesis of Single Thioether *c*-Type Cytochromes Provides Insight into Mechanisms Intrinsic to Holocytochrome *c* Synthase (HCCS)', *Biochemistry*, 56(26), pp. 3337–3346. doi: 10.1021/acs.biochem.7b00286.

Babbitt, S. E., Hsu, J. and Kranz, R. G. (2016) 'Molecular basis behind inability of mitochondrial holocytochrome *c* synthase to mature bacterial cytochromes: Defining A Critical Role for Cytochrome cα HELIX-1', *Journal of Biological Chemistry*, 291(34), pp. 17523–17534. doi: 10.1074/jbc.M116.741231.

Bahadir, O. (2013) 'Ion-Exchange Chromatography and Its Applications', in *Column Chromatography*. InTech. doi: 10.5772/55744.

Banci, L., Bertini, I., Turano, P. and Vicens Oliver, M. (1992) 'NOE and two-dimensional correlated 1H-NMR spectroscopy of cytochrome *c'* from *Chromatium vinosum*', *European Journal of Biochemistry*, 204(1), pp. 107–112. doi: 10.1111/j.1432-1033.1992.tb16611.x.

Baron, D., LaBelle, E., Coursolle, D., Gralnick, J. A. and Bond, D. R. (2009) 'Electrochemical measurement of electron transfer kinetics by *Shewanella oneidensis* MR-1.', *The Journal of biological chemistry*, 284(42), pp. 28865–73. doi: 10.1074/jbc.M109.043455.

Barrett, P. J., Chen, J., Cho, M.-K. K., Kim, J.-H. H., Lu, Z., Mathew, S., Peng, D., Song, Y., Horn, W. D. Van, Zhuang, T., Sönnichsen, F. D., Sanders, C. R., Van Horn, W. D., Zhuang, T., Sönnichsen, F. D. and Sanders, C. R. (2013) 'The quiet renaissance of protein nuclear magnetic resonance', *Biochemistry*, 52(8), pp. 1303–1320. doi: 10.1021/bi4000436.

Bertani, G. (2004) 'Lysogeny at Mid-Twentieth Century: P1, P2, and Other Experimental Systems', *Journal of Bacteriology*, 186(3), pp. 595–600. doi: 10.1128/JB.186.3.595-600.2004.

Bertini, I.; McGreevy, K. S.; Parigi, G. (2012) 'NMR and its Place in Mechanistic Systems Biology', in Bertini, I., McGreevy, K. S., and Parigi, G. (eds) *NMR of Biomolecules: Towards Mechanistic Systems Biology*. 1st edn. Weinheim, Germany: Wiley-Blackwell, pp. 3–6. doi: 10.1002/9783527644506.

Bertini, I., Dikiy, A., Luchinat, C., Macinai, R. and Viezzoli, M. S. (1998) '1H NMR Study of the Reduced Cytochrome *c*' from *Rhodopseudomonas palustris* Containing a High-Spin Iron(II) Heme Moiety', *Inorganic Chemistry*, 37(19), pp. 4814–4821. doi: 10.1021/ic980531c.

Bodenhausen, G. and Ruben, D. J. (1980) 'Natural abundance nitrogen-15

NMR by enhanced heteronuclear spectroscopy', *Chemical Physics Letters*, 69(1), pp. 185–189. doi: 10.1016/0009-2614(80)80041-8.

Brausemann, A., Zhang, L., Ilcu, L. and Einsle, O. (2021) 'Architecture of the membrane-bound cytochrome *c* heme lyase CcmF', *Nature Chemical Biology*, 17(7), pp. 800–805. doi: 10.1038/s41589-021-00793-8.

Bursac, T., Gralnick, J. A. and Gescher, J. (2017) 'Acetoin production via unbalanced fermentation in *Shewanella oneidensis*', *Biotechnology and Bioengineering*, 114(6), pp. 1283–1289. doi: 10.1002/bit.26243.

Caffrey, M., Simorre, J. P., Brutscher, B., Marion, D. and Cusanovich, M. (1995) 'NMR Assignment of Rhodobacter capsulatus Ferricytochrome c′, a 28 kDa Paramagnetic Heme Protein', *Biochemistry*, 34(17), pp. 5904–5912. doi: 10.1021/bi00017a020.

Cai, S. and Xiao, H. (2021) 'Discovery of enzymes responsible for cyclization and postmodification in triterpenoid biosynthesis', *Microbial Cell Factories Engineering for Production of Biomolecules*, pp. 37–49. doi: 10.1016/B978-0-12-821477-0.00028-3.

Camacho, C., Coulouris, G., Avagyan, V., Ma, N., Papadopoulos, J., Bealer, K. and Madden, T. L. (2009) 'BLAST+: Architecture and applications', *BMC Bioinformatics*, 10(1), pp. 1–9. doi: 10.1186/1471-2105-10-421.

Von Canstein, H., Ogawa, J., Shimizu, S. and Lloyd, J. R. (2008) 'Secretion of flavins by *Shewanella* species and their role in extracellular electron transfer', *Applied and Environmental Microbiology*, 74(3), pp. 615–623. doi: 10.1128/AEM.01387-07.

Carlson, H. K., Iavarone, A. T., Gorur, A., Yeo, B. S., Tran, R., Melnyk, R. A., Mathies, R. A., Auer, M. and Coates, J. D. (2012) 'Surface multiheme *c*-type cytochromes from *Thermincola potens* and implications for respiratory metal reduction by Gram-positive bacteria', *Proceedings of the National Academy of Sciences of the United States of America*, 109(5), pp. 1702–1707. doi:

10.1073/pnas.1112905109.

Chen, R. (2012) ‘Bacterial expression systems for recombinant protein production: *E. coli* and beyond’, *Biotechnology Advances*, 30(5), pp. 1102–1107. doi: 10.1016/j.biotechadv.2011.09.013.

Chew, S. C. and Yang, L. (2016) ‘Biofilms’, *Encyclopedia of Food and Health*, pp. 407–415. doi: 10.1016/B978-0-12-384947-2.00069-6.

Chiranjeevi, P. and Patil, S. A. (2020) ‘Strategies for improving the electroactivity and specific metabolic functionality of microorganisms for various microbial electrochemical technologies’, *Biotechnology Advances*, 39, p. 107468. doi: 10.1016/j.biotechadv.2019.107468.

Christensen, G. D., Simpson, W. A., Younger, J. J., Baddour, L. M., Barrett, F. F., Melton, D. M., Beachey", E. H., Christensen, [G D, Simpson, W. A., Beachey, E. H., Bisno, A. L. and Barrett, F. F. (1985) ‘Adherence of coagulase-negative *staphylococci* to plastic tissue culture plates: a quantitative model for the adherence of *staphylococci* to medical devices’, *Journal of Clinical Microbiology*, 22(6), pp. 996–1006. doi: 10.1128/JCM.22.6.996-1006.1985.

Clubb, R. T., Thanabal, V. and Wagner, G. (1992) ‘A constant-time three-dimensional triple-resonance pulse scheme to correlate intraresidue ^{1}HN, ^{15}N, and ^{13}C′ chemical shifts in ^{15}N^{13}C-labelled proteins’, *Journal of Magnetic Resonance (1969)*, 97(1), pp. 213–217. doi: 10.1016/0022-2364(92)90252-3.

Coenye, T. (2013) ‘Biofilms’, *Brenner’s Encyclopedia of Genetics: Second Edition*, pp. 335–337. doi: 10.1016/B978-0-12-374984-0.00154-6.

Costa, H. S., Santos, H. and Turner, D. L. (1996) ‘Ligand orientation and haem electronic structure in ferricytochrome c’’ from Methylophilus methylotrophus studied by 13C NMR’, *European Biophysics Journal*, 25(1), pp. 19–24. doi: 10.1007/S002490050011.

Costa, N. L., Carlson, H. K., Coates, J. D., Louro, R. O. and Paquete, C. M. (2015) 'Heterologous expression and purification of a multiheme cytochrome from a Gram-positive bacterium capable of performing extracellular respiration', *Protein Expression and Purification*, 111, pp. 48–52. doi: 10.1016/j.pep.2015.03.007.

Costa, N. L., Clarke, T. A., Philipp, L. A., Gescher, J., Louro, R. O. and Paquete, C. M. (2018) 'Electron transfer process in microbial electrochemical technologies: The role of cell-surface exposed conductive proteins', *Bioresource Technology*, 255. doi: 10.1016/j.biortech.2018.01.133.

Coursolle, D., Baron, D. B., Bond, D. R. and Gralnick, J. A. (2010) 'The Mtr respiratory pathway is essential for reducing flavins and electrodes in *Shewanella oneidensis*', *Journal of Bacteriology*, 192(2), pp. 467–474. doi: 10.1128/JB.00925-09.

Cytiva (2020) *Size Exclusion Chromatography*.

Cytiva (2021) *Ion Exchange Chromatography*.

Daltrop, O., Allen, J. W. A., Willis, A. C. and Ferguson, S. J. (2002) '*In vitro* formation of a *c*-type cytochrome', *Proceedings of the National Academy of Sciences*, 99(12), pp. 7872–7876. doi: 10.1073pnas.132259099.

Daltrop, O. and Ferguson, S. J. (2003) 'Cytochrome *c* maturation: The *in vitro* reactions of horse heart apocytochrome *c* and *Paracoccus denitrificans* apocytochrome c550 with heme', *Journal of Biological Chemistry*, 278(7), pp. 4404–4409. doi: 10.1074/jbc.M211124200.

Dantas, J. M., Morgado, L., Catarino, T., Kokhan, O., Pokkuluri, P. R. and Salgueiro, C. a (2014) 'Evidence for interaction between the triheme cytochrome PpcA from *Geobacter sulfurreducens* and anthrahydroquinone-2,6-disulfonate, an analog of the redox active components of humic substances.', *Biochimica et biophysica acta*, 1837(6), pp. 750–60. doi: 10.1016/j.bbabio.2014.02.004.

Davis, J. B. (1963) ‘Generation of Electricity by Microbial Action’, *Advances in Applied Microbiology*, 5(C), pp. 51–64. doi: 10.1016/S0065-2164(08)70006-6.

Davis, J. B. and Yarbrough, H. F. (1962) ‘Preliminary Experiments on a Microbial Fuel Cell’, *Science*, 137(3530), pp. 615–616. doi: 10.1126/SCIENCE.137.3530.615.

Delgado, V. P., Paquete, C. M., Sturm, G. and Gescher, J. (2019) ‘Improvement of the electron transfer rate in *Shewanella oneidensis* MR-1 using a tailored periplasmic protein composition’, *Bioelectrochemistry*, 129, pp. 18–25. doi: 10.1016/j.bioelechem.2019.04.022.

Díaz-Moreno, I., Hulsker, R., Skubak, P., Foerster, J. M., Cavazzini, D., Finiguerra, M. G., Díaz-Quintana, A., Moreno-Beltrán, B., Rossi, G.-L., Ullmann, G. M., Pannu, N. S., De la Rosa, M. a and Ubbink, M. (2014) ‘The dynamic complex of cytochrome c6 and cytochrome f studied with paramagnetic NMR spectroscopy.’, *Biochimica et biophysica acta*, 1837(8), pp. 1305–15. doi: 10.1016/j.bbabio.2014.03.009.

Dickerson, R. E. (1980) ‘Cytochrome c and the evolution of energy metabolism’, *Scientific American*, 242(3), pp. 136–153. doi: 10.1038/SCIENTIFICAMERICAN0380-136.

Dlouhy, A. C., Li, H., Albetel, A. N., Zhang, B., Mapolelo, D. T., Randeniya, S., Holland, A. A., Johnson, M. K. and Outten, C. E. (2016) ‘The Escherichia coli BolA Protein IbaG Forms a Histidine-Ligated [2Fe-2S]-Bridged Complex with Grx4’, *Biochemistry*, 55(49), pp. 6869–6879. doi: /10.1021/acs.biochem.6b00812.

Dolch, K., Danzer, J., Kabbeck, T., Bierer, B., Erben, J., Förster, A. H., Maisch, J., Nick, P., Kerzenmacher, S. and Gescher, J. (2014) ‘Characterization of microbial current production as a function of microbe–electrode-interaction’, *Bioresource Technology*, 157, pp. 284–292. doi:

10.1016/J.BIORTECH.2014.01.112.

Dressaire, C., Moreira, N., Barahona, S., Alves, P., Arraiano, M., Moreira, R. N., Barahona, S., Matos, A. P. A. and Arraiano, C. M. (2015) 'BolA Is a Transcriptional Switch That Turns Off Motility and Turns On Biofilm Development', *mBio*, 6(1), pp. 1–13. doi: 10.1128/mBio.02352-14.Editor.

Dumont, M. E., Ernst, J. F., Hampsey, D. M. and Sherman, F. (1987) 'Identification and sequence of the gene encoding cytochrome *c* heme lyase in the yeast *Saccharomyces cerevisiae*.', *The EMBO Journal*, 6(1), pp. 235–241. doi: 10.1002/j.1460-2075.1987.tb04744.x.

Echalier, A., Brittain, T., Wright, J., Boycheva, S., Mortuza, G. B., Fülöp, V. and Watmough, N. J. (2008) 'Redox-linked structural changes *c* peroxidase from *Pseudomonas aeruginosa*', *Biochemistry*, 47(7), pp. 1947–1956. doi: 10.1021/bi702064f.

Edel, M., Sturm, G., Sturm-Richter, K., Wagner, M., Ducassou, J. N., Couté, Y., Horn, H. and Gescher, J. (2021) 'Extracellular riboflavin induces anaerobic biofilm formation in Shewanella oneidensis', *Biotechnology for Biofuels*, 14(1), pp. 1–14. doi: 10.1186/s13068-021-01981-3.

Edel, M., Horn, H. and Gescher, J. (2019) 'Biofilm systems as tools in biotechnological production', *Applied Microbiology and Biotechnology*, (103), pp. 5095–5103. doi: 10.1007/s00253-019-09869-x.

Edeling, M. A., Guddat, L. W., Fabianek, R. A., Thöny-Meyer, L. and Martin, J. L. (2002) 'Structure of CcmG/DsbE at 1.14 Å resolution: High-fidelity reducing activity in an indiscriminately oxidizing environment', *Structure*, 10(7), pp. 973–979. doi: 10.1016/S0969-2126(02)00794-3.

Efron, B. (1979) 'Bootstrap Methods: Another Look at the Jackknife', *https://doi.org/10.1214/aos/1176344552*, 7(1), pp. 1–26. doi: 10.1214/AOS/1176344552.

Faustino, M. M., Fonseca, B. M., Costa, N. L., Lousa, D., Louro, R. O. and Paquete, C. M. (2021) 'Crossing the Wall: Characterization of the Multiheme Cytochromes Involved in the Extracellular Electron Transfer Pathway of *Thermincola ferriacetica*', *Microorganisms 2021, Vol. 9, Page 293*, 9(2), p. 293. doi: 10.3390/MICROORGANISMS9020293.

Ferguson, S. J. (2012) 'New perspectives on assembling *c*-type cytochromes, particularly from sulphate reducing bacteria and mitochondria', *Biochimica et Biophysica Acta - Bioenergetics*, 1817(10), pp. 1754–1758. doi: 10.1016/j.bbabio.2012.05.004.

Flemming, H.-C., Wingender, J., Szewzyk, U. and Steinberg, P. (2016) 'Biofilms: An emergent form of bacterial life Coral Spawning Monitoring View project Biofilm-Management View project', *Nature Reviews Microbiology*, 14, pp. 563–575. doi: 10.1038/nrmicro.2016.94.

Fleurie, A., Zoued, A., Alvarez, L., Hines, K. M., Cava, F., Xu, L., Davis, B. M. and Waldor, M. K. (2019) 'A *Vibrio cholerae* BolA-Like Protein Is Required for Proper Cell Shape and Cell Envelope Integrity', *mBio*, 10(4), pp. 1–15. doi: 10.1128/mbio.00790-19.

Fonseca, B. M., Saraiva, I. H., Paquete, C. M., Soares, C. M., Pacheco, I., Salgueiro, C. A. and Louro, R. O. (2009) 'The tetraheme cytochrome from *Shewanella oneidensis* MR-1 shows thermodynamic bias for functional specificity of the hemes', *Journal of Biological Inorganic Chemistry*, 14(3), pp. 375–385. doi: 10.1007/s00775-008-0455-7.

Fonseca, B. M., Tien, M., Rivera, M., Shi, L. and Louro, R. O. (2012) 'Efficient and selective isotopic labeling of hemes to facilitate the study of multiheme proteins.', *BioTechniques*, pp. 1–7. doi: 10.2144/000113859.

Fonseca, B. M., Paquete, C. M., Neto, S. E., Pacheco, I., Soares, C. M. C. and Louro, R. O. (2013) 'Mind the gap: cytochrome interactions reveal electron pathways across the periplasm of *Shewanella oneidensis* MR-1.',

The Biochemical journal, 449(1), pp. 101–8. doi: 10.1042/BJ20121467.

Fonseca, B. M., Silva, L., Trindade, I. B., Moe, E., Matias, P. M., Louro, R. O. and Paquete, C. M. (2019) 'Optimizing Electroactive Organisms: The Effect of Orthologous Proteins', *Frontiers in Energy Research*, 7, p. 2. doi: 10.3389/fenrg.2019.00002.

Fonseca, B. M., Soares, R. M., Paquete, C. M. and Louro, R. O. (2021) 'Bacterial Power: An Alternative Energy Source', *Enzymes for Solving Humankind's Problems*, pp. 215–246. doi: 10.1007/978-3-030-58315-6_8.

Fredrickson, J. K., Romine, M. F., Beliaev, A. S., Auchtung, J. M., Driscoll, M. E., Gardner, T. S., Nealson, K. H., Osterman, A. L., Pinchuk, G., Reed, J. L., Rodionov, D. A., Rodrigues, J. L. M., Saffarini, D. A., Serres, M. H., Spormann, A. M., Zhulin, I. B. and Tiedje, J. M. (2008) 'Towards environmental systems biology of *Shewanella*', *Nature Reviews Microbiology 2008 6:8*, 6(8), pp. 592–603. doi: 10.1038/nrmicro1947.

Freyman, M. C., Kou, T., Wang, S. and Li, Y. (2019) '3D printing of living bacteria electrode', *Nano Research*, pp. 1–5. doi: 10.1007/s12274-019-2534-1.

Garrigues, S., Martínez-Reyes, N. and de Vries, R. P. (2021) 'Genetic Engineering for Strain Improvement in Filamentous Fungi', *Encyclopedia of Mycology*, pp. 489–504. doi: 10.1016/B978-0-12-819990-9.00006-8.

Goodhew, C. F., Brown, K. R. and Pettigrew, G. W. (1986) 'Haem staining in gels, a useful tool in the study of bacterial *c*-type cytochromes', *BBA - Bioenergetics*, 852(2–3), pp. 288–294. doi: 10.1016/0005-2728(86)90234-3.

Gorby, Y. A. *et al.* (2006) 'Electrically conductive bacterial nanowires produced by *Shewanella oneidensis* strain MR-1 and other microorganisms', *Proceedings of the National Academy of Sciences*, 103(30), pp. 11358–11363. doi: doi:10.1073/pnas.0604517103.

Gralnick, J. A. and Newman, D. K. (2007) 'Extracellular respiration', *Molecular Microbiology*, 65(1), pp. 1–11. doi: 10.1111/j.1365-2958.2007.05778.x.

Grzesiek, S. and Bax, A. (1992a) 'An efficient experiment for sequential backbone assignment of medium-sized isotopically enriched proteins', *Journal of Magnetic Resonance (1969)*, 99(1), pp. 201–207. doi: 10.1016/0022-2364(92)90169-8.

Grzesiek, S. and Bax, A. (1992b) 'Correlating Backbone Amide and Side Chain Resonances in Larger Proteins by Multiple Relayed Triple Resonance NMR', *Journal of the American Chemical Society*, 114(16), pp. 6291–6293. doi: 10.1021/ja00042a003.

Guinote, I. B., Moreira, R. N., Freire, P. and Arraiano, C. M. (2012) 'Characterization of the BolA Homolog IbaG: A New Gene Involved in Acid Resistance', *J. Microbiol. Biotechnol.*, 22(4), pp. 484–493. doi: 10.4014/JMB.1107.07037.

Guinote, I. B., Moreira, R. N., Barahona, S., Freire, P., Vicente, M. and Arraiano, C. M. (2014) 'Breaking through the stress barrier: the role of BolA in Gram-negative survival', *World Journal of Microbiology and Biotechnology*, 30(10), pp. 2559–2566. doi: 10.1007/s11274-014-1702-4.

Guzha, A., McGee, R., Scholz, P., Hartken, D., Lüdke, D., Bauer, K., Wenig, M., Zienkiewicz, K., Herrfurth, C., Feussner, I., Vlot, A. C., Wiermer, M., Haughn, G. and Ischebeck, T. (2022) 'Cell wall-localized BETA-XYLOSIDASE4 contributes to immunity of *Arabidopsis* against *Botrytis cinerea*', *Plant Physiology*, 189(3), pp. 1794–1813. doi: 10.1093/PLPHYS/KIAC165.

Hau, H. H. and Gralnick, J. A. (2007) 'Ecology and Biotechnology of the Genus *Shewanella*', *Annual Review of Microbiology*, 61(1), pp. 237–258. doi: 10.1146/annurev.micro.61.080706.093257.

Heidelberg, J. F. *et al.* (2002) 'Genome sequence of the dissimilatory metal

ion–reducing bacterium *Shewanella oneidensis*', *Nature Biotechnology 2002 20:11*, 20(11), pp. 1118–1123. doi: 10.1038/nbt749.

Hernandez, C. A. and Osma, J. F. (2020) 'Microbial electrochemical systems: Deriving future trends from historical perspectives and characterization strategies', *Frontiers in Environmental Science*, 8, p. 44. doi: 10.3389/FENVS.2020.00044/BIBTEX.

Hernandez, M. E., Kappler, A. and Newman, D. K. (2004) 'Phenazines and other redox-active antibiotics promote microbial mineral reduction', *Applied and environmental microbiology*, 70(2), pp. 921–928. doi: 10.1128/AEM.70.2.921-928.2004.

Holtmann, D. and Harnisch, F. (2019) 'Electrification of biotechnology: Quo vadis?', *Advances in Biochemical Engineering/Biotechnology*, 167, pp. 395–411. doi: 10.1007/10_2018_75/COVER.

Hoppe-Seyler, F. (1890) 'About muscle dyes', *Zeitschrift für Physiologische Chemie*, 14, pp. 106–108.

IBA (2020) *Comprehensive comparison of the protein purification systems*. Available at: www.iba-lifesciences.com (Accessed: 13 December 2022).

Jadhav, D. A., Mungray, A. K., Arkatkar, A. and Kumar, S. S. (2021) 'Recent advancement in scaling-up applications of microbial fuel cells: From reality to practicability', *Sustainable Energy Technologies and Assessments*, 45, p. 101226. doi: 10.1016/J.SETA.2021.101226.

Jain, A., Coelho, A., Madjarov, J., Paquete, C. M. and Gralnick, J. A. (2022) 'Evidence for Quinol Oxidation Activity of ImoA, a Novel NapC/NirT Family Protein from the Neutrophilic Fe(II)-Oxidizing Bacterium *Sideroxydans lithotrophicus* ES-1', *mBio*, 13(5), p. e0215022. doi: 10.1128/mbio.02150-22.

Jiang, X. and Wang, X. (2004) 'Cytochrome *c*-Mediated Apoptosis', *Annual Review of Biochemistry*, 73(1), pp. 87–106. doi:

10.1146/annurev.biochem.73.011303.073706.

Kalathil, S., Khan, M. M., Lee, J. and Cho, M. H. (2013) 'Production of bioelectricity , bio-hydrogen , high value chemicals and bioinspired nanomaterials by electrochemically active biofilms', *Biotechnology Advances*, 31(6), pp. 915–924. doi: 10.1016/j.biotechadv.2013.05.001.

Kay, L. E., Ikura, M., Tschudin, R. and Bax, A. (1990) 'Three-dimensional triple-resonance NMR spectroscopy of isotopically enriched proteins', *Journal of Magnetic Resonance (1969)*, 89(3), pp. 496–514. doi: 10.1016/0022-2364(90)90333-5.

Keeler, J. (2005) *Understanding NMR Spectroscopy - 2nd Edition*. WILEY. doi: 978-0-470-74608-0.

Keilin, D. (1925) 'On cytochrome, a respiratory pigment, common to animals, yeast, and higher plants', *Proceedings of the Royal Society of London. Series B, Containing Papers of a Biological Character*, 98(690), pp. 312–339. doi: 10.1098/rspb.1925.0039.

Keller, R. (2004) *Optimizing the process of nuclear magnetic resonance spectrum analysis and computer aided resonance assignment*. Swiss federal institute of technology Zurich.

Khona, D. K., Dongre, S. S., Arraiano, C. M. and D'Souza, J. S. (2013) 'A BolA-like morphogene from the alga *Chlamydomonas reinhardtii* changes morphology and induces biofilm formation in *Escherichia coli*', *FEMS Microbiology Letters*, 339(1), pp. 39–47. doi: 10.1111/1574-6968.12051.

Kim, B. H., Kim, H. J., Hyun, M. S. and Park, D. H. (1999) 'Direct electrode reaction of Fe(III)-reducing bacterium, Shewanella putrefaciens', *Journal of Microbiology and Biotechnology*, 9(2), pp. 127–131.

Kiryu-Seo, S., Gamo, K., Tachibana, T., Tanaka, K. and Kiyama, H. (2006) 'Unique anti-apoptotic activity of EAAC1 in injured motor neurons', *The EMBO*

Journal, 25(14), pp. 3411–3421. doi: 10.1038/sj.emboj.7601225.

Koch, B. and Nybroe, O. (2006) 'Initial characterization of a *bolA* homologue from *Pseudomonas fluorescens* indicates different roles for BolA-like proteins in *P. fluorescens* and *Escherichia coli*', *FEMS Microbiology Letters*, 262(1), pp. 48–56. doi: 10.1111/j.1574-6968.2006.00359.x.

Koch, C. and Harnisch, F. (2016) 'Is there a Specific Ecological Niche for Electroactive Microorganisms?', *ChemElectroChem*, 3(9), pp. 1282–1295. doi: 10.1002/celc.201600079.

Korb, H. and Neupert, W. (1978) 'Biogenesis of Cytochrome *c* in *Neurospora crassa* Synthesis of Apocytochrome *c*, Transfer to Mitochondria and Conversion to Holocytochrome *c*', *European Journal of Biochemistry*, 91(2), pp. 609–620. doi: 10.1111/J.1432-1033.1978.TB12714.X.

Kovach, M. E., Elzer, P. H., Steven Hill, D., Robertson, G. T., Farris, M. A., Roop, R. M. and Peterson, K. M. (1995) 'Four new derivatives of the broad-host-range cloning vector pBBR1MCS, carrying different antibiotic-resistance cassettes', *Gene*, 166(1), pp. 175–176. doi: 10.1016/0378-1119(95)00584-1.

Kracke, F., Vassilev, I. and Krömer, J. O. (2015) 'Microbial electron transport and energy conservation - The foundation for optimizing bioelectrochemical systems', *Frontiers in Microbiology*, 6(JUN), pp. 1–18. doi: 10.3389/fmicb.2015.00575.

Kranz, R. G., Richard-Fogal, C., Taylor, J.-S. and Frawley, E. R. (2009) 'Cytochrome *c* biogenesis: mechanisms for covalent modifications and trafficking of heme and for heme-iron redox control.', *Microbiology and molecular biology reviews : MMBR*, 73(3), pp. 510–28, Table of Contents. doi: 10.1128/MMBR.00001-09.

Kumar, S., Stecher, G. and Tamura, K. (2016) 'MEGA7: Molecular Evolutionary Genetics Analysis Version 7.0 for Bigger Datasets', *Molecular biology and evolution*, 33(7), pp. 1870–1874. doi:

10.1093/MOLBEV/MSW054.

Lea-Smith, D. J., Bombelli, P., Vasudevan, R. and Howe, C. J. (2016) 'Photosynthetic, respiratory and extracellular electron transport pathways in cyanobacteria', *Biochimica et Biophysica Acta - Bioenergetics*, 1857(3), pp. 247–255. doi: 10.1016/j.bbabio.2015.10.007.

Lee, D. yeon D., Prindle, A., Liu, J. and Süel, G. M. (2017) 'SnapShot: Electrochemical Communication in Biofilms', *Cell*. Cell Press, pp. 214-214.e1. doi: 10.1016/j.cell.2017.06.026.

Leu, A. O., Cai, C., McIlroy, S. J., Southam, G., Orphan, V. J., Yuan, Z., Hu, S. and Tyson, G. W. (2020) 'Anaerobic methane oxidation coupled to manganese reduction by members of the *Methanoperedenaceae*', *ISME Journal*, 14(4), pp. 1030–1041. doi: 10.1038/s41396-020-0590-x.

Li, X., Liu, T., Wang, K. and Waite, T. D. (2015) 'Light-induced extracellular electron transport by the marine raphidophyte chattonella marina', *Environmental Science and Technology*, 49(3), pp. 1392–1399. doi: 10.1021/es503511m.

Lies, D. P., Hernandez, M. E., Kappler, A., Mielke, R. E., Gralnick, J. A. and Newman, D. K. (2005) '*Shewanella oneidensis* MR-1 uses overlapping pathways for iron reduction at a distance and by direct contact under conditions relevant for biofilms', *Applied and Environmental Microbiology*, 71(8), pp. 4414–4426. doi: 10.1128/AEM.71.8.4414-4426.2005.

Liu, T., Yu, Y. Y., Deng, X. P., Ng, C. K. K., Cao, B., Wang, J. Y., Rice, S. A. A., Kjelleberg, S. and Song, H. (2015) 'Enhanced *Shewanella* biofilm promotes bioelectricity generation', *Biotechnology and Bioengineering*, 112(10), pp. 2051–2059. doi: 10.1002/bit.25624.

Liu, Y., Wang, Z., Liu, J., Levar, C., Edwards, M. J., Babauta, J. T., Kennedy, D. W., Shi, Z., Beyenal, H., Bond, D. R., Clarke, T. A., Butt, J. N., Richardson, D. J., Rosso, K. M., Zachara, J. M., Fredrickson, J. K. and Shi, L. (2014) 'A

trans-outer membrane porin-cytochrome protein complex for extracellular electron transfer by *Geobacter sulfurreducens* PCA', *Environmental microbiology reports*, 6(6), pp. 776–85. doi: 10.1111/1758-2229.12204.

Logan, B. E., Hamelers, B., Rozendal, R., Schröder, U., Keller, J., Freguia, S., Aelterman, P., Verstraete, W. and Rabaey, K. (2006) 'Microbial fuel cells: Methodology and technology', *Environmental Science and Technology*, 40(17), pp. 5181–5192. doi: 10.1021/es0605016.

Logan, B. E., Rossi, R., Ragab, A. A. and Saikaly, P. E. (2019) 'Electroactive microorganisms in bioelectrochemical systems', *Nature Reviews Microbiology*, 17(5), pp. 307–319. doi: 10.1038/s41579-019-0173-x.

Logan, B. E. and Rabaey, K. (2012) 'Conversion of wastes into bioelectricity and chemicals by using microbial electrochemical technologies.', *Science*, 337(6095), pp. 686–90. doi: 10.1126/science.1217412.

Logan, B. E. and Regan, J. M. (2006) *Electricity-producing bacterial communities in microbial fuel cells*, *Trends in Microbiology*. doi: 10.1016/j.tim.2006.10.003.

Louro, R. O., Costa, N. L., Fernandes, A. P., Silva, A. V., Trindade, I. B., Fonseca, B. M. and Paquete, C. M. (2019) 'Exploring the Molecular Mechanisms of Extracellular Electron Transfer for Harnessing Reducing Power in METs: Methodologies and Approaches', in *Microbial Electrochemical Technology*. Elsevier, pp. 261–293. doi: 10.1016/B978-0-444-64052-9.00010-8.

MacDonell, M. T. and Colwell, R. R. (1985) 'Phylogeny of the Vibrionaceae, and Recommendation for Two New Genera, *Listonella* and *Shewanella*', *Systematic and Applied Microbiology*, 6(2), pp. 171–182. doi: 10.1016/S0723-2020(85)80051-5.

MacMunn, C. A. (1884) 'On Myohaematin, an intrinsic muscle-pigment of Vertebrates and Invertebrates, on Histohaematin, and on the Spectrum of the

Supra-renal Bodies.', *The Journal of Physiology*, 4(December 13), pp. xxiv–xxvi. doi: 10.1113/jphysiol.1885.sp000178.

Mallick, D., Sharma, S. D., Brahma, H. S., Nath, R., Bhowmik, R. and Kushwaha, A. (2022) 'Emerging commercial opportunities for conversion of waste to energy: aspect of gasification technology', *Waste-to-Energy Approaches Towards Zero Waste: Interdisciplinary Methods of Controlling Waste*, pp. 105–127. doi: 10.1016/B978-0-323-85387-3.00012-4.

Marsili, E., Baron, D. B., Shikhare, I. D., Coursolle, D., Gralnick, J. A. and Bond, D. R. (2008) '*Shewanella* secretes flavins that mediate extracellular electron transfer', *Proceedings of the National Academy of Sciences of the United States of America*, 105(10), pp. 3968–3973. doi: 10.1073/pnas.0710525105.

Di Matteo, A., Gianni, S., Schininà, M. E., Giorgi, A., Altieri, F., Calosci, N., Brunori, M. and Travaglini-Allocatelli, C. (2007) 'A strategic protein in cytochrome *c* maturation: Three-dimensional structure of CcmH and binding to apocytochrome *c*'', *Journal of Biological Chemistry*, 282(37), pp. 27012–9. doi: 10.1074/jbc.M702702200.

Di Matteo, A., Calosci, N., Gianni, S., Jemth, P., Brunori, M. and Travaglini-Allocatelli, C. (2010) 'Structural and functional characterization of CcmG from *Pseudomonas aeruginosa*, a key component of the bacterial cytochrome *c* maturation apparatus', *Proteins: Structure, Function and Bioinformatics*, 78(10), pp. 2213–2221. doi: 10.1002/prot.22733.

Mavridou, D. a I., Ferguson, S. J. and Stevens, J. M. (2013) 'Cytochrome *c* assembly.', *IUBMB life*, 65(3), pp. 209–16. doi: 10.1002/iub.1123.

Mendez, D. L., Lowder, E. P., Tillman, D. E., Sutherland, M. C., Collier, A. L., Rau, M. J., Fitzpatrick, J. A. J. and Kranz, R. G. (2022) 'Cryo-EM of CcsBA reveals the basis for cytochrome *c* biogenesis and heme transport', *Nature Chemical Biology*, 18(1), pp. 101–108. doi: 10.1038/s41589-021-00935-y.

Mil-homens, D., Barahona, S., Moreira, R. N., Silva, I. J., Pinto, S. N. and Fialho, A. M. (2018) 'Stress Response Protein BolA Influences Fitness and Promotes Salmonella enterica Serovar Typhimurium Virulence', *Applied and Environmental Microbiology*, 84(8), pp. 1–13.

Miller, J. H. (1972) *Experiments in Molecular Genetics*. Edited by J. H. Miller. Cold Spring Harbor Laboratory.

Min, D., Cheng, L., Zhang, F., Huang, X.-N., Li, D., Liu, D., Lau, T.-C., Mu, Y. and Yu, H. (2017) 'Enhancing Extracellular Electron Transfer of *Shewanella oneidensis* MR-1 through Coupling Improved Flavin Synthesis and Metal-Reducing Conduit for Pollutant Degradation', *Environmental Science & Technology*, 51(9), pp. 5082–5089. doi: 10.1021/acs.est.6b04640.

Mohan, S. V., Varjani, S. and Pandey, A. (2019) *Microbial Electrochemical Technology: Sustainable Platform for Fuels, Chemicals and Remediation*. 1st edn. Edited by S. V. Mohan, S. Varjani, and A. Pandey. Elsevier.

Monkara, F., Bingham, S. J., Kadir, F. H. A., McEwan, A. G., Thomson, A. J., Thurgood, A. G. P. and Moore, G. R. (1992) 'Spectroscopic studies of *Rhodobacter capsulatus* cytochrome *c′* in the isolated state and in intact cells', *BBA - Bioenergetics*, 1100(2), pp. 184–188. doi: 10.1016/0005-2728(92)90080-L.

Morar, A. S., Kakouras, D., Young, G. B., Boyd, J. and Pielak, G. J. (1999) 'Expression of 15N-labeled eukaryotic cytochrome *c* in *Escherichia coli*', *Journal of Biological Inorganic Chemistry*, 4(2), pp. 220–222. doi: 10.1007/s007750050307.

Moreira, R. N., Dressaire, C., Barahona, S., Galego, L., Kaever, V., Jenal, U. and Arraiano, C. M. (2017) 'BolA Is Required for the Accurate Regulation of c-di-GMP, a Central Player in Biofilm Formation.', *mBio*, 8(5). doi: 10.1128/mBio.00443-17.

Myers, C. R. and Nealson, K. H. (1988) 'Bacterial Manganese Reduction and

Growth with Manganese Oxide as the Sole Electron Acceptor', *Science*, 240(4857), pp. 1319–1321. doi: 10.1126/SCIENCE.240.4857.1319.

Nations, U. (2015) 'Transforming Our World: The 2030 Agenda for Sustainable Development', in *A New Era in Global Health*. doi: 10.1891/9780826190123.ap02.

Nei, M. and Kumar, S. (2000) *Molecular Evolution and Phylogenetics*, *Oxford University Press*.

Neto, S. E., Fonseca, B. M., Maycock, C. and Louro, R. O. (2014) 'Analysis of the residual alignment of a paramagnetic multiheme cytochrome by NMR.', *Chemical communications (Cambridge, England)*, 50(35), pp. 4561–3. doi: 10.1039/c3cc49135h.

Newman, D. K. and Kolter, R. (2000) 'A role for excreted quinones in extracellular electron transfer.', *Nature*, 405(6782), pp. 94–7. doi: 10.1038/35011098.

Nicholls, D. G. and Ferguson, S. J. (2013) *Bioenergetics*. Fourth Edi. Elsevier. doi: 10.1016/C2010-0-64902-9.

O'Leary, N. A. *et al.* (2016) 'Reference sequence (RefSeq) database at NCBI: current status, taxonomic expansion, and functional annotation', *Nucleic Acids Research*, 44(Database issue), p. D733. doi: 10.1093/NAR/GKV1189.

O'Toole, G. A. (2011) 'Microtiter dish biofilm formation assay', *Journal of visualized experiments : JoVE*, (47). doi: 10.3791/2437.

Olteanu, A., Patel, C. N., Dedmon, M. M., Kennedy, S., Linhoff, M. W., Minder, C. M., Potts, P. R., Deshmukh, M. and Pielak, G. J. (2003) 'Stability and apoptotic activity of recombinant human cytochrome *c*.', *Biochemical and biophysical research communications*, 312(3), pp. 733–40. doi: 10.1016/j.bbrc.2003.10.182.

Ouyang, N., Gao, Y.-G., Hu, H.-Y. and Xia, Z.-X. (2006) 'Crystal Structures of

E. coli CcmG and its Mutants Reveal Key Roles of the N-Terminal b-Sheet and the Fingerprint Region', *PROTEINS: Structure, Function, and Bioinformatics*, 65, pp. 1021–1031. doi: 10.1002/prot.

Ow, Y.-L. P., Green, D. R., Hao, Z. and Mak, T. W. (2008) 'Cytochrome *c*: functions beyond respiration', *Nature Reviews Molecular Cell Biology*, 9(7), pp. 532–542. doi: 10.1038/nrm2434.

Paquete, C. M., Fonseca, B. M., Cruz, D. R., Pereira, T. M., Pacheco, I., Soares, C. M. C. M. and Louro, R. O. (2014) 'Exploring the molecular mechanisms of electron shuttling across the microbe/metal space', *Frontiers in Microbiology*, 5(JUN), pp. 1–12. doi: 10.3389/fmicb.2014.00318.

Paquete, C. M., Rusconi, G., Silva, A. V., Soares, R. and Louro, R. O. (2019) 'A brief survey of the "cytochromome"', *Advances in Microbial Physiology*, 75, pp. 69–135. doi: 10.1016/bs.ampbs.2019.07.005.

Patel, C. N., Lind, M. C. and Pielak, G. J. (2001) 'Characterization of horse cytochrome *c* expressed in *Escherichia coli*', *Protein Expression and Purification*, 22(2), pp. 220–224. doi: 10.1006/prep.2001.1438.

Patriarca, A., Polticelli, F., Piro, M. C., Sinibaldi, F., Mei, G., Bari, M., Santucci, R. and Fiorucci, L. (2012) 'Conversion of cytochrome *c* into a peroxidase: Inhibitory mechanisms and implication for neurodegenerative diseases', *Archives of Biochemistry and Biophysics*, 522(1), pp. 62–69. doi: 10.1016/j.abb.2012.03.028.

Peñacoba-Antona, L., Ramirez-Vargas, C. A., Wardman, C., Carmona-Martinez, A. A., Esteve-Núñez, A., Paredes, D., Brix, H. and Arias, C. A. (2022) 'Microbial Electrochemically Assisted Treatment Wetlands: Current Flow Density as a Performance Indicator in Real-Scale Systems in Mediterranean and Northern European Locations', *Frontiers in Microbiology*, 13. doi: 10.3389/FMICB.2022.843135.

Pettigrew, G. W. and Moore, G. R. (1987) *Cytochromes c Biological Aspects*,

International Journal of Biochemistry. doi: 10.1007/978-3-642-72698-9.

Pirbadian, S., Barchinger, S. E., Leung, K. M., Byun, H. S., Jangir, Y., Bouhenni, R. A., Reed, S. B., Romine, M. F., Saffarini, D. A., Shi, L., Gorby, Y. A., Golbeck, J. H. and El-Naggar, M. Y. (2014) 'Shewanella oneidensis MR-1 nanowires are outer membrane and periplasmic extensions of the extracellular electron transport components', *Proceedings of the National Academy of Sciences of the United States of America*, 111(35), pp. 12883–12888. doi: 10.1073/PNAS.1410551111.

Pitts, K. E., Dobbin, P. S., Reyes-Ramirez, F., Thomson, A. J., Richardson, D. J. and Seward, H. E. (2003) 'Characterization of the *Shewanella oneidensis* MR-1 decaheme cytochrome MtrA: Expression in *Escherichia coli* confers the ability to reduce soluble FE(III) chelates', *Journal of Biological Chemistry*, 278(30), pp. 27758–27765. doi: 10.1074/jbc.M302582200.

Pollock, W. B., Rosell, F. I., Twitchett, M. B., Dumont, M. E. and Mauk, a G. (1998) 'Bacterial expression of a mitochondrial cytochrome *c*. Trimethylation of lys72 in yeast iso-1-cytochrome *c* and the alkaline conformational transition.', *Biochemistry*, 37(17), pp. 6124–31. doi: 10.1021/bi972188d.

Pollock, W. B. R., Rosell, F. I., Twitchett, M. B., Dumont, M. E. and Mauk, A. G. (1998) 'Bacterial expression of a mitochondrial cytochrome *c*. Trimethylation of Lys72 in yeast iso-1-cytochrome *c* and the alkaline conformational transition', *Biochemistry*, 37(17), pp. 6124–6131. doi: 10.1021/bi972188d.

Potter, M. C. (1911) 'Electrical effects accompanying the decomposition of organic compounds', *Proceedings of the Royal Society of London. Series B, Containing Papers of a Biological Character*, 84(571), pp. 260–276. doi: 10.1098/rspb.1911.0073.

Promega (no date) *Bacterial Strain JM109(DE3)*, *2022*. Available at: https://worldwide.promega.com/products/cloning-and-dna-markers/bacterial-

strains-and-competent-cells/bacterial-strain-jm109_de3_/?catNum=P9801.

Rabaey, K., Boon, N., Siciliano, S. D., Verhaege, M. and Verstraete, W. (2004) 'Biofuel cells select for microbial consortia that self-mediate electron transfer', *Applied and Environmental Microbiology*, 70(9), pp. 5373–5382. doi: 10.1128/AEM.70.9.5373-5382.2004.

Rabaey, K. and Rozendal, R. A. (2010) 'Microbial electrosynthesis — revisiting the electrical route for microbial production', *Nature Reviews Microbiology*, 8(10), pp. 706–716. doi: 10.1038/nrmicro2422.

Razdan, A. (2000) *Affinity Chromatography Handbook, Vol. 2: Tagged Proteins*. Available at: www.gelifesciences.com (Accessed: 23 March 2020).

Reguera, G., McCarthy, K. D., Mehta, T., Nicoll, J. S., Tuominen, M. T. and Lovley, D. R. (2005) 'Extracellular electron transfer via microbial nanowires', *Nature*, 435(7045), pp. 1098–1101. doi: 10.1038/nature03661.

Reguera, G., Nevin, K. P., Nicoll, J. S., Covalla, S. F., Woodard, T. L. and Lovley, D. R. (2006) 'Biofilm and nanowire production leads to increased current in *Geobacter sulfurreducens* fuel cells', *Applied and environmental microbiology*, 72(11), pp. 7345–7348. doi: 10.1128/AEM.01444-06.

Reguera, G. and Kashefi, K. (2019) 'The electrifying physiology of *Geobacter bacteria*, 30 years on', *Advances in Microbial Physiology*, 74, pp. 1–96. doi: 10.1016/bs.ampbs.2019.02.007.

Richardson, D. J. (2000) 'Bacterial respiration: A flexibe process for a changing environment', *Microbiology*, 146(2000), pp. 551–571. doi: so.

Richardson, D. J., Butt, J. N., Fredrickson, J. K., Zachara, J. M., Shi, L., Edwards, M. J., White, G., Baiden, N., Gates, A. J., Marritt, S. J. and Clarke, T. A. (2012) 'The "porin-cytochrome" model for microbe-to-mineral electron transfer', *Molecular Microbiology*, 85(2), pp. 201–212. doi: 10.1111/j.1365-2958.2012.08088.x.

Richardson, D. J., Fredrickson, J. K. and Zachara, J. M. (2012) 'Electron transport at the microbe-mineral interface: a synthesis of current research challenges.', *Biochemical Society transactions*, 40(6), pp. 1163–6. doi: 10.1042/BST20120242.

Rosano, G. L., Ceccarelli, E. A., Neubauer, P., Bruno-Barcena, J. M. and Schweder, T. (2014) 'Recombinant protein expression in *Escherichia coli*: advances and challenges'. doi: 10.3389/fmicb.2014.00172.

Rosano, G. L., Morales, E. S. and Ceccarelli, E. A. (2019) 'New tools for recombinant protein production in *Escherichia coli*: A 5-year update', *Protein Science*. Blackwell Publishing Ltd, pp. 1412–1422. doi: 10.1002/pro.3668.

Ross, D. E., Brantley, S. L. and Tien, M. (2009) 'Kinetic characterization of OmcA and MtrC, terminal reductases involved in respiratory electron transfer for dissimilatory iron reduction in Shewanella oneidensis MR-1', *Applied and Environmental Microbiology*, 75(16), pp. 5218–5226. doi: 10.1128/AEM.00544-09.

Rotaru, A. E., Shrestha, P. M., Liu, F., Markovaite, B., Chen, S., Nevin, K. P. and Lovley, D. R. (2014) 'Direct interspecies electron transfer between *Geobacter metallireducens* and *Methanosarcina barkeri*', *Applied and Environmental Microbiology*, 80(15), pp. 4599–4605. doi: 10.1128/AEM.00895-14.

Saltikov, C. W. and Newman, D. K. (2003) 'Genetic identification of a respiratory arsenate reductase.', *Proceedings of the National Academy of Sciences of the United States of America*, 100(19), pp. 10983–8. doi: 10.1073/pnas.1834303100.

San Francisco, B., Bretsnyder, E. C. and Kranz, R. G. (2013) 'Human mitochondrial holocytochrome *c* synthase's heme binding, maturation determinants, and complex formation with cytochrome *c*.', *Proceedings of the National Academy of Sciences of the United States of America*, 110(9), pp.

E788-97. doi: 10.1073/pnas.1213897109.

San Francisco, B., Sutherland, M. C. and Kranz, R. G. (2014) 'The CcmFH complex is the System I holocytochrome *c* synthetase: engineering cytochrome *c* maturation independent of CcmABCDE.', *Molecular microbiology*, 91(5), pp. 996–1008. doi: 10.1111/mmi.12510.

Sanders, C., Turkarslan, S., Lee, D.-W., Onder, O., Kranz, R. G. and Daldal, F. (2008) 'The Cytochrome *c* Maturation Components CcmF, CcmH, and CcmI Form a Membrane-integral Multisubunit Heme Ligation Complex *'. doi: 10.1074/jbc.M805413200.

Sanders, C., Turkarslan, S., Lee, D.-W. and Daldal, F. (2010) 'Cytochrome *c* biogenesis: the Ccm system', *Trends in Microbiology*, 18(6), pp. 266–274. doi: 10.1016/j.tim.2010.03.006.

Sanders, C., Wethkamp, N. and Lill, H. (2001) 'Transport of cytochrome *c* derivatives by the bacterial Tat protein translocation system', *Molecular Microbiology*, 41(1), pp. 241–246. doi: 10.1046/j.1365-2958.2001.02514.x.

Satomi, M. (2014) '*Shewanella*', *Encyclopedia of Food Microbiology: Second Edition*, pp. 397–407. doi: 10.1016/B978-0-12-384730-0.00307-4.

Schröder, U., Harnisch, F. and Angenent, L. T. (2015) 'Microbial electrochemistry and technology: terminology and classification', *Energy & Environmental Science*, 8(2), pp. 513–519. doi: 10.1039/C4EE03359K.

Shevket, S. H., Gonzalez, D., Cartwright, J. L., Kleanthous, C., Ferguson, S. J., Redfield, C. and Mavridou, D. A. I. (2018) 'The CcmC-CcmE interaction during cytochrome *c* maturation by System I is driven by protein-protein and not protein-heme contacts', *Journal of Biological Chemistry*, 293(43), pp. 16778–16790. doi: 10.1074/jbc.RA118.005024.

Shi, L., Dong, H., Reguera, G., Beyenal, H., Lu, A., Liu, J., Yu, H. Q. and Fredrickson, J. K. (2016) 'Extracellular electron transfer mechanisms

between microorganisms and minerals', *Nature Reviews Microbiology*, 14(10), pp. 651–662. doi: 10.1038/nrmicro.2016.93.

Silva, A. V., Edel, M., Gescher, J. and Paquete, C. M. (2020) 'Exploring the Effects of *bolA* in Biofilm Formation and Current Generation by *Shewanella oneidensis* MR-1', *Frontiers in Microbiology*, 11, p. 815. doi: 10.3389/FMICB.2020.00815/BIBTEX.

Silva, A. V., Firmino, M. O., Costa, N. L., Louro, R. O. and Paquete, C. M. (2022) 'Investigation of the Molecular Mechanisms of the Eukaryotic Cytochrome-*c* Maturation System', *Biomolecules*, 12(4), p. 549. doi: 10.3390/BIOM12040549/S1.

Di Silvio, E., Di Matteo, A., Malatesta, F. and Travaglini-Allocatelli, C. (2013) 'Recognition and binding of apocytochrome *c* to *P. aeruginosa* CcmI, a component of cytochrome *c* maturation machinery.', *Biochimica et biophysica acta*, 1834(8), pp. 1554–61. doi: 10.1016/j.bbapap.2013.04.027.

Simonte, F., Sturm, G., Gescher, J. and Sturm-Richter, K. (2019) 'Extracellular Electron Transfer and Biosensors', in Harnisch, F. and Holtmann, D. (eds) *Bioelectrosynthesis*. Cham: Springer International Publishing, pp. 15–38. doi: 10.1007/10_2017_34.

Sisler, F. D. (1962) 'Electrical Energy from Microbiological Processes', *Journal of the Washington Academy of Sciences*, 52(8), pp. 181–87.

Slavotinek, A. (2019) 'Genetics of anophthalmia and microphthalmia. Part 2: Syndromes associated with anophthalmia–microphthalmia', *Human Genetics*, 138(8–9), pp. 831–846. doi: 10.1007/s00439-018-1949-1.

Sturm, G., Dolch, K., Richter, K., Rautenberg, M. and Gescher, J. (2012) 'Metal reducers and reduction targets. A short survey about the distribution of dissimilatory metal reducers and the multitude of terminal electron acceptors', in *Microbial Metal Respiration: From Geochemistry to Potential Applications*. Berlin, Heidelberg: Springer-Verlag Berlin Heidelberg, pp. 129–159. doi:

10.1007/978-3-642-32867-1_6.

Sturm, G., Richter, K., Doetsch, A., Heide, H., Louro, R. O. and Gescher, J. (2015) 'A dynamic periplasmic electron transfer network enables respiratory flexibility beyond a thermodynamic regulatory regime', *The ISME Journal*, 9(8), pp. 1802–1811. doi: 10.1038/ismej.2014.264.

Sugase, K., Dyson, H. J. and Wright, P. E. (2007) 'Mechanism of coupled folding and binding of an intrinsically disordered protein', *Nature*, 447(7147), pp. 1021–1025. doi: 10.1038/nature05858.

Sutherland, M. C., Jarodsky, J. M., Ovchinnikov, S., Baker, D. and Kranz, R. G. (2018) 'Structurally Mapping Endogenous Heme in the CcmCDE Membrane Complex for Cytochrome *c* Biogenesis', *Journal of Molecular Biology*, 430(8), pp. 1065–1080. doi: 10.1016/j.jmb.2018.01.022.

Sutherland, M. C., Tran, N. L., Tillman, D. E., Jarodsky, J. M., Yuan, J. and Kranz, R. G. (2018) 'Structure-Function Analysis of the Bifunctional CcsBA Heme Exporter and Cytochrome *c* Synthetase', *mBio*. Edited by M. R. Chapman, 9(6). doi: 10.1128/mBio.02134-18.

Sutherland, M. C., Mendez, D. L., Babbitt, S. E., Tillman, D. E., Melnikov, O., Tran, N. L., Prizant, N. T., Collier, A. L. and Kranz, R. G. (2021) '*In vitro* reconstitution reveals major differences between human and bacterial cytochrome c synthases', *eLife*, 10. doi: 10.7554/eLife.64891.

Sydow, A., Krieg, T., Mayer, F., Schrader, J. and Holtmann, D. (2014) 'Electroactive bacteria—molecular mechanisms and genetic tools', *Applied Microbiology and Biotechnology*, 98(20), pp. 8481–8495. doi: 10.1007/S00253-014-6005-Z.

Tahirov, T. H., Misaki, S., Meyer, T. E., Cusanovich, M. A., Higuchi, Y. and Yasuoka, N. (1996) 'High-resolution Crystal Structures of Two Polymorphs of Cytochrome *c′* from the Purple Phototrophic Bacterium *Rhodobacter capsulatus*', *Journal of Molecular Biology*, 259(3), pp. 467–479. doi:

10.1006/JMBI.1996.0333.

Takamatsu, H., Kodama, T., Nakayama, T. and Watabe, K. (1999) ‘Characterization of the *yrbA* gene of *Bacillus subtilis* involved in resistance and germination of spores’, *Journal of bacteriology*, 181(16), pp. 4986–4994. doi: 10.1128/JB.181.16.4986-4994.1999.

Tartoff, K. D. and Hobbs, C. A. (1987) ‘Improved media for growing plasmid and cosmid clones’, *Bethesda Research Laboratories Focus*, 9, pp. 12–16.

Teravest, M. A. and Ajo-Franklin, C. M. (2015) ‘Transforming exoelectrogens for biotechnology using synthetic biology’, *Biotechnology and Bioengineering*, 113(4), pp. 687–697. doi: 10.1002/bit.25723.

Thompson, J. D., Higgins, D. G. and Gibson, T. J. (1994) ‘CLUSTAL W: improving the sensitivity of progressive multiple sequence alignment through sequence weighting, position-specific gap penalties and weight matrix choice’, *Nucleic acids research*, 22(22), pp. 4673–4680. doi: 10.1093/NAR/22.22.4673.

Thony-Meyer, L., Fischer, F., Kunzler, P., Ritz, D. and Hennecke, H. (1995) ‘*Escherichia coli* genes required for cytochrome *c* maturation.’, *Journal of Bacteriology*, 177(15), p. 4321. doi: 10.1128/JB.177.15.4321-4326.1995.

Thormann, K. M., Duttler, S., Saville, R. M., Hyodo, M., Shukla, S., Hayakawa, Y. and Spormann, A. M. (2006) ‘Control of Formation and Cellular Detachment from *Shewanella oneidensis* MR-1 Biofilms by Cyclic di-GMP Control of Formation and Cellular Detachment from *Shewanella oneidensis* MR-1 Biofilms by Cyclic di-GMP’. doi: 10.1128/JB.188.7.2681.

Trindade, B. and Louro, R. O. (2020) ‘Introduction to nuclear magnetic resonance and metals’, in. Elsevier, pp. 155–199. doi: 10.1016/B978-0-444-64225-7.00005-5.

Trindade, I. B., Coelho, A., Cantini, F., Piccioli, M. and Louro, R. O. (2022)

‘NMR of paramagnetic metalloproteins in solution: Ubi venire, quo vadis?’, *Journal of Inorganic Biochemistry*, 234, p. 111871. doi: 10.1016/J.JINORGBIO.2022.111871.

Ucar, D., Zhang, Y. and Angelidaki, I. (2017) ‘An Overview of Electron Acceptors in Microbial Fuel Cells’, *Frontiers in Microbiology*, 8, p. 643. doi: 10.3389/fmicb.2017.00643.

Ueki, T., Nevin, K. P., Woodard, T. L., Aklujkar, M. A., Holmes, D. E. and Lovley, D. R. (2018) ‘Construction of a *Geobacter* strain with exceptional growth on cathodes’, *Frontiers in Microbiology*, 9(JUL), pp. 1–7. doi: 10.3389/fmicb.2018.01512.

Venkateswaran, K., Moser, D. P., Dollhopf, M. E., Lies, D. P., Saffarini, D. A., MacGregor, B. J., Ringelberg, D. B., White, D. C., Nishijima, M., Sano, H., Burghardt, J., Stackebrandt, E. and Nealson, K. H. (1999) ‘Polyphasic taxonomy of the genus *Shewanella* and description of *Shewanella oneidensis sp. nov.*’, *International Journal of Systematic Bacteriology*, 49(2), pp. 705–724. doi: 10.1099/00207713-49-2-705/CITE/REFWORKS.

Verissimo, A. F., Yang, H., Wu, X., Sanders, C. and Daldal, F. (2011) ‘CcmI Subunit of CcmFHI Heme Ligation Complex Functions as an Apocytochrome c Chaperone during c -Type Cytochrome Maturation *’, *The Journal of biological chemistry*, 286(47), pp. 40452–40463. doi: 10.1074/jbc.M111.277764.

Verissimo, A. F., Sanders, J., Daldal, F. and Sanders, C. (2012) ‘Engineering a prokaryotic apocytochrome *c* as an efficient substrate for *Saccharomyces cerevisiae* cytochrome *c* heme lyase’, *Biochemical and Biophysical Research Communications*, 424(1), pp. 130–135. doi: 10.1016/j.bbrc.2012.06.088.

Verissimo, A. F. and Daldal, F. (2014) ‘Cytochrome *c* biogenesis System I: an intricate process catalyzed by a maturase supercomplex?’, *Biochimica et biophysica acta*, 1837(7), pp. 989–98. doi: 10.1016/j.bbabio.2014.03.003.

Verissimo, A. F., Shroff, N. P. and Daldal, F. (2015) 'During Cytochrome *c* Maturation CcmI chaperones Class I Apocytochromes until the Formation of their *b*-type Cytochrome Intermediates', *Journal of Biological Chemistry*, 290(27), p. jbc.M115.652818. doi: 10.1074/jbc.M115.652818.

Vieira, H. L. A., Freire, P. and Arraiano, C. M. (2004) 'Effect of Escherichia coli Morphogene bolA on Biofilms', *Applied and Environmental Microbiology*, 70(9), pp. 5682–5684. doi: 10.1128/AEM.70.9.5682-5684.2004.

de Vitry, C. and Vitry, C. de (2011) 'Cytochrome *c* maturation system on the negative side of bioenergetic membranes: CCB or System IV.', *The FEBS journal*, 278(22), pp. 4189–97. doi: 10.1111/j.1742-4658.2011.08373.x.

Wah Tang, P., San Chua, P., Kee Chong, S., Saberi Mohamad, M., Wen Choon, Y., Deris, S., Omatu, S., Manuel Corchado, J., Howe Chan, W. and Abdul Rahim, R. (2015) 'A Review of Gene Knockout Strategies for Microbial Cells', *Recent Patents on Biotechnology*, 9(3), pp. 176–197. doi: 10.2174/1872208310666160517115047.

Watanabe, K. and Woodward, D. F. (2015) 'Prostamide F2α Biosynthesizing Enzymes', *The Endocannabinoidome: The World of Endocannabinoids and Related Mediators*, pp. 101–110. doi: 10.1016/B978-0-12-420126-2.00007-9.

White, G. F., Edwards, M. J., Gomez-Perez, L., Richardson, D. J., Butt, J. N. and Clarke, T. A. (2016) *Mechanisms of Bacterial Extracellular Electron Exchange*. 1st edn, *Advances in microbial physiology*. 1st edn. Elsevier Ltd. doi: 10.1016/bs.ampbs.2016.02.002.

Williamson, M. P., Suzuki, Y., Bourne, N. T. and Asakura, T. (2006) 'Binding of amyloid β-peptide to ganglioside micelles is dependent on histidine-13', *Biochemical Journal*, 397(3), pp. 483–490. doi: 10.1042/BJ20060293.

Williamson, M. P. (2013) 'Using chemical shift perturbation to characterise ligand binding', *Progress in Nuclear Magnetic Resonance Spectroscopy*, 73, pp. 1–16. doi: 10.1016/j.pnmrs.2013.02.001.

Wimplinger, I., Morleo, M., Rosenberger, G., Iaconis, D., Orth, U., Meinecke, P., Lerer, I., Ballabio, A., Gal, A., Franco, B. and Kutsche, K. (2006) 'Mutations of the Mitochondrial Holocytochrome *c*–Type Synthase in X-Linked Dominant Microphthalmia with Linear Skin Defects Syndrome', *The American Journal of Human Genetics*, 79(5), pp. 878–889. doi: 10.1086/508474.

Wishart, D. S., Bigam, C. G., Holm, A., Hodges, R. S. and Sykes, B. D. (1995) '^{1}H, ^{13}C and ^{15}N random coil NMR chemical shifts of the common amino acids. I. Investigations of nearest-neighbor effects.', *Journal of biomolecular NMR*, 5(1), pp. 67–81. doi: 10.1007/BF00227471.

Xu, Z., Liang, Y., Lin, S., Chen, D., Li, B., Li, L. and Deng, Y. (2016) 'Crystal Violet and XTT Assays on Staphylococcus aureus Biofilm Quantification', *Current Microbiology*, 73(4), pp. 474–482. doi: 10.1007/S00284-016-1081-1.

Yang, Y., Ding, Y., Hu, Y., Cao, B., Rice, S. A., Kjelleberg, S. and Song, H. (2015) 'Enhancing Bidirectional Electron Transfer of *Shewanella oneidensis*by a Synthetic Flavin Pathway', *ACS Synthetic Biology*, 4(7), pp. 815–823. doi: 10.1021/sb500331x.

Yong, Y.-C., Yu, Y.-Y., Zhang, X. and Song, H. (2014) 'Highly Active Bidirectional Electron Transfer by a Self-Assembled Electroactive Reduced-Graphene-Oxide-Hybridized Biofilm', *Angewandte Chemie International Edition*, 53(17), pp. 4480–4483. doi: 10.1002/anie.201400463.

Yu, Y., Chen, H.-L., Yong, Y., Kim, D. and Song, H. (2011) 'Conductive artificial biofilm dramatically enhances bioelectricity production in *Shewanella* -inoculated microbial fuel cells', *ChemComm*, 47(C), pp. 12825–12827. doi: 10.1039/c1cc15874k.

Zajdel, T. J., Baruch, M., Méhes, G., Stavrinidou, E., Berggren, M., Maharbiz, M. M., Simon, D. T. and Ajo-Franklin, C. M. (2018) 'PEDOT:PSS-based Multilayer Bacterial-Composite Films for Bioelectronics', *Scientific Reports*, 8(1), p. 15293. doi: 10.1038/s41598-018-33521-9.

Zhao, J., Li, F., Cao, Y., Zhang, X., Chen, T., Song, H. and Wang, Z. (2021) ‘Microbial extracellular electron transfer and strategies for engineering electroactive microorganisms’, *Biotechnology Advances*, 53, p. 107682. doi: 10.1016/J.BIOTECHADV.2020.107682.